Dor Leviathan Offshore Platform Environmental Report Review and Simulation

Supplementary Report

ORION-Joint Research and Development Center

Date of Issue: 22/November/2019

Doc	Name	Signature	Degree	Date	Role
Approved by	Evis Drousiotis	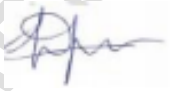	M.Sc.	22/11/2019	ORION CEO
Approved by	Ziv Deshe		B.Sc. Agr. Eng.	22/11/2019	Mayor Local Council Zichron-Ya'akov Israel
Approved by	Avigdor Brillant		B.Sc. EE Senior member IEEE	22/11/2019	Gas Cabinet Zichron-Ya'akov
Approved by	Avigdor Klein	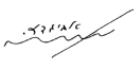	B.Sc. ME Eng.	22/11/2019	Gas Cabinet Zichron-Ya'akov

This page is intentionally left blank

Peer Approval Table

Doc	Name	Signature	Degree	Date	Role
Prepared by	1. George Zodiatis		Ph.D.		Oil spill modeling
	2. Svitlana Liubartseva		Ph.D.		Oil spill modeling
	3. Loizos Loizides		M.Sc.		Marine Pollution
	4. Marco Pellegatta		M.Sc.		Air pollution
	5. Giovanni Coppini		Ph.D.		Oil spill modeling
	6. Hari Radhakrishnan		Ph.D.		Oil spill modeling
	7. Roberto Bonarelli		M.Sc.		Oil spill modeling
	8. George Kallos		Ph.D.		Atmospheric data
	9. Christina Kalogeri		Ph.D.		Atmospheric data
	10. Robin Lardner		Ph.D.		Oil spill modeling
	11. Panikos Nikolaides		M.Sc.		Marine pollution
Reviewed by	George Zodiatis		Ph.D.		Oil spill modeling
	Loizos Loizides		M.Sc.		Marine pollution

Revision Control

#	Date	Rev	Originator	Description
1.				
2.				

This page is intentionally left blank

Table of Contents

List of Figures

List of Tables

This page is intentionally left blank

1. Executive Summary

1.1. Background

This report is a supplementary report to report number LSR-OR-ZY-04-08-2019-R-A [13], ordered by the Local Council of Zichron-Ya'akov Israel as third party second opinion report. The report examines Product water discharges from the Leviathan offshore fixed platform rig located at the proximity of 10km from the shoreline of Dor Israel within the Regional municipality of Hof-Carmel jurisdiction and pip-rupture spill event evaporation. The Dor rig coordinates are provided in chapter *3 Problem Definition* The report comprises five main parts:

1. Evaluation review of the performed environmental risk assessments and spill size documents provided by Noble Energy to the Ministry of Energy and Ministry of Environmental Protection having the following information:
   1.1. LPP-ON-NEM-EHS-STY-0002 Rev-A Dec. 2016 applicable document *[1]* in *Table 2*
      1.1.1. Annex 6.3 Noble Energy pp. 242- 261
         1.1.1.1. DOC: LPP-PM-NEM-EHS-PLN-0006 Noble Energy pp.243-251*[1.1]*.
         1.1.1.2. DOC: LPP-PM-NEM-EHS-BOD-0402 Noble Energy pp.252-261 *[1.2]*.
      1.1.2. Annex 6.4 DOC: J20813-Y-TN-24004 Rev-B2 March 2016 Genesis OSCAR modeling summary pp262-293 *[1.3]*.
         1.1.2.1. Table 3-2 page 275,
            1.1.2.1.1. scenario 1: Volume 194m^3(1220bbls)
            1.1.2.1.2. scenario 2-3:Volume 159m^3 (1000bbls)
      1.1.3. Annex 6.4 DOC J20813B-YPN-25005 Rev-D1May 2016 Genesis OSCAR Oil spills results pp294-371 *[1.4]*.
      1.1.4. Annex 6.9 Brenner MEDSLIK report Feb 2016 modelling the dispersion of condensate spills from the proposed gas processing pipeline. pp. 440-537*[1.5]*.
         1.1.4.1. Volume 1220bbls for the pipeline rupture. Page 449
         1.1.4.2. 12 simulation runs.
         1.1.4.3. API=43.2, SG=0.8099, page 449.
   1.2. LPP-ON-NEM-EHS-STY-0005 applicable document *[2]*in *Table 2*
      1.2.1. Annex 6.4 DOC: J20979A-Y-TN-24003/REV B1 May 2017 Genesis OSCAR simulation spillage Pipeline Rupture Modeling Summary pp. 293-325 *[2.3]*.
         1.2.1.1. Table 3-2: Volume 192m^3(1207bbls), rate 69.5m^3/h (437), page 306.
      1.2.2. Annex 6.5: Brenner MEDSLIK report Feb 2016 pp. 326-385 (as in *1.1.4*) *[2.4]*.
         1.2.2.1. Data is at page 346.
   1.3. TAMA 37-H Effects on Marine Environment pp.51- 68, applicable document [16] in *Table 2*.
      1.3.1. Table 3.4.6 page 68 shows 2446bbls (minimum potential pipe rupture spill).

2. Spillage event of 3000 bbls of condensate from Dor rig pipe rupture event to the CVS at the proximity of 1Km from the shoreline of Dor.

2.1. Toxic vapor cloud due to;

2.1.1. Pipe rupture event of 3000 bbls (not included in this report and is analyzed in supplementary report)

2.1.2. Comparing pipe rupture spillage beaching to results to Annex 6.9 pipeline rupture simulation by Brenner using MEDSLIK. Page 449 applicable document *[1.5]* against simulation in LSR-OR-ZY-04-08-2019-R-A [13].

2.1.3. Comparing pipe rupture spillage beaching to results to Annex 6.4 DOC: J20979A-Y-TN-24003/REV B1 May 2017 Genesis OSCAR simulation spillage Pipeline Rupture Modeling Summary pp. 293-325 *[2.3]*. Table 3-2: Volume 192m^3(1207bbls), rate 69.5m^3/h (437), page 306 against simulation in LSR-OR-ZY-04-08-2019-R-A [13].

2.2. Product water discharges impact on sea marine life and desalination plans.

3. Concluding reaction time to pipe rupture spillage event and identifying the time where levels of contamination at shoreline crosses the threshold of 0.03 Ton/Km or 0.19 bbls/Km.
4. Checking the evaporation levels against international standards
5. Monitoring and prevention.

Massive near coast condensate spills (3000 bbls) are likely to result into temporary exceedances of the 24-hours Ambient Air Quality Value of Benzene (3.9 ug/m^3), but within the permitted number of exceedances by the National Regulation (maximum 3 days of exceedance, against 7 yearly permitted events).

On the other side, no exceedance of Acute Exposure Guidelines (PAC/AEGLs) are anticipated for Benzene and the other BTEXs, simulated levels being at least 1 order of magnitude lower than the relevant Tier-1 thresholds (the lowest being: Benzene 8h: 9 ppm; Ethylbenzene 1h: 22 ppm) .

Low-wind conditions could result in high coastal concentrations of Total VOCs, with levels on the same order of magnitude of emergency public exposure guidelines (PAC2) for C10, C11 and C12 alkanes (respectively: 6.6 ppm, 2.3 ppm and 1.7 ppm).

The lack of detailed data about hydrocarbon speciation of potential spilled condensate does not allow to get an ultimate judgment on the harmfulness of VOC vapor mixture on potential exposed communities in case of Massive near coast condensate spills.
While maximum estimated onshore levels of Benzene are well below internationally recognized emergency thresholds (USEPA PACs/AEGLs) and maximum total VOCs do not reach available tier-1 thresholds for hydrocarbon mixtures (relevant to gasoline and jet fuels), the cautionary comparison of maximum onshore concentration of total VOCs with selected C10-C12 Alkanes threshold raise concerns. Tier-2 effects (irreversible or other serious, long-lasting, adverse health effects or an impaired ability to escape), cannot be excluded for the potentially exposed population in case of massive condensate spill event such as those under study.

The speciation and concentration of airborne volatile compounds should be carefully monitored in case of spill. In the absence of additional data, a warning communication plan should also be activated in order to alert communities and minimize their exposure to vapor plumes in the area of major impact, especially in case of a near-coast spill with low-winds blowing towards coast.

It is worth to be noted that no threshold level was found in literature for Total VOC. This means that the above reported comparison may be overly conservative, although the presence of other compounds than alkanes and the effects of the overall mixture should be considered. This requires detailed information about the composition of the spilled condensate. The concentration of airborne volatile compounds should be carefully monitored in case of spill.

The plan for having offshore platform at such proximity to shoreline requires monitoring and readiness for spill event. Monitoring must be reliable and continuous. It is recommended to perform continuous monitoring on the platform, monitoring seawater and monitoring the air quality at several fix stations to different locations. Monitoring requirement is critical in case of growth plans as elaborated in Chapter *7Growth Impact to Four platforms in the Polygon* .

Since spill events occur at such proximity to shoreline, the response time is critical. Hence it is recommended to have a local response facility with all required equipment. Chapter *9 Monitoring* details the means and technology for monitoring levels.

1.2. What Condensate is

The term condensate is defined in applicable document [13] section 4.1 page 42. The definition used is cited in the Environment Canada Document 2016 Natural Gas condensate Screening Assessment for relevant legislation[1]. In this definition Condensate is clearly a liquid oil product.

In addition the condensate used for the model scenario has a specific **API**[2] [3]a term used only for **Liquid** petroleum products.

[1] http://publications.gc.ca/collections/collection_2017/eccc/En14-270-2017-eng.pdf
[2] https://www.sciencedirect.com/topics/earth-and-planetary-sciences/gas-condensate
[3] https://www.sciencedirect.com/topics/engineering/oil-gravity

2. Overview

2.1. Scope

This supplementary report request is from The Local Council of Zichron-Ya'akov Israel. The report examines the product water discharge from Dor fixed offshore platform (OSP) on the shore-line of Israel. In addition it examines the evaporation due to pipe rupture at the proximity of 1km from shoreline. The data for this report is based on applicable documents listed in *Table 2*.

The present simulations are based on MEDSLIK/ MEDSLIK II solvers, which are utilized for many years in the Levantine and the Mediterranean Sea during real oil spill incidents. The current simulations spillage results are compared to the Leviathan results of OSCAR and MEDSLIK by Brenner mentioned in *Table 2* . The current simulations assume larger spillage size (compared to OSCAR and MEDSLIK by Brenner previous simulations), as described by the official letters of the Ministry of Energy [7] and the Ministry of Environmental Protection [8].

Under this assumption the condensate spillage size in pipe rupture event is 3000 bbls against analysis provided by *LPP-ON-NEM-EHS-STY-0002* [1] pipe rupture evaporation of 1220 bbls, as appears and simulated in annex 6.4, 6.9 [1.3,1.5] OSCAR by Genesis and MEDSLIK by Brenner. In the analysis provided by *LPP-ON-NEM-EHS-STY-0005*[2] annex 6.4 [2.3] and annex 6.5 [2.4] maintain low spillage during operation. Annex 6.2 [2.1] and 6.3 [2.2] provide diesel oil spill of 2000 bbls.
The recent permit [9] request of Noble Energy asks for 6300 bbls at the second phase of operation, however since there is no official approval from the State of Israel for that request, the current condensate spillage size remains for 5300bbls.

The present report examines the following scenario:

1- Condensate evaporation due to spillage of 3000 bbls from the pipe rupture located 1 km from the Israel shore.

The results of the spillage concentrations at key coordinates are compared to the results in the applicable documents [1], [2] and their annexes, in order to conclude the magnitude of contamination. In addition, contamination levels at the coastline of the Hadera desalination plan is reported, as well as the levels at the coastline of the Atlit old Crusades Fort reservation, Ma'agan-Michael and Caesarea national parks located at *Figure 5*, *Figure 6*, *Figure 7*, *Figure 8*, *Figure 9* are reported.

2.2. Abbreviation list

Table 1: Abbreviations

#	Abbreviation	Meaning
1.	API	American Petroleum Number
2.	BAT	Best Available Technology
3.	bbls	Barrels
4.	CDF	Cumulative Density Function
5.	CUMSUM	Cumulative Summation
6.	CMEMS	Copernicus Marine Environmental Monitoring Service
7.	CVS	Coastal Valve Station
8.	CYCOFOS	Cyprus Coastal Ocean Forecasting and Observing System
9.	ECMWF	European Centre for Medium-Range Weather Forecasts
10.	EEZ	Exclusive Economic Zone
11.	EMSA	European Maritime Safety Agency
12.	EPA	Environmental Protection Agency
13.	FPSO	Floating Production Storage and Offloading
14.	GEBCO	General Bathymetric Chart of the Oceans
15.	GFS	Global Forecast System
16.	IEC	Israel Electrical Company
17.	ITOPF	International Tanker Owners Pollution Federation Limited
18.	LPP	Leviathan Production Platform
19.	MARPOL	Marine Pollution (UN convention)
20.	MFC -Med	Monitoring and Forecasting Center - Mediterranean
21.	MFSTEP	Mediterranean Forecasting System Toward Environmental Predictions
22.	MMscfd	Million Standard Cubic Feet Per Day
23.	MONGOOS	Mediterranean Oceanography Network for Global Ocean Observing System
24.	MOON	Mediterranean Operational Oceanography Network
25.	NCEP	National Center of Environmental Prediction
26.	NEML	Noble Energy Mediterranean Limited
27.	OSCAR	Oil Spill Contingency and Response (SINTEF)
28.	OSCP	Oil Spill Contingency Plan
29.	OSLR	Oil Spill Response Limited
30.	OSP	Offshore Platform
31.	POLMAR	Pollution Maritime
32.	MEDSLIK, MEDSLIK II	Mediterranean oil spill and trajectory predictions model
33.	REMPEC	Regional Marine Pollution Emergency Response Centre for the Mediterranean Sea
34.	RRTM	Rapid Radiative Transfer Model
35.	SG	Specific Gravity
36.	SINTEF	Norwegian: Stiftelsen for Industriell og TEknisk Forskning
37.	SST	Sea Surface Temperature
38.	TH	Threshold
39.	USCG	United States Coast Guard
40.	USGS	United States Geological Survey

2.3. Applicable documents

Table 2: Applicable documents

#	Standard/Doc	Description	Rev.	Date
1.	LPP-ON-NEM-EHS-STY-0002	AMPHIBIO Leviathan Marine Environmental report	Rev. A,	04 December 2016
1.1.	LPP-PM-NEM-EHS-PLN-0006	Annex 6.3 Air Discharges Noble Energy pp. 243-251	Rev. B	07 June 2016
1.2.	LPP-PM-NEM-EHS-BOD-0402	Annex 6.3 Air Discharges Noble Energy pp. 252-261	Rev. 0	06 July 2016
1.3.	J20813-Y-TN-24004	Annex 6.4 Genesis OSCAR Modelling summary pp. 262-293	Rev. B2	22 March 2016
1.4.	J20813B-YPN-25005	Annex 6.4 Genesis OSCAR Oil spill results pp. 294-371	Rev. D1	25 May 2016
1.5.	None	Annex 6.9 Steve Brenner MEDSLIK Modelling pp. 440-537	None	February 2016
2.	LPP-ON-NEM-EHS-STY-0005	AMPHIBIO Leviathan Marine Environmental report	Rev. 2,	26 October 2017
2.1.	J20979A-Y-TN-24001	Annex 6.2 Genesis Analysis OSCAR Diesel Modelling Summary pp. 200-232	Rev. B2	03 May 2017
2.2.	None	Annex 6.3 Steve Brenner modeling spillage during construction pp.234-292	None	March 2017
2.3.	J20979A-Y-TN-24003	Annex 6.4Genesis OSCAR Pipeline Rupture Modelling Summary pp. 293- 325	Rev. B1	04 May 2017
2.4.	None	Annex 6.5 Steve Brenner modeling spillage during operation pp. 326-385	None	February 2016
3.	Official Translation www.Globus-Translations.com LPP-ON-NEM-EHS-STY-0002	AMPHIBIO Leviathan Marine Environmental report Chapters 3, 4, 5	None	January 2018
4.	Marine and Coastal Environment Division Ministry of the Environment	Environmental Quality Standards for the Mediterranean Sea in Israel		August 2002
5.	Ministry of National Infrastructure, Energy, and Water Resources, Natural Resources Administration Ministry of Environmental Protection Marine Environment Protection Division	Framework Guidelines for Preparing the Environmental Statement Enclosed with the Exploration License - Exploration Well Application Name and Production Tests in the License (License Name)		30May, 2016
6.	Prevention of Sea-Water Pollution by Oil Ordinance			
7.	Ministry of Energy Letter from 12 – July-2018 to Mrs. Anat Gal, "Rotzim Lehyot" signed by general manager ministry of energy Mr. Udi Adiri	Page 4, QTY is 5000bbls as a minimum		12July 2018
8.	Ministry of Environmental Protection letter from 05-May-2018, to Dror Laufer Home Guardians	Page 6, QTY is 5300 bbls max		05May 2018

#	Standard/Doc	Description	Rev.	Date
9.	Form 2.1.1- Leviathan	Request for 6300bbls (1000m^3)		20January 2019
10.	LPP-PM-NEM-EIA-PLN-0002 Genesis No: J20813A-Y-RT-24001 Rev0	Environmental Impact Assessment for Installation, Operation and Maintenance of pipelines and Submarine Systems for Leviathan Field Development	Rev0	July 2016
11.	Benzene Content - Leviathan Field	Report	None	10-June-2019
12.	Condensate data	Memorandum from Local Council Zichron-Ya'akov		9/April/2019
13.	LSR-OR-ZY-04-08-2019-R-A	Dor Leviathan Offshore Platform Environmental Report Review and Simulation ORION-Joint Research and Development Center	A	04/August/2019
14.	Clarifications to Dr. Zodiatis. Local Council Zichron-Ya'akov	Coordinates Location of DOR offshore Pipe Rupture		4/June/2019
15.	SOW Local Council Zichron-Ya'akov	Statement of Work for Environmental Risk Analysis and Review (SOW-ERAR)		5/February/2019
16.	ETHOS - Architecture, Planning and Environment ltd. 5 Habanai St. Hod-Hasharon 45319, Israel www.ethos-group.co.il Lerman Architects and City Designesign LTD 120 Ygal Alon Street Tel-Aviv 67443 http://www.lerman.co.il/	TAMA 37-H Effects on Marine Environment Sections C to E		June 2013
17.	Israel Electrical Company IEC Link is here	Monitoring of the Marine and Shoreline Environment at the Site of Orot Rabin Power Station, Desalination Hadera Facility H2ID report for 2017		April 2018
18.	TAMA 37-H Ministry of Energy and Water Lerman Architects Office	Environmental Effects Review Sections Gimel - Het Marine Environment		June 2013
19.	National Outline Plan NOP 37/H For Natural Gas Treatment Facilities Environmental Impact	Survey Chapters 3 – 5 – Marine Environment		June 2013

3. Problem Definition

The Leviathan natural gas field was discovered in 2010 and is located approximately120 km offshore Israel beach line within the Israeli exclusive economic zone (EEZ). Water depth at the field is varying between 1540 and1800 m. Phase one of the development plan involves drilling of 4 subsea wells. Production will be delivered via flow lines to a fixed platform with full processing capabilities, situated roughly 10 km off the coastline of Israel. Processed gas will connect to the Israel Natural Gas Lines onshore transportation grid in the northern part of the country and to regional markets via onshore export pipelines.

Drilling is anticipated completed during 2018. Offshore installation should be followed by the start of commissioning in 4Q 2019, ahead of the planned year-end 2019 start-up.
A partnership of Noble Energy, Delek Drilling, Avner Oil Exploration and Ratio Oil Exploration is behind the plan for development of the field, including preparation of an Environmental Impact Assessment [10] (dated July 2016; *Environmental Impact Assessment for Installation, Operation and Maintenance of pipelines and Submarine Systems for Leviathan Field Development*).
In phase one the processing platform will handle about 1.4 MSm3/hr natural gas and 2500 barrels/day of condensate, volumes increasing with 40-50% in phase two.

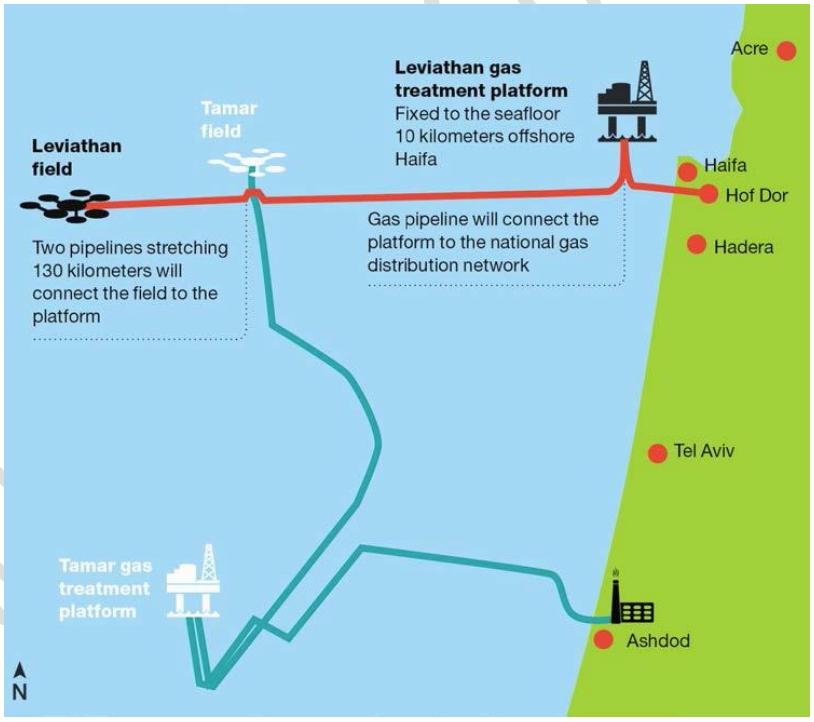

Figure 1: Layout of phase 1 of the Leviathan discovery/facilities offshore Israel (Source: Delek drilling)

The petroleum activity in such proximity to the shoreline, and onshore settlement, has created skepticism among local communities, and the Council of Zichron - Ya'akov has by letter dated 18/11/2018 approached ORION to perform a 3rd party review of the EIA documentation and undertake independent modeling of pollution and assess potential impacts on the environment and public health.

Their stake is that the field should rather be developed by a FPSO located 120 km offshore to reduce pollution risk along the coastline and likewise reduce public health risk from air pollution.

The fixed platform is located 10km west to Dor village as depicted in *Figure 2* and *Figure 3*. Coordinates and water depth of the Dor fixed platform are provided in *Table 3*, *Table 4* (translated in English) and *Table 5*. There are several design documents with slight different coordinates (see *Table 5*)

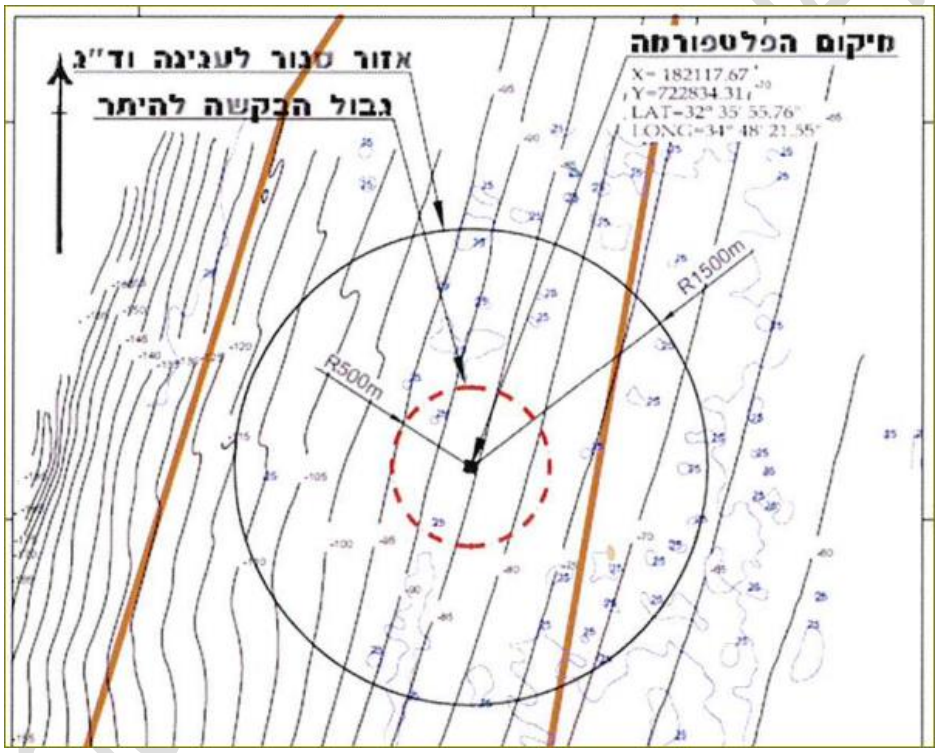

Figure 2: DOR offshore fix platform location and coordinates X/Y and UTM

(From LPP-ON-NEM-EHS-STY-0002 Rev. A, Fig 2.1 page 15 reference [1] as Fig 2.1B)

X=182117.67
Y= 722834.31
LAT= 32°35'55.76"
LONG= 34°48'21.55"
Water Depth 86 meters.

Table 3: Dor fixed platform coordinates water depth and distances from beach line and towns (Hebrew)

(From LPP-ON-NEM-EHS-STY-0002 Rev. A Table 2.1 page 16 reference [1])

מרחקים (ק"מ)				קואורדינטות UTM		קואורדינטות		
דור	חדרה	ראש כרמל	חוף קרוב	Y (m)	X (m)	E מזרח	N צפון	עומק מים (מטר)
10.9	19.5	29.5	9.7	360825.35	669479.57	34.805993	32.598825	86

Table 4: Dor fixed platform coordinates water depth and distances from beach-line and towns (translation)

Distances [Km]				Coordinates [UTM]		Coordinates		Water Depth [m]
Dor	Hadera	Carmel Peak	Near Beach	Y [m]	X [m]	East LONG	North LAT	
10.9	19.5	29.5	9.7	360825.35	669479.57	34.805993	32.598825	86

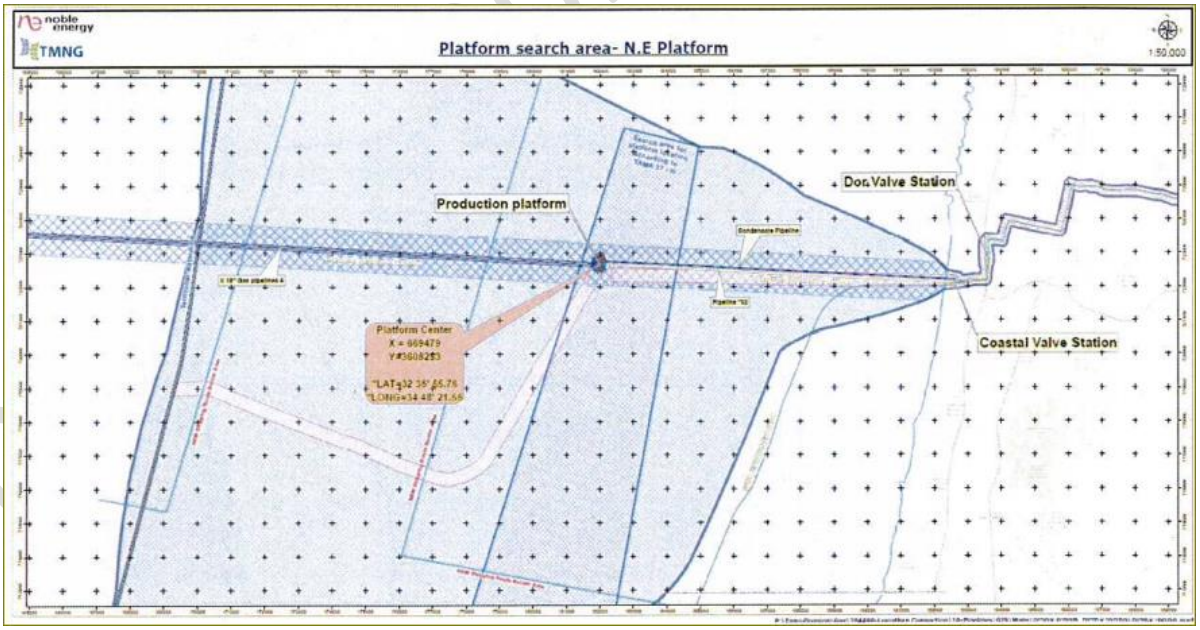

Figure 3: Dor fixed platform offshore location and coordinates X/Y and UTM

Table 5: Dor fixed platform coordinates water depth and distances from beach - line and towns (translation)

Documentation	Coordinates [UTM]		Coordinates		Water Depth [m]
	Y [m]	X [m]	East LONG	North LAT	
LPP-ON-NEM-EHS-STY- 0002 Rev-A 2016 (Environmental Doc ref [1])	360825.35	669479.57	34.805993	32.598825	86
Emission request Noble 8/11/2016 page 6	360825.35	669479.57	34.850993	32.598815	--
LEVIATHAN DOC 2016	360825.65	669479.11	34.805988	32.598818	--

Condensate spillage size dated January 20 2019 [9] is as follows (see *Figure 4*):

1. Rig capacity at first phase 572 cubic meters /day 3600 bbls
2. Rig capacity at second phase 1002 cubic meters /day 6300 bbls this is planed operation 1000 bbls larger than simulation in this report, which is 5300 bbls according to [7] and [8].
3. Conversion m^3 to bbls calculator is provided:
   3.1. https://www.metric-conversions.org/volume/cubic-meters-to-us-oil-barrels.htm

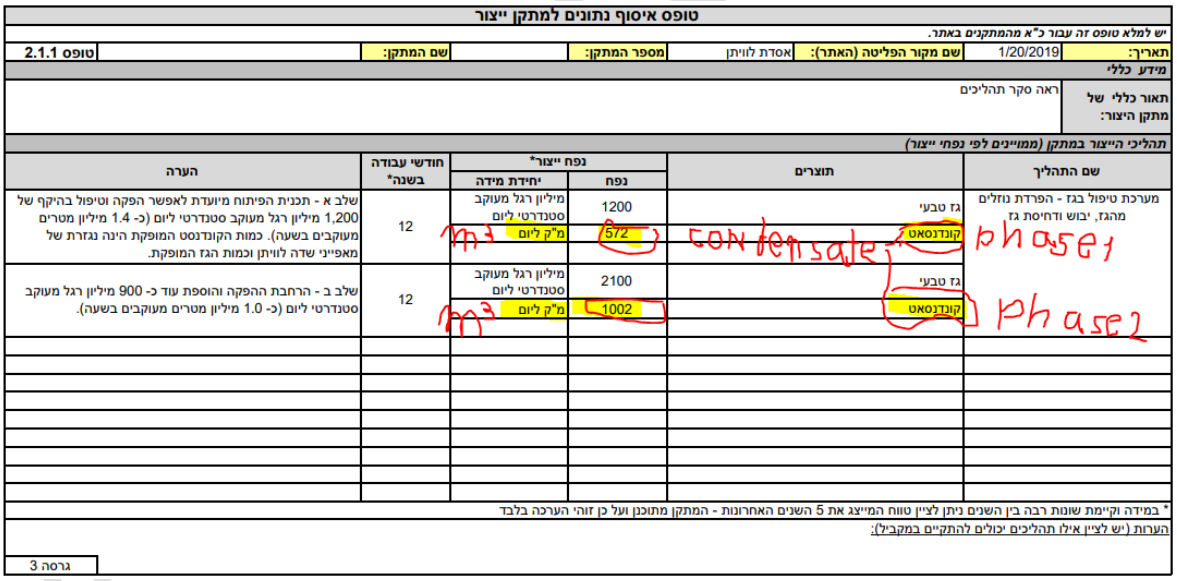

טופס איסוף נתונים למתקן ייצור

יש למלא טופס זה עבור כ"א מהמתקנים באתר.

תאריך:	1/20/2019	שם מקור הפליטה (האתר):	אסדת לוויתן	מספר המתקן:		שם המתקן:		טופס 2.1.1

מידע כללי

תאור כללי של מתקן היצור:	ראה סקר תהליכים

תהליכי הייצור במתקן (ממויינים לפי נפחי ייצור)

שם התהליך	תוצרים	נפח ייצור* נפח	נפח ייצור* יחידת מידה	חודשי עבודה בשנה*	הערה
מערכת טיפול בגז - הפרדת נוזלים מהגז, יבוש ודחיסת גז	גז טבעי	1200	מיליון רגל מעוקב סטנדרטי ליום	12	שלב א - תכנית הפיתוח מיועדת לאפשר הפקה וטיפול בהיקף של 1,200 מיליון רגל מעוקב סטנדרטי ליום (כ- 1.4 מיליון מטרים מעוקבים בשעה). כמות הקונדנסט המופקת הינה נגזרת של מאפייני שדה לוויתן וכמות הגז המופקת.
	קונדנסאט	572	מ"ק ליום		
	גז טבעי	2100	מיליון רגל מעוקב סטנדרטי ליום	12	שלב ב - הרחבת ההפקה והוספת עוד כ- 900 מיליון רגל מעוקב סטנדרטי ליום (כ- 1.0 מיליון מטרים מעוקבים בשעה).
	קונדנסאט	1002	מ"ק ליום		

* במידה וקיימת שונות רבה בין השנים ניתן לציין טווח המייצג את 5 השנים האחרונות - המתקן מתוכנן ועל כן זוהי הערכה בלבד

הערות (יש לציין אילו תהליכים יכולים להתקיים במקביל):

גרסה 3

Figure 4: Condensate spillage size increase request by Noble Energy reference [9]

Hadera desalination plant, as well as the Atlit old Crusades Fort reservation, Ma'agan-Michael and Caesarea national parks coordinates are provided in *Figure 6*, *Figure 7*, *Figure 8*, and *Figure 9* , as provided by the Local Council of Zichron-Ya'akov.

Figure 5: Hadera desalination plant coordinates Google map (near by the electric station)

Figure 6: Hadera desalination plant near by the electric station

Figure 7: Atlit national park coordinates (32.699642, 34.931749 Google map)

Figure 8: Ma'agan Michael national park coordinates (32.539724, 34.902258 Google map)

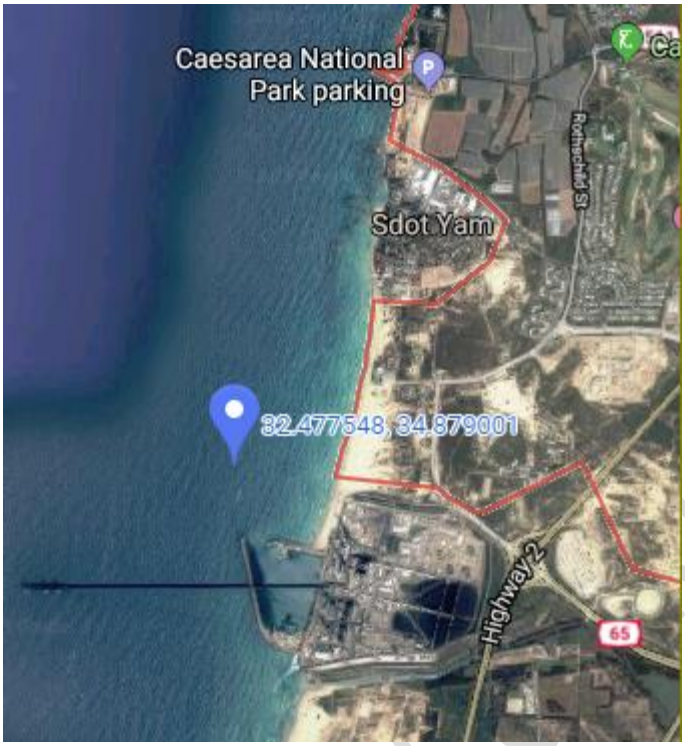

Figure 9: Caesarea national park coordinates (32.477548, 34.879001 Google map)

Desalination facility is located south to the Orot-Rabin Hadera Electrical Company power station. Pipe depth is 10meters below sea level and 5 meters above the sea bottom [17]. The intake of the pipe is 1250m from the shoreline estuary of the Hadera-River [4] coordinates shown at *Figure 5*. There are three intake pipes where each pipe outer diameter is 1.6m per Prof. Guy Ramon from Technion Israel Institute of Technology (IIT). The OMIS report[5] (Yaron Egozy) details 3 pipes with 1.8m diameter with 1.25km length and 15m depth submerging of intake, see *Figure 14* and *Figure 15*.

The production capacity of the H2ID desalination facility is 135milion cubic meters per year according to return ratio of $0.55m^3/0.45m^3$ which is the ratio of reverse osmosis of current desalination facilities technology. It results is suction of 165milion cubic meters per year[6] which is equal to capacity of $19{,}097m^3$/hour assuming 360 working days for a year at a constant rate. The intake map is provided by applicable document [17] figures 2.2 and 2.3 pages 10 and 11, please see here *Figure 10* and *Figure 11*. Coordinates, shown in *Figure 12* and *Figure 13*, are DD 32.465556, 34.870264.

[4] https://www.eib.org/attachments/pipeline/1755_nts_en.pdf
[5] http://gwri-ic.technion.ac.il/pdf/IDS/398.pdf
[6] 165=135 x 0.55/0.45

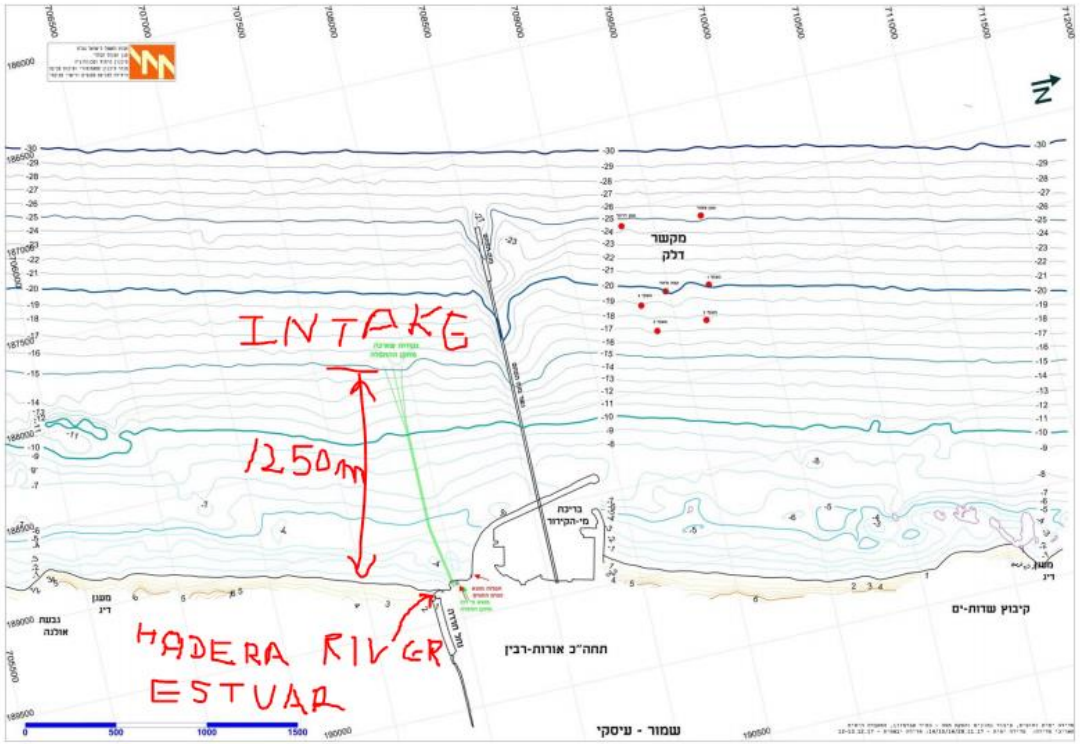

Figure 10: H2ID desalination intake location map [17] Figure 2.2 Bathymetric map

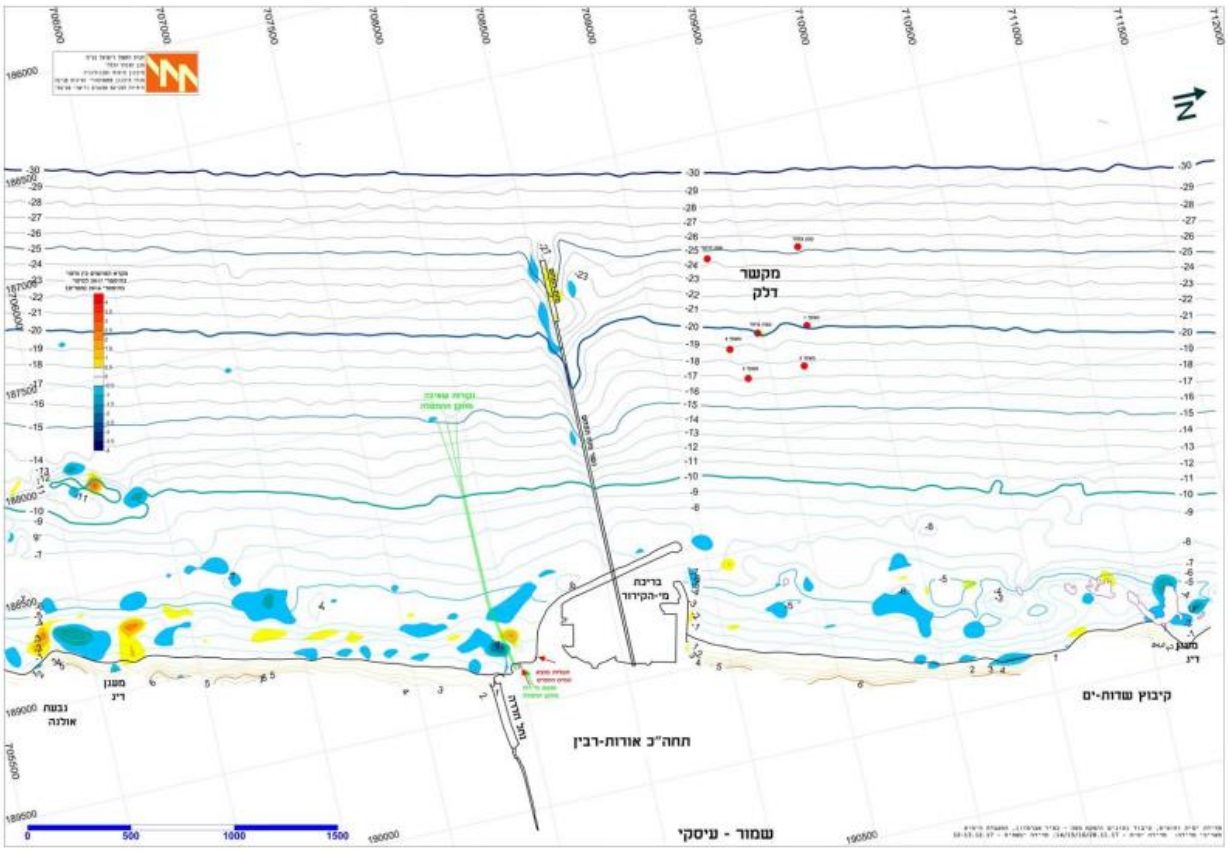

Figure 11: H2ID desalination intake location map [17] Figure 2.3 difference map Oct 2016

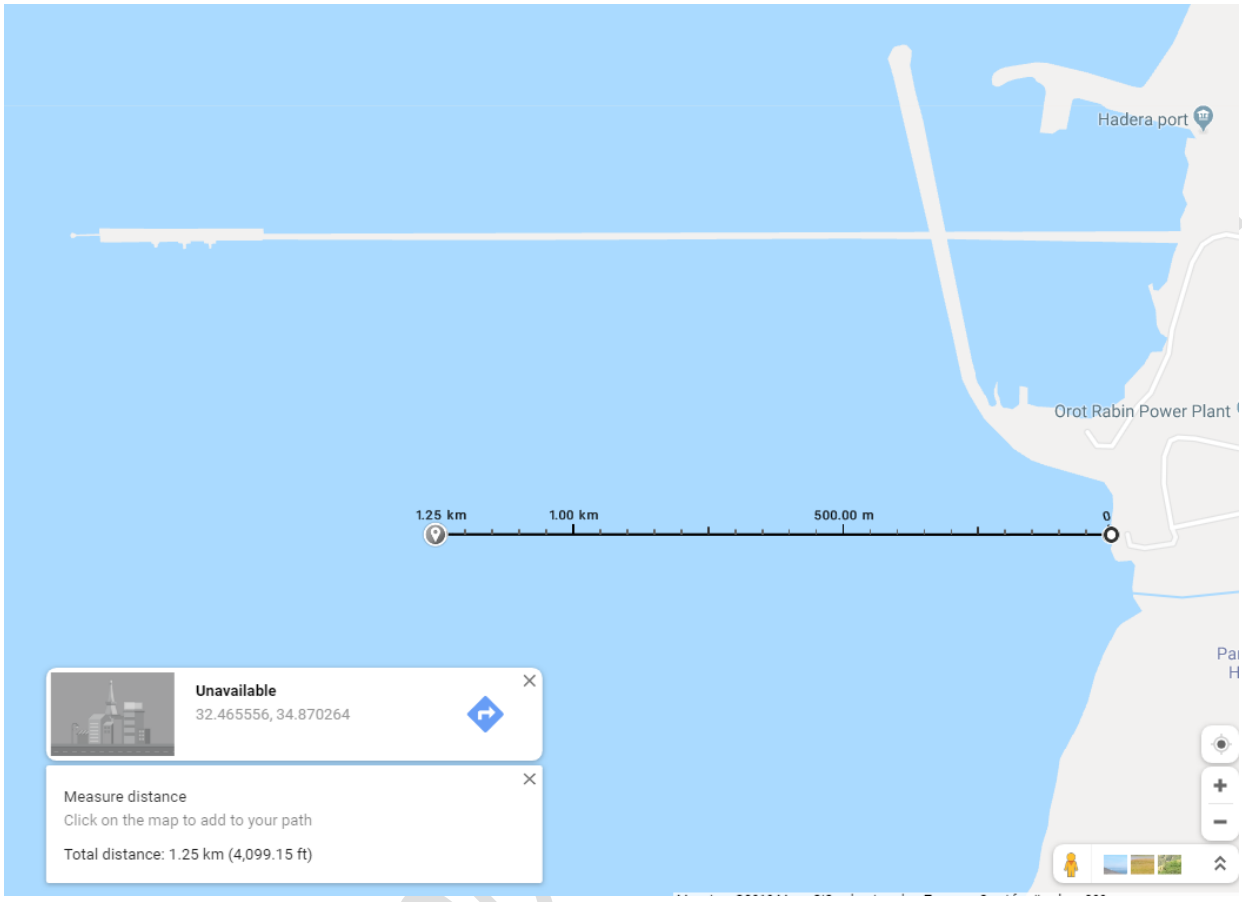

Figure 12: H2ID desalination intake coordinates DD 32.465556, 34.870264 Google Map

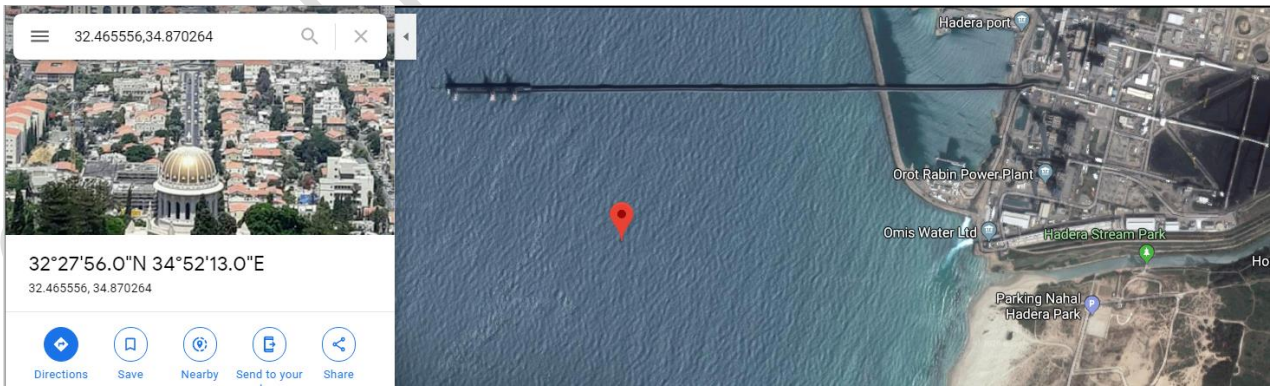

Figure 13: H2ID desalination intake coordinates DD 32.465556, 34.870264 Google Map

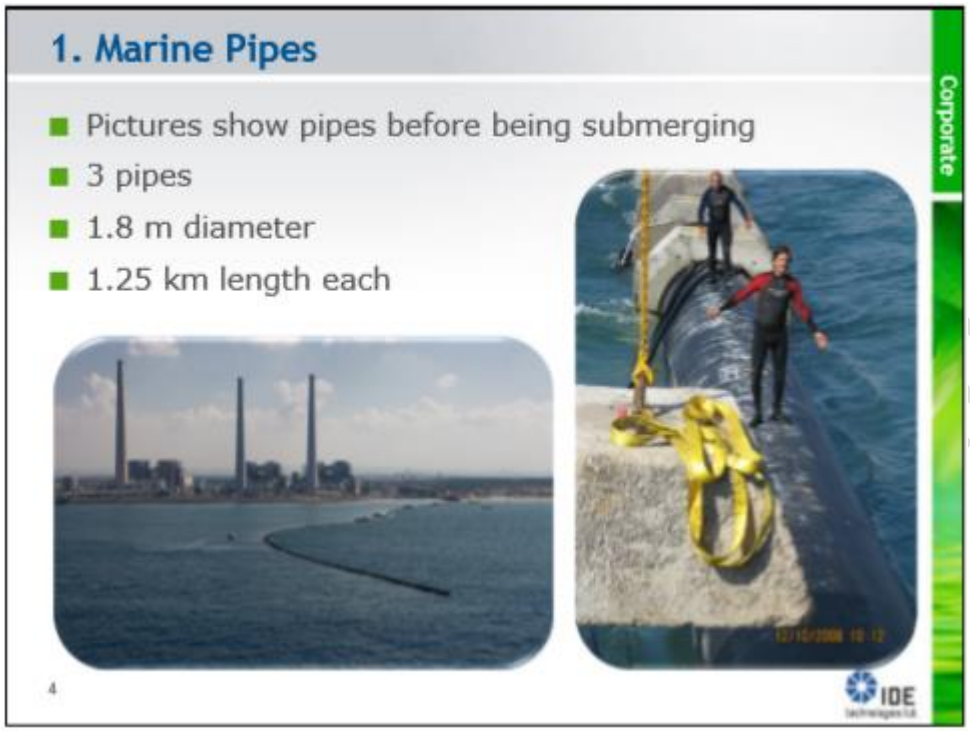

Figure 14: H2ID desalination intake pipes data (Yaron Egozy)

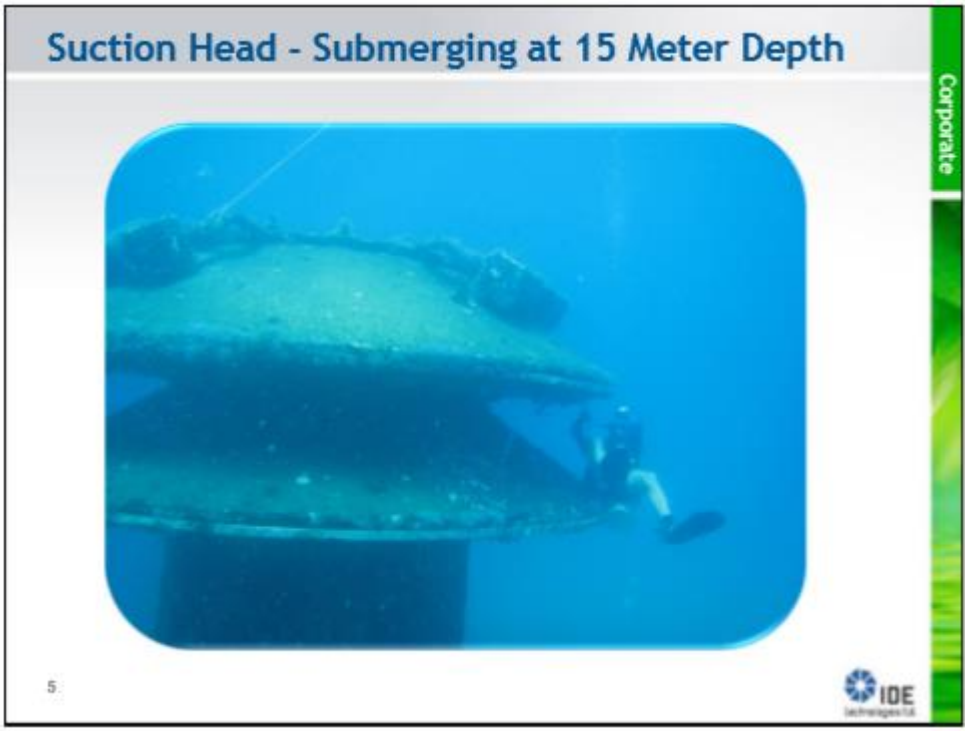

Figure 15: H2ID desalination intake head (Yaron Egozy)

4. General Sea Surface Circulation in the SE Levantine Basin and Offshore Israel

4.1. Introduction

The general circulation in the Eastern Mediterranean Levantine Basin as inferred in 60s and 70s (Ovchinnikov, et al., 1976) shows an anticlockwise flow with sub-basin features in the Levantine Basin, while in the 80s, during the POEM (Physical Oceanography of the Eastern Mediterranean) mesoscale field experiments (The POM Group, 1992) it was documented that in the Levantine Basin an offshore cross-basin jet, named as the Mid Mediterranean Jet-MMJ is generated as a result of the interaction between the mesoscale cyclonic (Rhodes gyre) and the anti-cyclonic (Mersa Matruch and Shikmona gyres) flow features during the eastward spreading of the surface and subsurface waters of Atlantic origin, after passing the Cretan passage.

The use of satellite sea level anomaly (SLA) nowadays is documented to provide a true background of the sea surface circulation. This is the main reason that these remote sensing data are assimilated into the numerical models producing accurate enough operational sea surface flow forecasts in the Mediterranean Sea by the Copernicus marine service- CMEMS MFC Med. The use of a series of SLA patterns of the Mediterranean Sea has made possible the direct estimation of the general sea surface circulation (Pascual, Pujol, G, Le Traon, & Rio, 2005). This SLA-derived circulation has been used for simulating the pathways of passive tracers in the Mediterranean, where particles released in the Western Mediterranean spread after traversing the Cretan Passage, diverging from the south-western coast of the Levantine Basin, from where they crossed the Levantine Basin, more or less following a similar bath, as the one of the MMJ shown to cross the Levantine Basin during the POEM experiments in the 80s.

In-situ investigations in the SE Levantine Basin from 1995 to 2015 in the frame of CYBO, CYCLOPS, MSM/14 cruises and NEMED Argo floats deployments, made possible to give strong evidences about the seasonal and inter-annual fluctuation of the MMJ, the Cyprus warm eddy variability, the Shikmona eddy generation and the periodical re-establishment of the Shikmona gyre (Zodiatis, Drakopoulos, Brenner, & Groom, 2005) , (Zodiatis, Hayes, Gertman, & Samuel-Rhodes, 2010), (Zodiatis, Gertman, Poulain, & Menna, 2015), (Menna, Poulain, Zodiatis, & Gertman, 2012).

In addition, numerical datasets from CYCOFOS and SELIPS forecasting systems, both downscaled from the CMEMS MFC Med, reveal that the dominant flow features in the SE Levantine are: the Cyprus warm core eddy, the Shikmona eddy, which is generated during periods when the Cyprus eddy becomes weaker and or shifted westward or southward from Eratosthenes seamount, and when the strong northward current flowing along the Israel-Lebanese coast becomes unstable. The latter is evidently also from drifters trajectories, deployed during the PERSEUS project

(Menna, Poulain, Zodiatis, & Gertman, 2012) , (Zodiatis, Gertman, Poulain, Menna, & Sofianos, 2016). The drifters trajectories shown an anticyclonic eddy to be detached from the prevailed northward current along the Israel coast. .

The in-situ and numerical data sets obtained in the SE Levantine from 1995-2015, provides a detailed picture of the general circulation in the Se Levantine Please see *Figure 16*, where: a) the Cyprus and Shikmona eddies, as well as the MMJ are the dominant flow features; b) the Cyprus warm eddy undertakes strong spatial and temporal variability; c) the variability of the displacement of the Cyprus warm eddy affects the MMJ and the eastward transfer of the AW; d) The Shikmona eddy found to be established for certain periods, when the Cyprus eddy shifts to the west, south-west; e) the MMJ flows along the northern periphery of the Cyprus eddy and is the major current transferring the AW in the area.

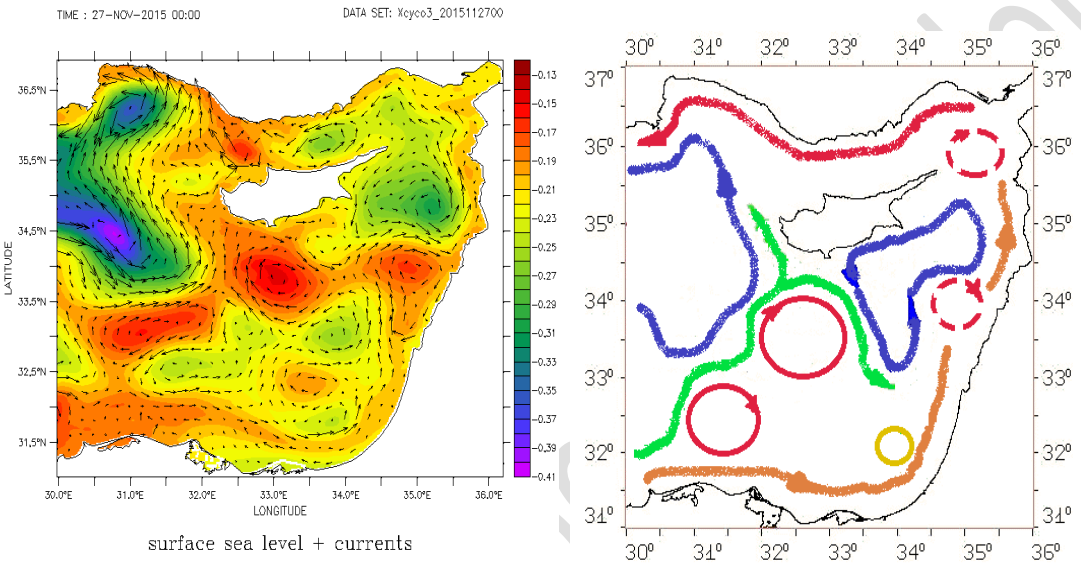

Figure 16 : surface sea currents from CYCOFOS on the 27/11/2015 shown the main mesoscale features of the Levantine Basin, similarly as were documented from in-situ data, b) schematic circulation in the Levantine Basin based on long-term numerical models and in-situ data, the last two decades from 1995 to 2016 (Zodiatis, Gertman, Poulain, Menna, & Sofianos, 2016) .

4.2. General circulation offshore Israel (2015-2018)

The sea currents used for the oil spill modelling applications in the framework of the *"Dor Leviathan Offshore Platform Environmental Report Review"* are: a) the hourly CMEMS MFC Med data, with a horizontal resolution of 1/16 degree (~6.5 km), forced with the 6-hourly ECMWF at a horizontal resolution of 0.125 degree (~12.5 km) and b) those of the CYCOFOS downscaled forecasts with a resolution of 1.8 km, forced with the hourly SKIRON at a resolution of 10 km.

For the needs of the current report the maps of the mean monthly averaged sea surface currents were reproduced for the period 2015-2018, in order to show the main flow patterns dominated at the offshore and coastal sea areas along the Israel coastline (*Figure 17* to *Figure 22*).

The general flow patterns indicate the northward current to flow along the coastline of Israel with mean monthly averaged currents between 10-20 cm/s. The monthly mean averaged sea surface current variability indicates that during February and March the sea surface currents close to the Israel coast are quite weak, with mean averaged currents much less than 5 cm/s, while during the rest months the along the Israel coastline, the sea surface currents are very well pronounced with much higher velocities.

The Dor offshore fixed platform located at the eastern periphery of the strong northward current during the months April to December, while during the months February to March its location influenced by the along the coast zone of insignificant currents velocities.

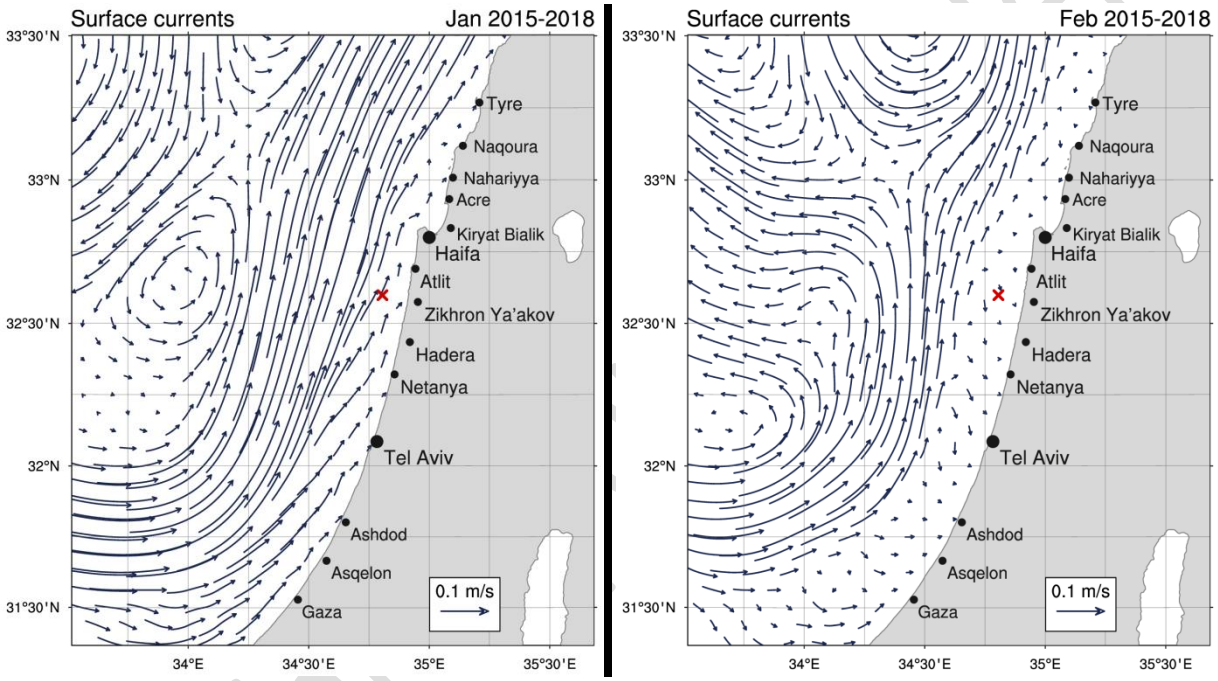

Figure 17: a) Mean averaged sea surface currents for January and b) for February, both based on the reanalysis products of the CMEMS MFC Med for the period 2015-2018. The red color "x" indicate the location of the Dor offshore fixed platform.

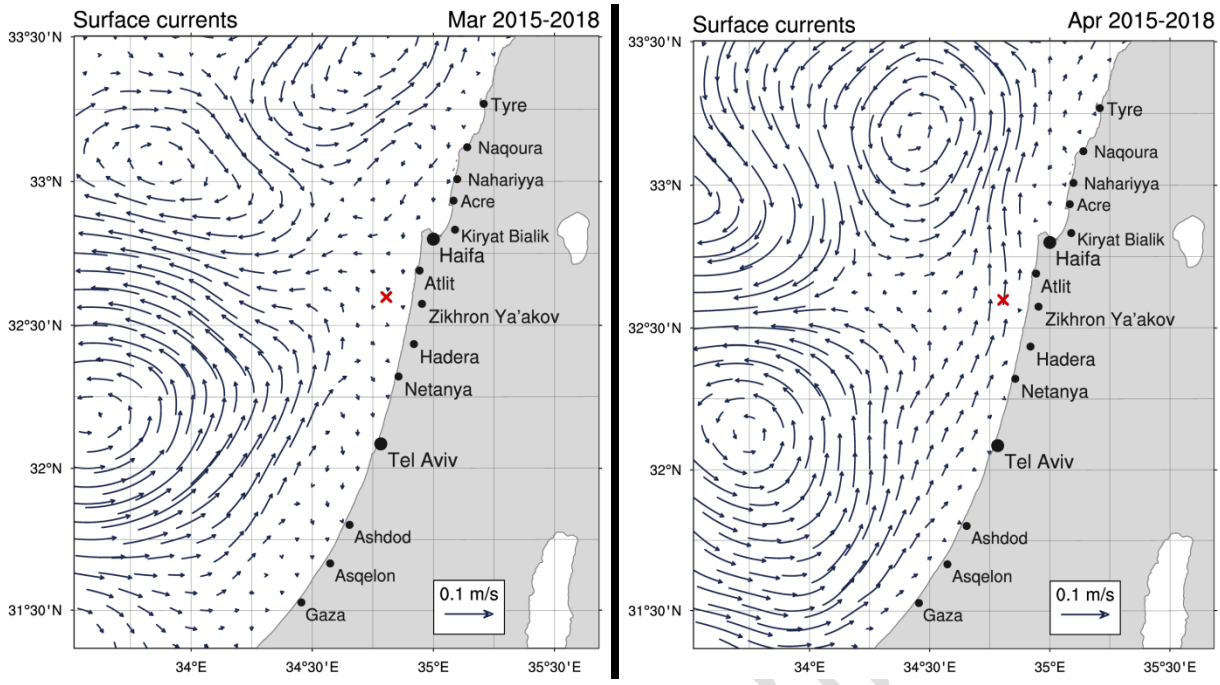

Figure 18: a) Mean averaged sea surface currents for March and b) for April, both based on the reanalysis products of the CMEMS MFC Med for the period 2015-2018. The red color "x" indicate the location of the Dor offshore fixed platform.

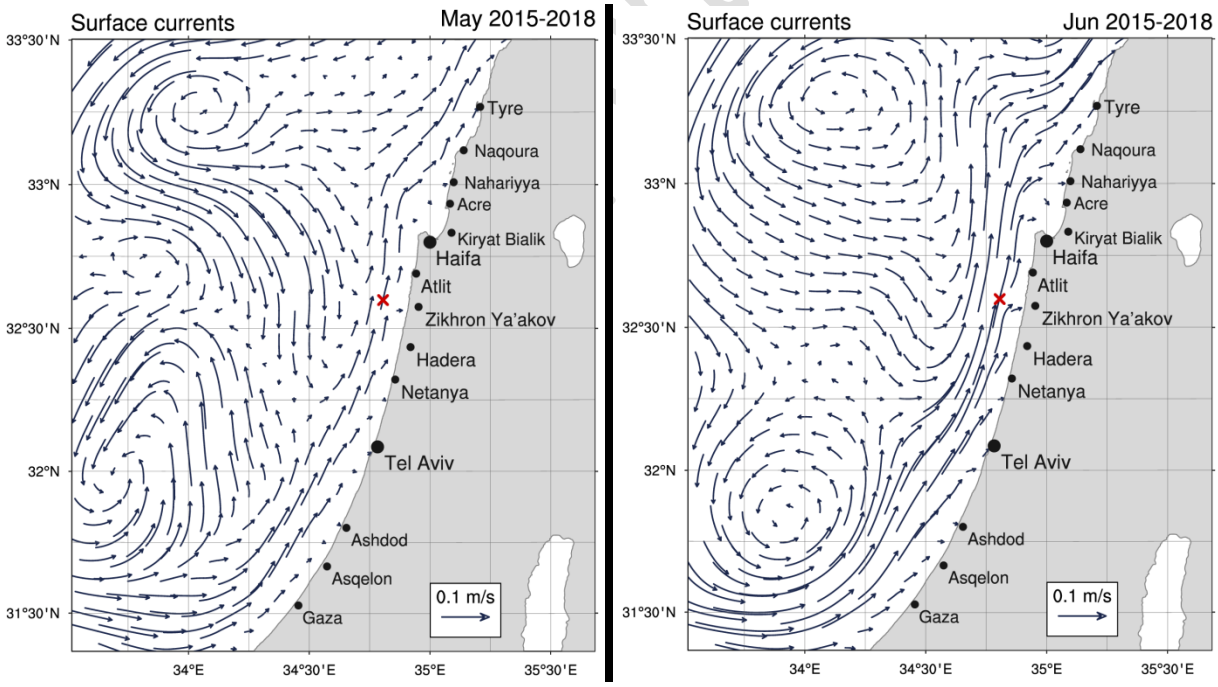

Figure 19: a) Mean averaged sea surface currents for May and b) for June, both based on the reanalysis products of the CMEMS MFC Med for the period 2015-2018. The red color "x" indicate the location of the Dor offshore fixed platform.

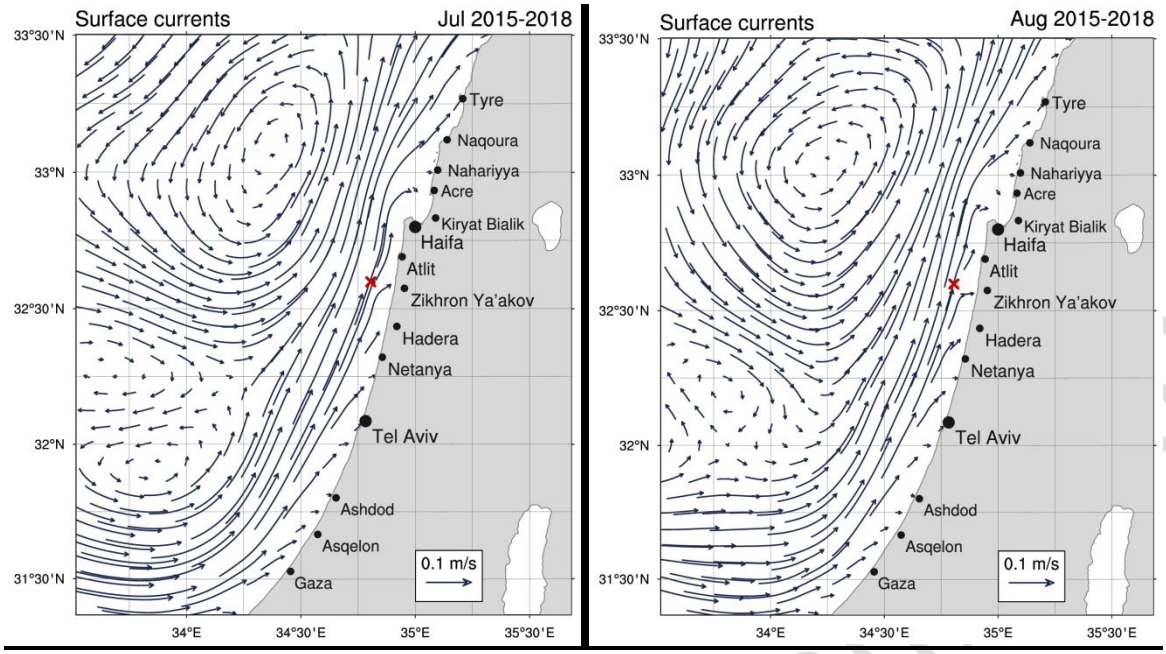

Figure 20: a) Mean averaged sea surface currents for July and b) for August, both based on the reanalysis products of the CMEMS MFC Med for the period 2015-2018. The red color "x" indicate the location of the Dor offshore fixed platform.

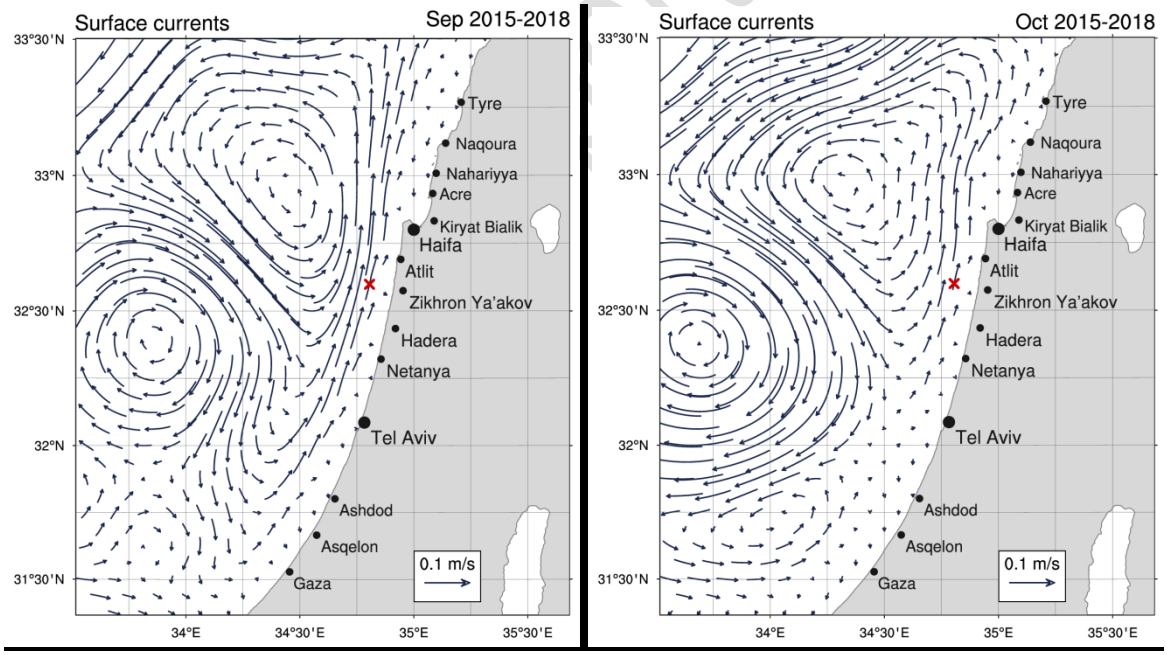

Figure 21: a) Mean averaged sea surface currents for September and b) for October, both based on the reanalysis products of the CMEMS MFC Med for the period 2015-2018. The red color "x" indicate the location of the Dor offshore fixed platform.

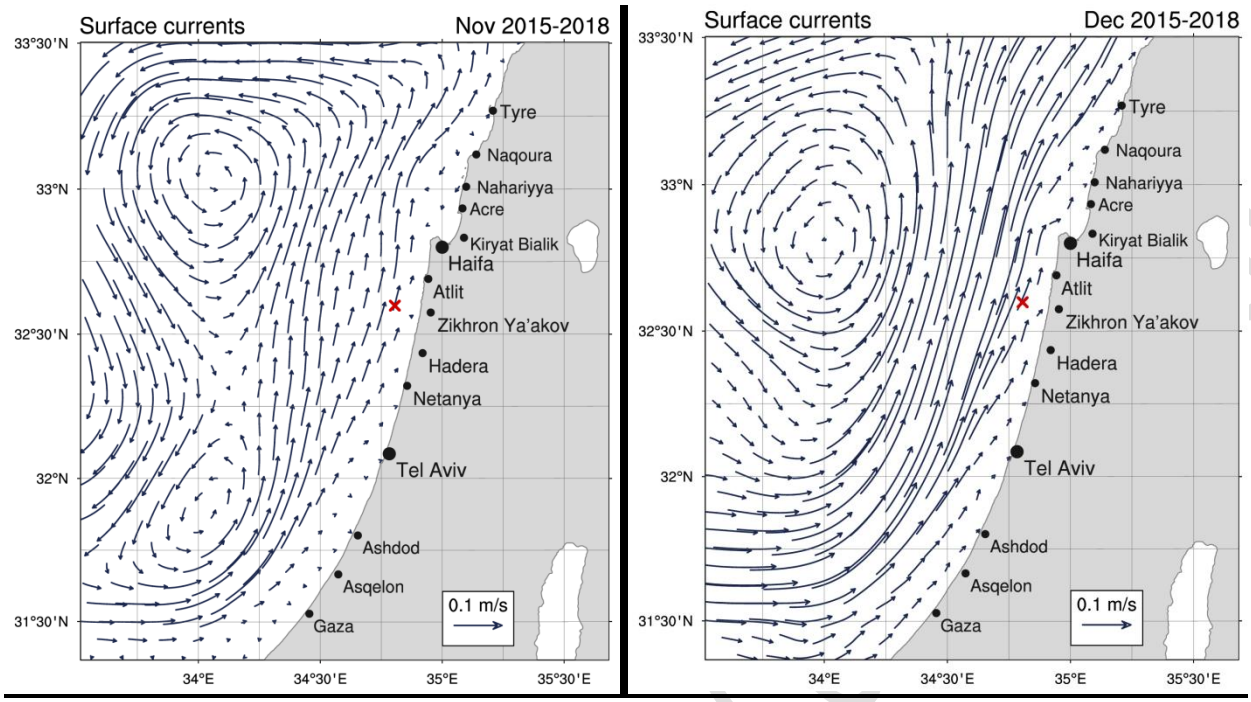

Figure 22: a) Mean averaged sea surface currents for November and b) for December, both based on the reanalysis products of the CMEMS MFC Med for the period 2015-2018. The red color "x" indicate the location of the Dor offshore fixed platform.

5. Pipe Rupture and Evaporation

5.1. Data

Pipe rupture coordinates are provided in applicable document [14] memorandum from Local Council Zichron-Ya'akov dated 4/June/2019 entitled Coordinates Location of DOR offshore Pipe Rupture and per applicable document [2.3] page 306 Table 3-1 Marin discharge location (*Figure 27*). Coordinates of rupture location are **32.6*00743*, 34.9*05234*.** The rupture leakage of 3000bbls is based upon Local Council Zichron-Ya'akov SOW definitions [15] and clarification letters in applicable documents [7] [8] and [9] against 1200bbls Brenner [1.5] page 449, 1200bbls Genesis [1.3] page 274 Table 3-1 coordinates, page 275 Table 3-2 volume ,1200bbls Genesis [2.3] page 306 Table 3-1 and 1200bbls Brenner [2.4] page 346.

According to the TAMA 37-H plan [16] section 3.2 page 51 Eastern marine pipe corridor it is stated that the condensate pipe diameter is 8 inches and it refers to correction drawing 3.2.1-2 (*Figure 31*). In addition drawing 3.2-1 page 52 describes the area of burial of deployed pipe see *Figure 29*. Burial cross section is provided by [16] in Drawing 3.2-2 page 53 see *Figure 30*. Table 3.3.1-1 page 61 in [16] defines the condensate riser to onshore to be 8 inches (*Table 8*).

Drawing 3.2.1-4 page 60 in [16] describes in detail the HDD with respect to DOR shoreline. It can be seen that HDD is 800 meters from shoreline. Having this data and 12km distance the pipe volume can be estimated according to *Equation 1* resulting as ~2446bbls Table 3.4.6 [16] page 68 (see *Table 6* and translation *Table 7*). Hence 1200bbls in [2.3] and [2.4] is underestimation by half quantity.

Equation 1 $$\boldsymbol{V[m^3] = \frac{\Phi^2 \pi}{4}[m^2] \times L[m] = 0.25 \times (8 \times 0.0254)^2 \times 12{,}000 = 389[m^3]}$$

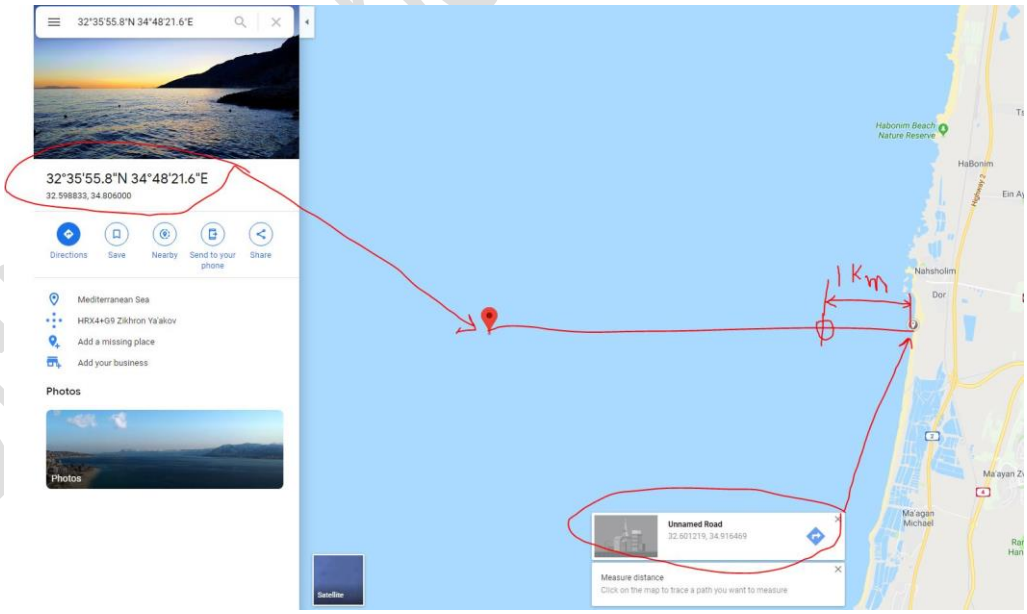

Figure 23: Valve location, rig location and measurement process [14]

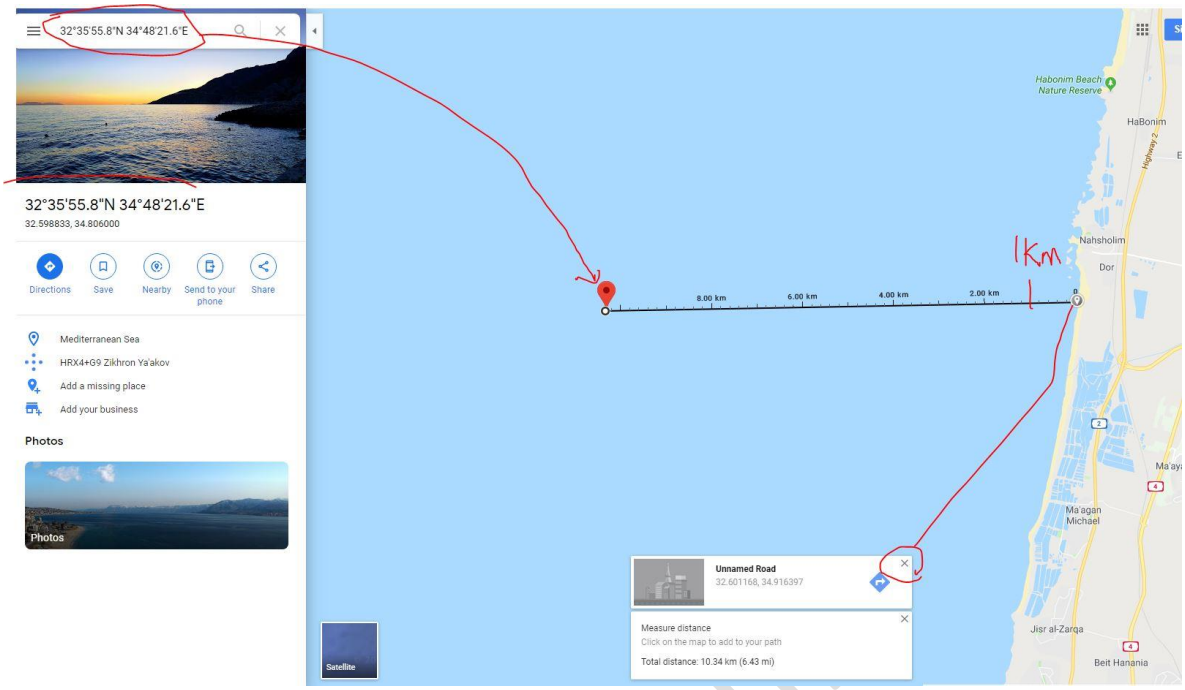

Figure 24: distance between valve-station to offshore place [14]

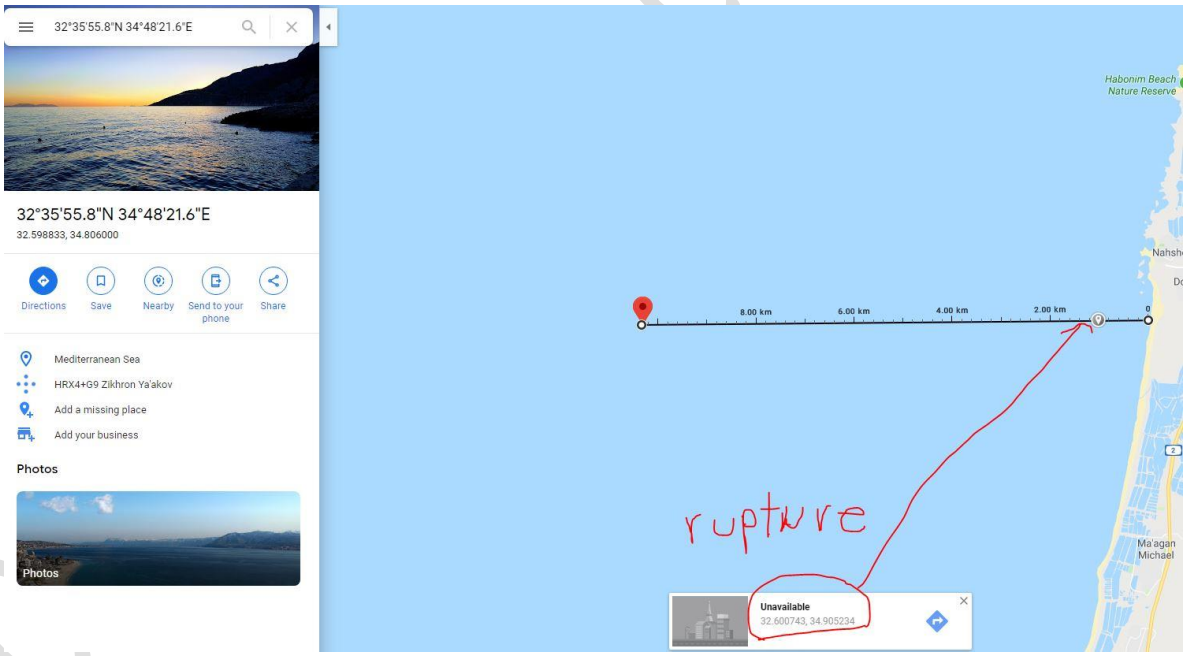

Figure 25: Sliding to 1km from shoreline and getting coordinates [14]

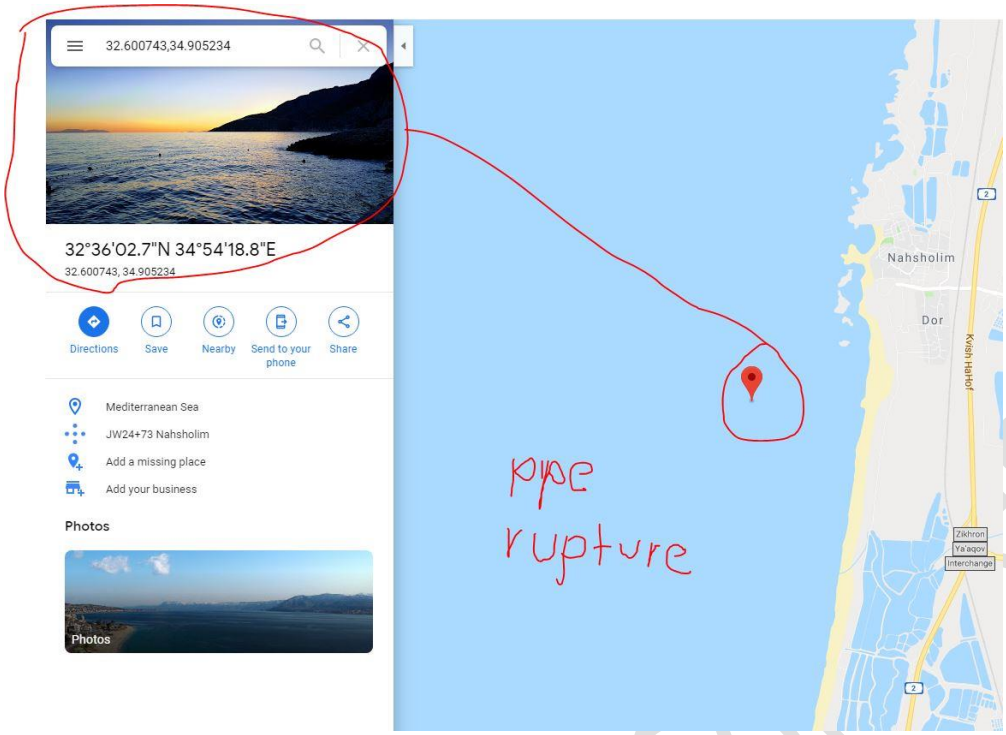

Figure 26: Rupture coordinates for simulation (32.3600743, 34.905234 Google map) [14]

Table 3-1 Marine Discharge Location

Scenario	Value	
Pipeline Condensate Release	Longitude	034° 51' 40.2" E
	Latitude	032° 36' 11.1" N
	Depth	1 m (Above Sea Bed)

Figure 27: Rupture coordinates for simulation Genesis OSCAR [2.3] page 306

Table 3-2: Discharge Volume

Scenario	Discharge Volume (m^3)	Discharge Rate (m^3/hr)
Pipeline Condensate Release	194	69.5

Figure 28: Rupture spill size for simulation Genesis OSCAR [2.3] page 306

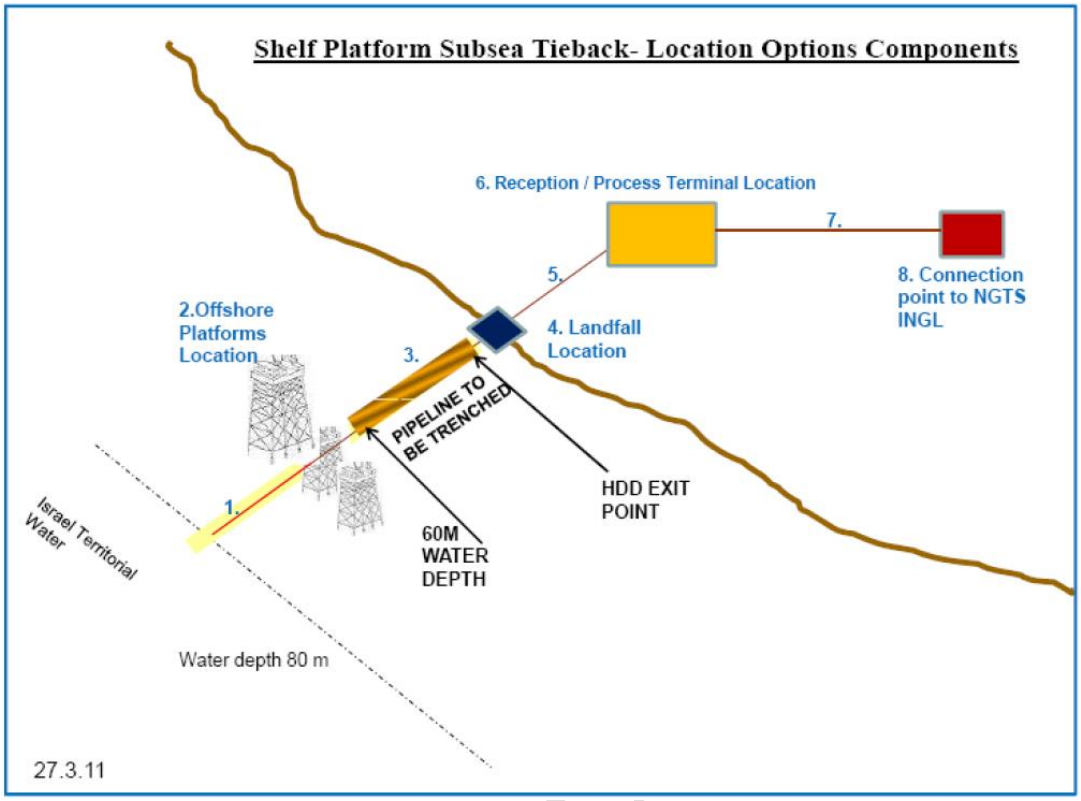

Figure 29: Pipeline deployment [16] page 52

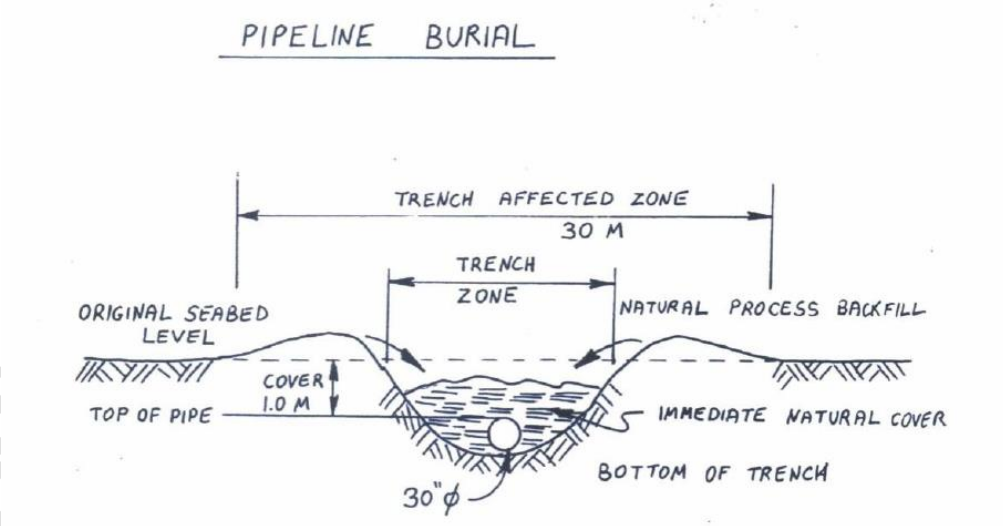

Figure 30: Pipeline burial in a trench [16] page 53

תשריט 3.2.1-2: חתך אופייני של מסדרון הצנרת הימית המזרחי

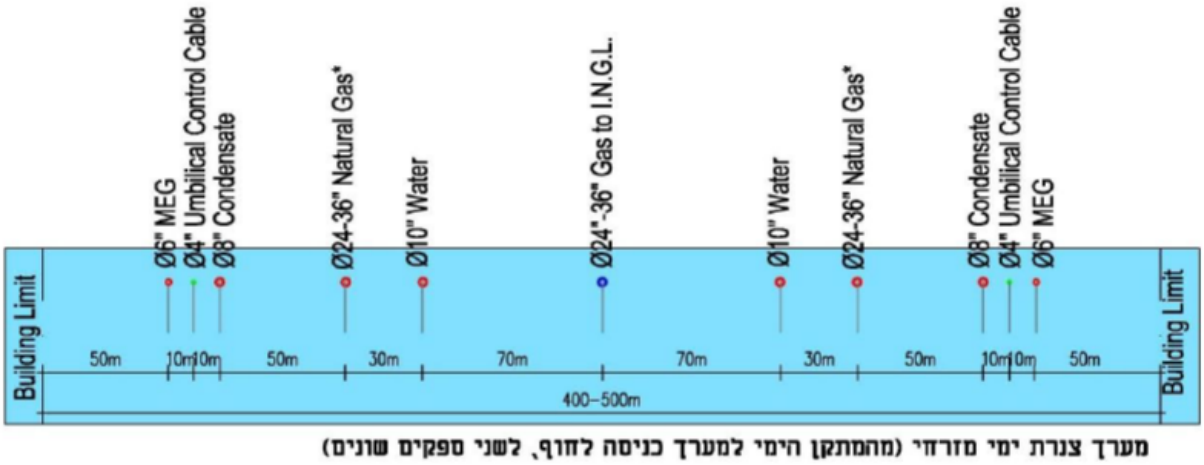

מערך צנרת ימי מזרחי (מהמתקן הימי למערך כניסה לחוף, לשני ספקים שונים)

Figure 31: Typical cross section of the eastern marine pipe corridor [16] page 59

Table 6: Composition and flow data [16] page 68

טבלה 3.4.6: נתוני הרכב וזרימה[4]

נפח כולל [מ"ק]	משטר זרימה בצינור	מספר קווים	קוטר [אינץ']	אורך הקו [ק"מ]	הרכב משוער	ספיקה [מ"ק/יום]	
389	מלא	1	8	12	Decanes, מעל 90% Heptanes,Hexanes Octanes &	2802-2159	Condensate פחמימנים מעובים
195	מלא	2	4	12	72% גליקול, 28% מים	437	MEG – גליקול מונו-אתיל

Table 7: Composition and flow data [16] page 68 (translation of *Table 6*)

Liquid	Capacity [M^3/Day]	Estimated Composition	Pipe line [Knm]	Dia [Inch]	Num of Pipes	Pipe Flow Regime	Tot Vol. [M^3]
Condensate	2802-2159	Over 90% Decanes, Heptanes, Hexanes & Octanes	12	8	1	Full	389
MEG Monoethylene Glycol	437	72% Glycol 28% Water	12	4	2	Full	195

Table 8: Main design guidelines of the sea installation [16] page 61 Table 3.3.1-1

טבלה 3.3.1-1: עקרונות התכנון המרכזיים של מתקן הטיפול הימי

Item	Value
Manning	Manned – up to 35 personnel (no allowance made for security personnel).
Helideck	Assumed to be required for crew transfer and rescue
Incoming Risers	3 x 16" pipeline risers 1 x 6" MEG transfer riser (for possible MEG reclamation)
Outgoing Risers	1 x 36" gas pipeline Riser 1 x 8" condensate riser to onshore 1x 8" condensate riser to storage vessel 1 x 6" MEG transfer riser (for possible MEG reclamation) 3 x MEG lines to the wellheads 3 x umbilical J-tube risers
HP: LP interface	At the incoming riser ESVs on the RP
J-Tube Risers	Required for umbilicals (detail not required for indicative design)
Wellhead Control	MCS and HPU included with control from the onshore DCS.
Water Depth	80 m suitable for jacket sub-structure
Flare Radiation	1.9 kW/m^2 for Helideck - 6.3 kW/m^2 for personnel exposure: **limiting value** - 15.8 kW/m^2 for equipment exposure -

5.2. Spill spread comparison to Amphibio reports

Under this assumption the condensate spillage size is 3000 bbls against analysis provided by *LPP-ON-NEM-EHS-STY-0002* [1] of pipe rupture of 1220 bbls, as appears and simulated in annex 6.4, 6.9 [1.3,1.5] OSCAR by Genesis and MEDSLIK by Brenner. In the analysis provided by *LPP-ON-NEM-EHS-STY-0005*[2] annex 6.4 [2.3] and annex 6.5 [2.4] maintain low spillage during operation. Annex 6.2 [2.1] and 6.3 [2.2] provide diesel oil spill of 2000bbls.

The recent permit [9] request of Noble Energy asks for 6300bbls at the second phase of operation, however since there is no official approval from the State of Israel for that request, the current condensate spillage size remains for 5300bbls.

5.3. Introduction

Desalinated water is part of the domestic demands in most Mediterranean countries while this in the major and only sources in the Arabian Gulf. Oil spill accidents in the Arabian Gulf have resulted in a shutdown of several coastal desalination plants in the United Arab Emirates (W. El-Sayed Elshorbagy, A. Awad Elhakeem, 2012).

The basic desalination methods used are the Multistage Flash Distillation (MSF) and the Reverse Osmosis (RO).

The RO process is much like a modern campers water purifier executed on a much longer scale. Saline water is passed through a membrane which separates it from the salts and other foreign matter. RO requires no heating, however it does requires energy for pressurizing the feed water (O.K. Buros, 2000).

The MSF is based in the theory and methods used to desalinate water for thousands of many cooperation chamber arrange in series each with successively lower pressures and temperatures that cause sudden (flash) evaporation of hot water brine followed by condensation of tubes in the upper portion of oil chamber (O.K. Buros, 2000) .

5.4. Threat of oil spills to the desalination plants

Oil spill is a threat to desalination plants for two main reasons. Oils contain pollutions basically Hydrocarbons not normally found in sea water that the desalination plants (processes) do not normally have to remove. Aromatic Hydrocarbons is a real threat to human health, for instance, benzene is considered as human carcinogenic in concentration which exceed 5 part per billion (ppb) in potable water (J. W. Doerffer, 1992).

Second and perhaps the most obvious reason oil threatens desalination plants is the damage it can do to sea water intakes filters , heat exchanges for MSF and the membranes of the RO plants. Oil in seawater can take the form of the well-recognized slick, but it can also form tar balls and “sunken oil glops” that can be drawn into intakes filters (J. W. Doerffer, 1992).

Obviously the oil can then foul the filters limiting the amount of water intakes, as well as full internal membranes disturbing the reverse osmosis process, if oil effecting a reverse osmosis facility.

A study related to potential problems associated with the desalination performance of reverse osmosis (RO) unit in conditions, when feed may be contaminated with crude oil and fuel oil spillages was carried out (T. Hodgkiess, W. T. Hanbury , G.B. Law, T.Y. Al-Ghasham, 2001) .The results demonstrated serious degradation of desalination performance after exposure to

some, but not all of the contaminating fluids. The “pure” hydrocarbons and also when they are in emulsion form with water caused extreme serve reduction in RO membrane performance as opposed

to the situation when they are in solution in the aqueous phase (T. Hodgkiess, W. T. Hanbury , G.B. Law, T.Y. Al-Ghasham, 2001).

5.5. Hadera desalination plant data implementation

The Hadera desalination is located west of Hadera town, north of the Hadera stream in north central Israel. It is of a Reverse Osmosis technology with capacity of 525,000m^3/day (Abraham Tenne (Head of Desalination Division Chairman of the WDA), 2010).

The sea water is fed in the plant via a pipe from 1,250 meters long from a sea water depth of 15 meters. Intake with three pipe ports are five meters above the sea floor and ten meters from the sea surface. *Figure 5* shows the exact side of the plant, while *Figure 10* depicts the exact site of the Hadera desalination along with the intake pipe superimposed with the bathymetric map of the area *Figure 11* (Applicable doc. [17] Fig.2.3 p19).

The maps in *Figure 12* and *Figure 13* show the exact intake point of Hadera desalination while pipe rapture is depicted in *Figure 25*, *Figure 26*, *Figure 27* and *Figure 28*. Further information is elaborated in section *5.1Data*.

5.5.1. Basic principles

In order to access the impact of condensate and diesel oil spills on the destination plant the key factors to be considered are the characteristics and behaviors of oil and their fate to the environment on one hand, and the type of intake and its distance from the shore, the depth of pumping site and of course the outcomes of the oil spill simulations.

5.5.2. Criteria for evaluation of impacts

1. As the impact of the desalination plant will be through the water intake, the amount of the beached condensate at the area of desalination plant will be considered only if it goes back to sea at the site of water intake
2. The concentrations of the condensate, which is dispersed and dissolve in the water after the oil spill accident is critical.
3. The concentrations of the dispersed and dissolved condensate at the side of intake.

5.6. Spill Simulation

5.6.1. Method

In order to provide the spatial and temporal distribution of the **dispersed condensate** from the pipe rupture, the results obtained from the MEDLIK current oil spill simulations described in App. Doc [13] sections 8.5.1 pp. 142 and 8.5.2 pp. 143 and were used herein.

Overall **104 MEDSLIK current simulations were produced** during the period 2015-2018 for the condensate pipe rupture located 1 km from the Israel shore, including the results on the dispersed condensate. The same ENI's simulation methodology implemented for 10 planned offshore platforms in the EEZ of Cyprus (Alves M. T., et al., 2015) was applied for the current pipe rupture, i.e., each simulation initiated every 15 days for 20 days ahead **during the entire examined period 2015-2018**, using the SKIRON winds, the CYCOFOS sea currents and the CYCOFOS wave data for the above period.

In contrary, OSCAR and MEDSLIK Brenner oil spill simulations for the condensate pipe rupture **were limited only to 12** each, for 4 small time windows covering partially the examined period 2007-2011.

While OSCAR results provide only the peak value of the water column concentration of the condensate for each of the examined period in the entire OSCAR model domain, Brenner does not provide any particular information on the dispersed condensate, expect the fate parameters plots for each of the examined period in the entire model domain. Therefore, the examination of the OSCAR and Brenner results on the possible impact of the dispersed condensate at the intake of the Hadera desalination plan, is indirectly evaluated based on the OSCAR sea surface maps of the condensate concentration from the pipe rupture.

Similarly, as it was mentioned in App. Doc [13], the major source of the dispersed condensate differences between the current and the previous simulations, is the very limited number of simulations, **12 in total**, carried out by OSCAR and MEDSLIK by Brenner for 4 small time windows, not covering the entire period under examination, compared to the **104 of the current simulations covered the entire examined period**. Moreover, a secondary significant source of differences of the results between OSCAR against the currents simulations and those obtained by Brenner is the use of a much lighter type of condensate in OSCAR simulations, resulted in higher evaporation, and hence less dispersed condensate into the water column.

5.6.2. Results from the application of different oil spill models

5.6.2.1. Oscar model (condensate) from pipe rupture (2016)

Scenarios of spill from the Leviathan offshore platform are described in App. Doc. [1.3] section 5.0 - Results pp. 278-279 (pipe rupture summary) and charts are as in App. Doc [1.4]. The below listed summarizes the repot of Genesis using OSCAR simulation tool. Results are for pipe rupture spill size of 1200bbls 0.8Km from shoreline as detailed in section *5.1 Data* (Please note that actual rupture spill size is larger). The OSCAR/Genesis results does not provide any maps with the dispersed condensate from the pipe rupture, except the peak value of the water column concentration of the condensate for each of the examined period in the entire OSCAR model domain. Therefore, the examination of the OSCAR results on the possible impact of the dispersed condensate at the intake of the Hadera desalination plan, is indirectly evaluated based on the OSCAR sea surface maps of the condensate concentration from the pipe rupture.

1. Extreme winter storm Period (17 Dec.2010 to 31 Dec.2010)

No impact on the Hadera desalination plant, as the condensate plume experienced some dispersion at sea before being driven quickly towards the shore. Large quantities of condensate stranded on the beaches between Atlit and Kfar-Galim. Very negligible amounts were seen at Shikmona. (see App. Doc. [1.4] pp.300-301) The maximum peak water column concentration of the condensate for this period was 161 ppm; 165 mg/L in the entire OSCAR model domain.

2. Typical winter conditions (11 Feb.2008 to 25 Feb. 2018)

No impacts on the Hadera desalination plant, as the condensate dispersed to a small degree before reaching the beach. Medium to low level of condensate stranded over a wide area between Dor and Atlit. Negligible amount of stranded condensate were seen around Shikmona. (see App. Doc. [1.4] pp.308-309) The maximum peak water column concentration of the condensate for this period was 420 ppm; 431 mg/L in the entire OSCAR model domain.

3. Typical summer conditions (17 July 2008 to 31 July 2008)

No impact on Hadera desalination plant, as the calm conditions resulted in small amount of dispersion of the plume before it beached heavily along the shoreline from Dor to Atlit. (see App. Doc. [1.4] pp.310-311) The maximum peak water column concentration of the condensate for this period was 145 ppm; 149 mg/L in the entire OSCAR model domain.

4. Transition season (4 Oct. 2007 to 18 Oct.2007)

No severe impact on the Hadera desalination Plant, as the calm conditions resulted a heavily beached of condensate along the shoreline, impacted mainly the Dor area, with smaller quantities of condensate in the north and South of Dor area.

The Hadera desalination plant found to be *slightly impacted* with small quantities in the south of the Dor and with very high peak water column concentration: 375ppm, 386 mg/L in the entire OSCAR model domain (see App. Doc. [1.4] pp.318-319).

5.6.2.2. Oscar model (condensate) pipe rupture (2017)

OSCAR model setup and results are provided in App Doc [2.3] pp.301-325. Spill size is underestimated and used 1200bbls vs. 3000bbls in this report. The data in section *5.1 Data* herein elaborates the differences. The OSCAR pipe rupture results are listed in page 310 in App Doc [2.3]

Table 9: Pipe rupture results OSCAR [2.3]

Table 5-1: Summary of Condensate Fate and Coastal Stranding

Simulation period		Evaporation percentage		Peak concentration		Time of first stranding	Peak stranded mass		Most affected location	Affected coastline length
		24 hours	14 days	ppm	mg/L	hours	tonnes	%		km
Extreme Winter storm	09 Dec – 23 Dec 2010	65	76	161	165	45	0.5	0.4	Acre	2.5
	17 Dec – 31 Dec 2010	57	65	82	84	17	16	12	Atlit	8
	25 Dec 2010 – 8 Jan 2011	66	76	157	161	n/a	n/a	n/a	n/a	n/a
Typical Winter	26 Jan – 9 Feb 2008	64	75	106	109	41	10	7.8	Atlit	6
	3 Feb – 17 Feb 2008	66	69	420	431	n/a	n/a	n/a	n/a	n/a
	11 Feb – 25 Feb 2008	63	74	188	193	20	33	25	Atlit Dor	8 2
Typical Summer	17 Jul – 31 Jul 2008	63	75	145	149	25	51	38	Dor Atlit	9
	25 Jul – 8 Aug 2008	62	75	122	125	17	49	36	Dor	13
	2 Aug – 16 Aug 2008	62	76	112	115	30	55	41	Atlit	15
Transition Season	26 Sep – 10 Oct 2007	62	69	153	157	30	18	13	Mikhmoret	8
	4 Oct – 18 Oct 2007	63	76	114	117	23	50	37	Dor	5
	11 Oct – 25 Oct 2007	64	75	376	386	32	48	36	Sdot Yam	11

5.6.2.3. MEDSLIK by Steve Brenner

Scenarios of spill from the Leviathan offshore platform are described in Brenner Report using the MEDSLIK simulation tool, as described App. Doc. [1.5] section 7 pp. 498- 535 spill from pipe rupture. Results are for spill size of 1200bbls. Brenner report does not provide any particular information or maps on the dispersed condensate, expect the fate parameters plots for each of the examined period. The report does not provided any dedicated information regarding the location of the maximum dispersed condensate. Therefore, the examination of the Brenner results on the possible impact of the dispersed condensate at the intake of the Hadera desalination plan, is indirectly evaluated based on the sea surface maps of the condensate concentration from the pipe rupture.
Pipe rupture analysis simulation and results are described in App Doc [2.4] pp.329-385. It is a report from 2016 even though the overall report is dated from October 26th 2017. The simulations assumed a nearly instantaneous discharge of 1220 barrels for the pipeline rupture with API of 43.2, SG = 0.8099 (details provided by Noble Energy Mediterranean and Genesis, Ltd.). Thus a total of 12 simulations were conducted. See details herein in section *5.1 Data.*

1. Extreme winter storm Period (9 Dec.2010 to 9 Jan.2011)

No impact on Hadera desalination plant. The slick is slowly transported to the north, northwest from the offshore platform. The center of mass of the slick between 6 and 12 hours after the spillage moves very slowly, while between 12 and 24 hours after the spillage the slick spreads and moves north *(Figure 53, App. Doc.[1.5] p.59 DPF page 499).* The most affected regions at the end of this period are the Carmel beach and Atlit *(Table 3, App. Doc.[1.5] p 95 PDF page 535).*

2. Typical winter conditions Period (26 Jan.2008 to 26 Feb.2008)

No severe impact on the Hadera desalination plant for the period 26 Jan – 10 Feb 2008. The slick transported to the north *(Figure 62, App. Doc.[1.5] p 69* PDF page 509). The main impact is projected to occur along 7-8 km along the coast near Atlit (*Figure 63, Doc.[1.5] p 70* PDF page 510).

The Hadera desalination was ***slightly impacted*** during the period between 3 Feb. to 18 Feb.2008,as shown from the oil spreading at sea surface at 6, 12 and 24 hours after the spillage. The slick is quickly transported to the southwest and eastward (*Figure 65, App. Doc.[1.5] p72* PDF page 512). The pattern of the coastal deposition at the end of 15 days after the spillage is shown at Figure 66 (*App. Doc.[1.5]* p73 PDF page 513). The main impact is projected to occur along a 15 km long shoreline near Netanya, including the Hadera desalination Plant.

3. Typical summer conditions period (17 Jul. 2008 to17 Aug.2008)

No impact on the Hadera desalination plant during this period. Spreading of condensate at sea surface at 6, 12 and 24 hours after the spillage is shown at Figure 71 (*App. Doc.[1.5]* p78 PDF page 518). Most of the non-evaporated condensate is deposited over the next 10-12 hours. The length of the coastline potentially impacted is 42.1 km, and is located mostly from Atlit to Netanya with projected deposition being largest at Neve-Yam.

4. Transition period (25 Sep.2008 to 26 Oct.2008)

The Hadera desalination plant is ***medium impacted***. Figure 80 (*App. Doc. [1.5]* p87 PDF page 527) shows spreading of the surface at 6 hrs, 12 hrs and 24hrs after the spillage. During this period the slick is transported southward until intersecting with the coast, just north of Hadera. The pattern of the coastal deposition at the end of the 10th day from the spillage is shown in the Figure 81(*App. Doc. [1.5] p88 PDF page 528*). The most adverse impact is projected along a 2.3 km coastline near Givat-Olga, where the maximum concentration of condensate is 260.3 bbl/km. Although in most of this zone the concentration was less than 100 bbls/km.

5.6.3. MEDSLIK current Simulations

1. <u>Extreme winter storm period December -January 2015-2018</u>

No actual impact from the dispersed condensate from the spillage on the Hadera desalination plant, except after the 7th day amounts between 5-100 bbls/km2 of dispersed condensate affecting the broader area of Zichron Ya'akov. On the second day (*Figure 32* a) the condensate reaches the shore at the area between Zichron-Ya'akov and Atlit. On day third (*Figure 32* b) the condensate spreads further North and less quantity to South and only on the 7th day (*Figure 33* a) most on the condensate moves further North, with very minor quantity at the Hadera desalination plant, without significant impact. On the day 10th (*Figure 33* b) the quantities at Hadera plant are negligible. On the day 20th there are small minor patches near the Hadera desalination plant with no impact on it (*Figure 34*).The same picture as above appearance for December 201-2018.

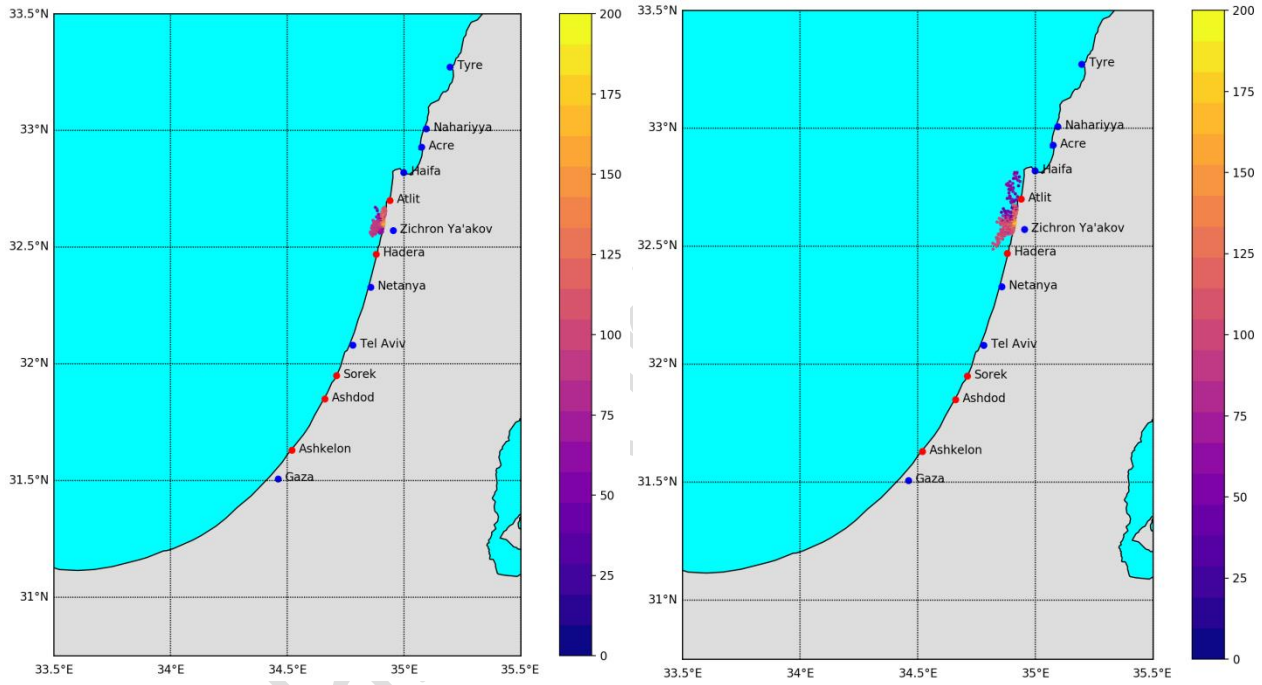

Figure 32: Mean averaged concentration of the dispersed condensate (bbls/km^2)

Figure 32 a (left): Mean averaged concentration of the dispersed condensate (bbls/km^2) from the pipe rupture on the 2nd day from the spillage, January 2015-2018.
Figure 32 b (right): Mean averaged concentration of the dispersed condensate (bbls/km^2) from the pipe rupture on the 3rd day from the spillage, January 2015-2018.

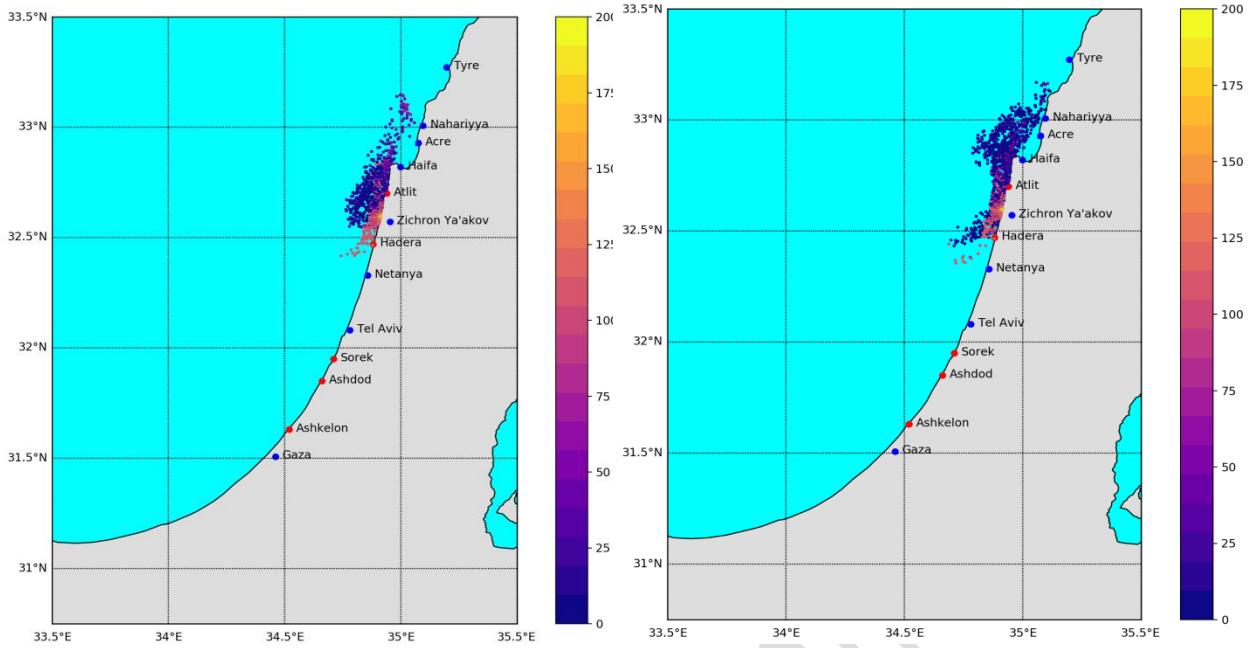

Figure 33: Mean averaged concentration of the dispersed condensate (bbls/km²)

Figure 33 a (left): Mean averaged concentration of the dispersed condensate (bbls/km^2) from the pipe rupture on the 7th day from the spillage, January 2015-2018.

Figure 33 b (right): Mean averaged concentration of the dispersed condensate (bbls/km^2) from the pipe rupture on the 10th day from the spillage, January 2015-2018.

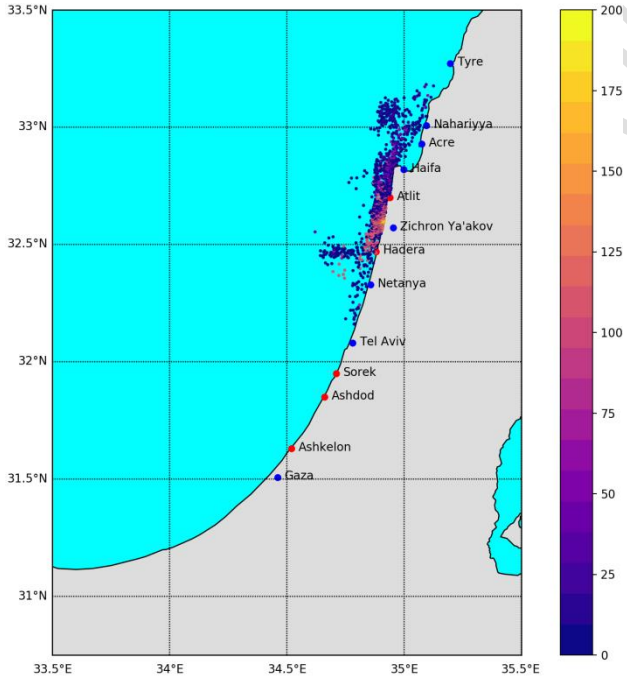

Figure 34: Mean averaged concentration of the dispersed condensate (bbls/km²)

Mean averaged concentration of the dispersed condensate (bbls/km^2) from the pipe rupture on the 20th day from the spillage, January 2015-2018.

2. Typical winter end January - February 2015-2018 (week 04)

No actual impact from the dispersed condensate from the spillage on the Hadera desalination plant, except after the 7 day from the spillage with small amount ~5 bbls/km2 of dispersed condensate. The dispersed condensate remains very close to the shore on day 1st (*Figure 35*a) and continue to remain on days 2nd (*Figure 35*b) and 3rdday (*Figure 36* a) between Zichron-Ya'aKov and Atlit. On day 7th (*Figure 36* b) small amounts of dispersed condensate moves to South with very small amounts ~5 bbls/km2 in the Hadera desalination plant, which is not considered to create significant impact on the Hadera desalination plant. On day 10th (*Figure 37*) slightly increased amount >5 bbls/km2 of dispersed condensate in the Hadera desalination plant intake might cause light impact on the Hadera desalination plant.

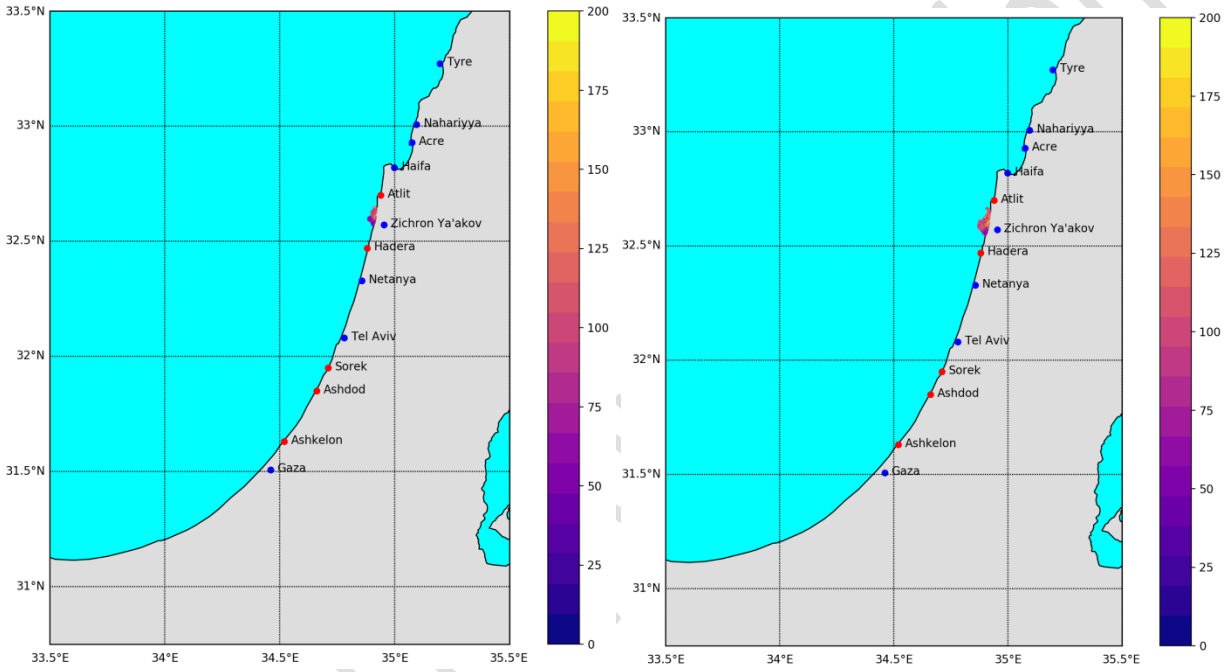

Figure 35: Mean averaged concentration of the dispersed condensate (bbls/km^2)

Figure 35 a (left): Mean averaged concentration of the dispersed condensate (bbls/km^2) from the pipe rupture on the 1st day from the spillage, end January - February 2015-2018.

Figure 35 b (right): Mean averaged concentration of the dispersed condensate (bbls/km^2) from the pipe rupture on the 2nd day from the spillage, end January- February 2015-2018.

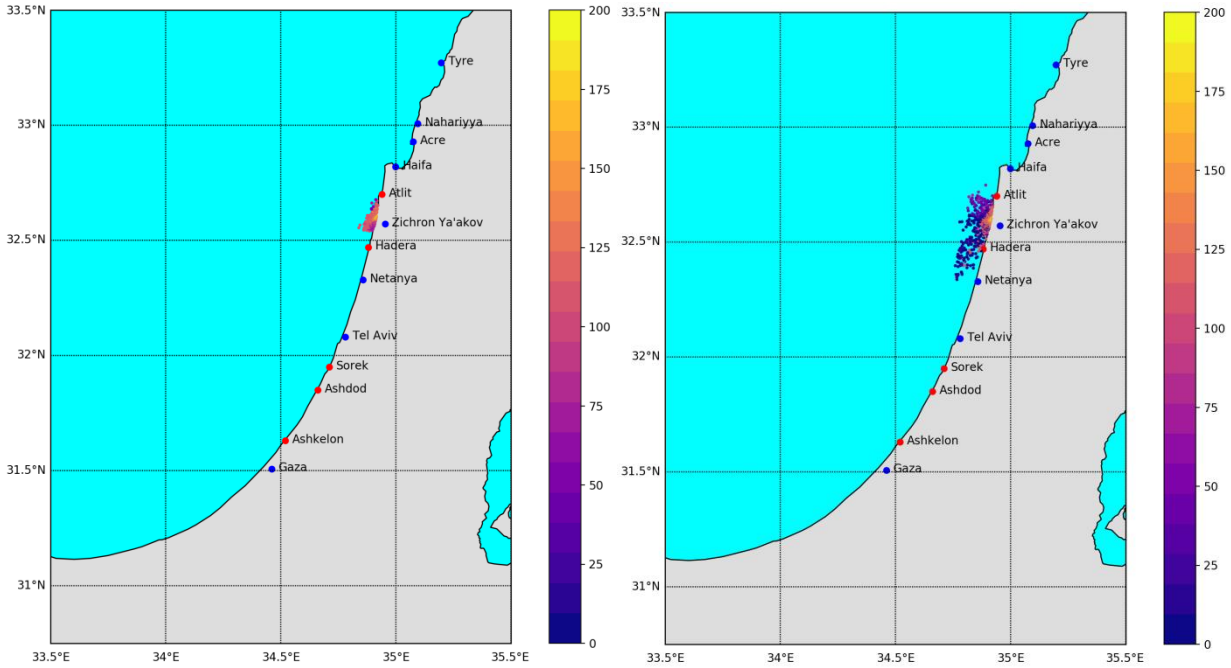

Figure 36: Mean averaged concentration of the dispersed condensate (bbls/km²)

Figure 36 a (left): Mean averaged concentration of the dispersed condensate (bbls/km^2) from the pipe rupture on the 3rd day from the spillage, end January - February 2015-2018.

Figure 36 b (right): Mean averaged concentration of the dispersed condensate (bbls/km^2) from the pipe rupture on the 7th day from the spillage, end January- February 2015-2018.

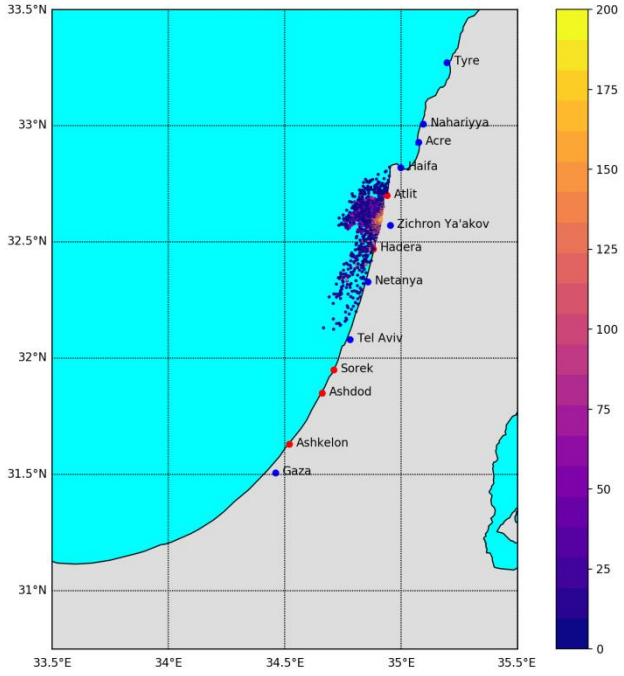

Figure 37: Mean averaged concentration of the dispersed condensate (bbls/km²)

Mean averaged concentration of the dispersed condensate (bbls/km^2) from the pipe rupture on the 10th day from the spillage, end January- February 2015-2018.

3. Typical Summer July –August 2015-2018 (week 28)

No impact from the dispersed condensate from the spillage on the Hadera desalination plant this period. The dispersed condensate remains very close to the shore the 1st day in the area between Zichron-Ya'akov and Atlit (*Figure 38*a). Continues to remain in the same near shore area during the 2nd, 3rd, 7th, 10th and 20th days (*Figure 38*b, *Figure 39*a, *Figure 39* b, *Figure 40* a, and *Figure 40* b). However, from the 3rd to the 20th day from the spillage the dispersed condensate is increased from 100 to 150 bbls/km2, away from the Hadera desalination plant. Similar patterns appears for August 2015-2018.

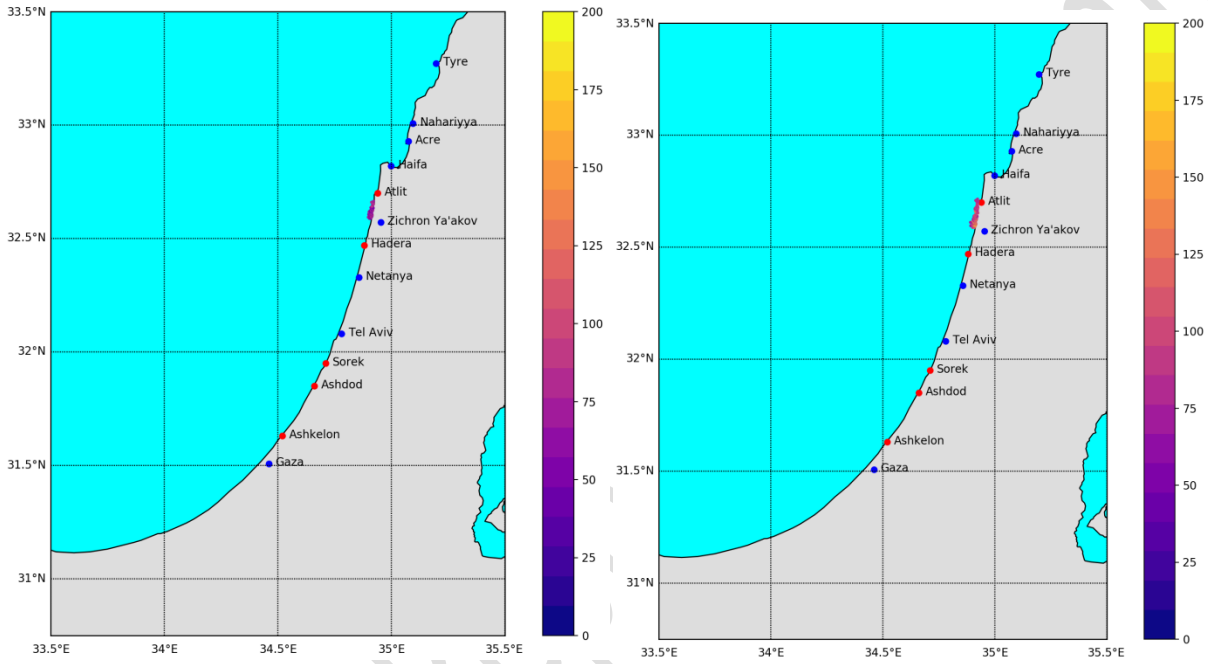

Figure 38: Mean averaged concentration of the dispersed condensate (bbls/km²)

Figure 38 a (left): Mean averaged concentration of the dispersed condensate (bbls/km²) from the pipe rupture on the 1st day from the spillage, July 2015-2018.

Figure 38 b (right): Mean averaged concentration of the dispersed condensate (bbls/km²) from the pipe rupture on the 2nd day from the spillage, July 2015-2018.

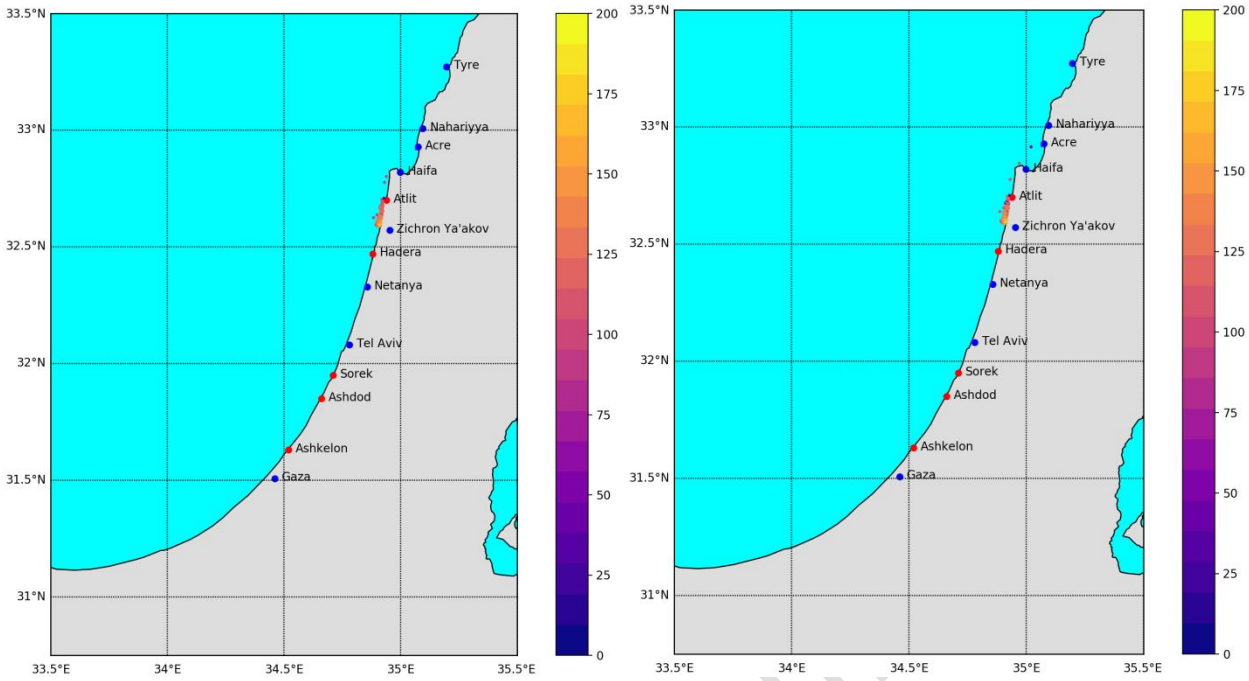

Figure 39: Mean averaged concentration of the dispersed condensate (bbls/km^2)

Figure 39 a(left): Mean averaged concentration of the dispersed condensate (bbls/km^2) from the pipe rupture on the 3rd day from the spillage, July 2015-2018.

Figure 39 b (right): Mean averaged concentration of the dispersed condensate (bbls/km^2) from the pipe rupture on the 7th day from the spillage, July 2015-2018.

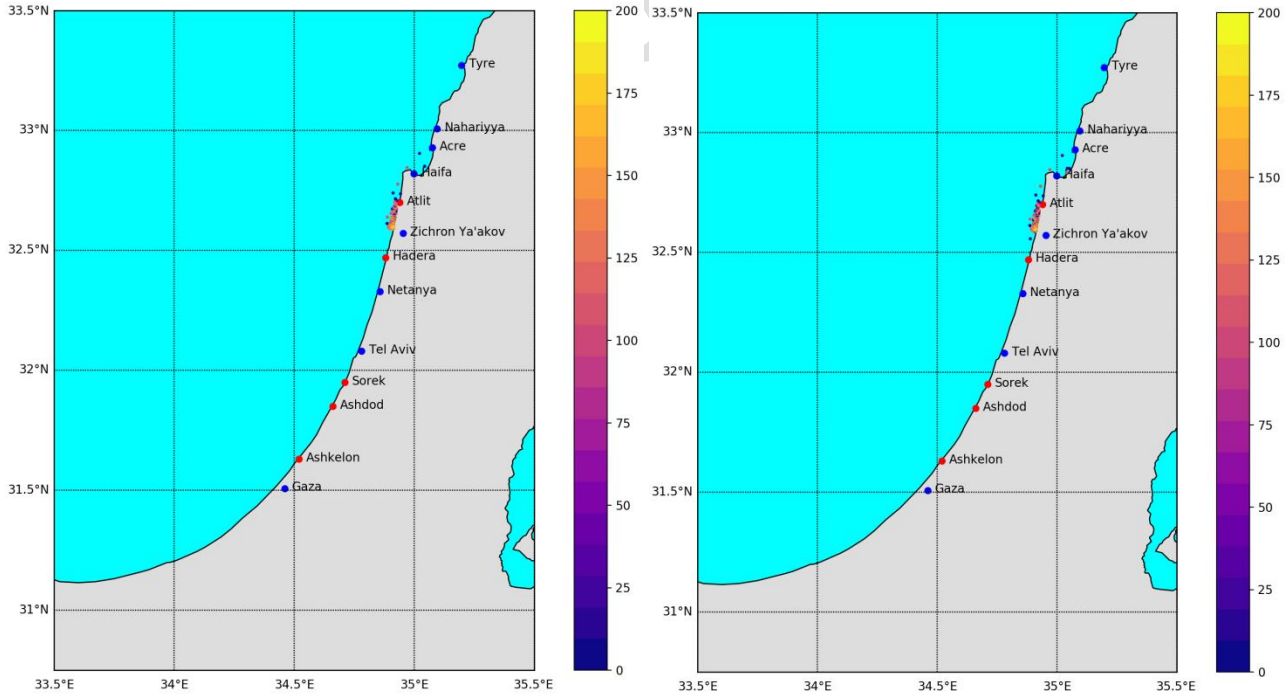

Figure 40: Mean averaged concentration of the dispersed condensate (bbls/km^2)

Figure 40 a (left): Mean averaged concentration of the dispersed condensate (bbls/km^2) from the pipe rupture on the 10th day from the spillage, July 2015-2018.
Figure 40 b (right): Mean averaged concentration of the dispersed condensate (bbls/km^2) from the pipe rupture on the 20th day from the spillage, July 2015-2018.

4. Transition period September – October 2015-2018

4.1. Transition period: September 2015 - 2018

No impact from the dispersed condensate from the spillage on the Hadera desalination plant during September. The dispersed condensate gathered very close to the shore areas of Zichron-Ya'akov on the 2st day (*Figure 41*a) move further South, but did not reach the Hadera desalination plant even during the following days 3nd , 7th,10th and 20th as it is seen on the Figures *Figure 41*b, *Figure 42* a, *Figure 42* b.

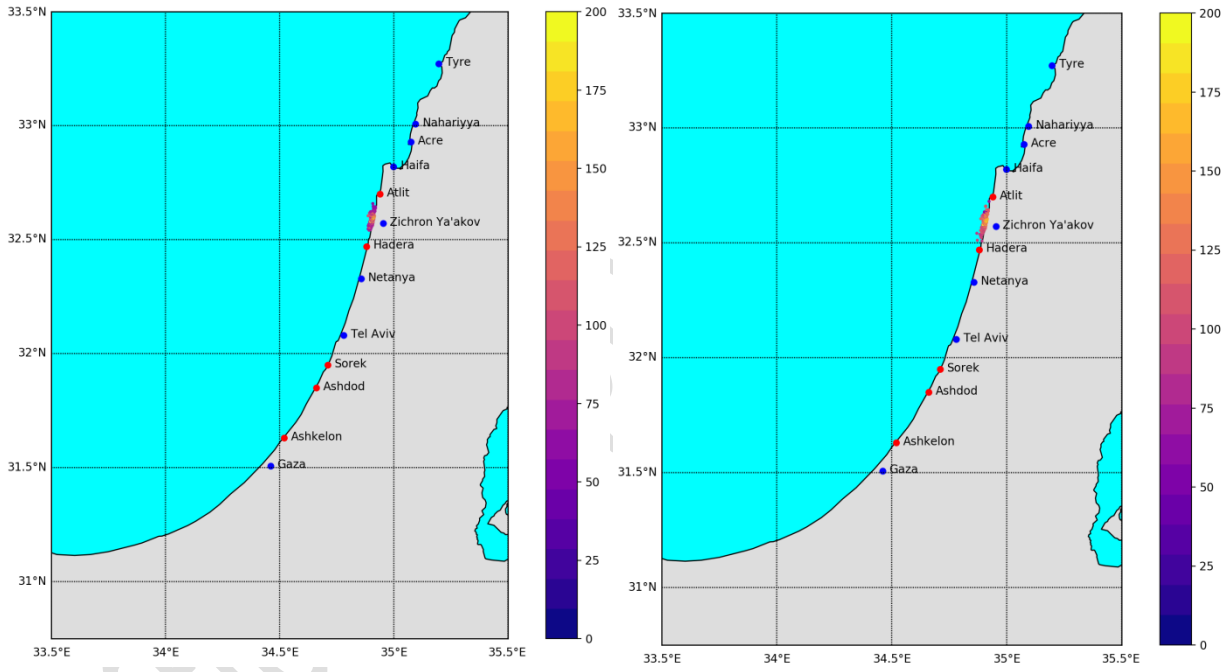

Figure 41: Mean averaged concentration of the dispersed condensate (bbls/km^2)
Figure 41 a (left): Mean averaged concentration of the dispersed condensate (bbls/km^2) from the pipe rupture on the 2nd day from the spillage, September 2015-2018.
Figure 41 b (right): Mean averaged concentration of the dispersed condensate (bbls/^{km2}) from the pipe rupture on the 3rd day from the spillage, September 2015-2018.

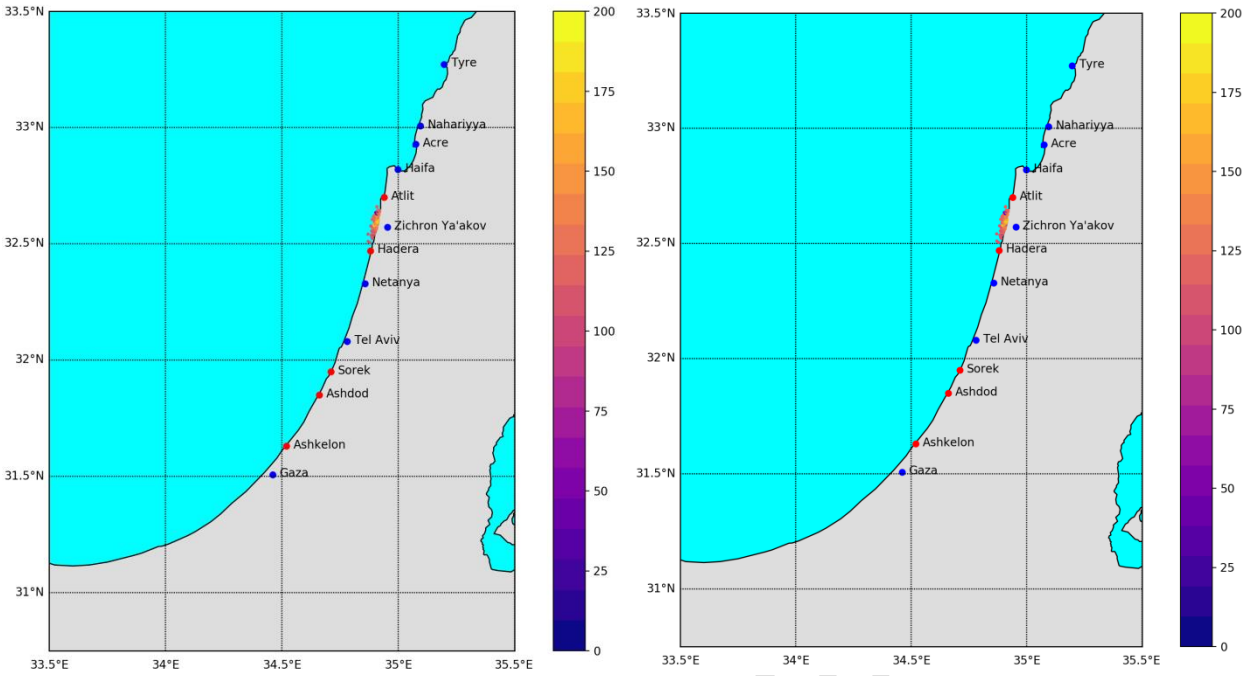

Figure 42: Mean averaged concentration of the dispersed condensate (bbls/km^2)

Figure 42a (left): Mean averaged concentration of the dispersed condensate (bbls/km^2) from the pipe rupture on the 7th day from the spillage, September 2015-2018.
Figure 42b (right): Mean averaged concentration of the dispersed condensate (bbls/km^2) from the pipe rupture on the 10th day from the spillage, September 2015-2018.

4.2. Transition period: October 2015-2018

During this period the Hadera desalination plant is ***impacted with mean averaged concentration of the dispersed condensate ~100 bbl/km2 on the th 7th day from the spillage.*** During the 1st day (*Figure 43*a) the dispersed condensate was close to the shore at the area of Zihron-Ya'akov and continues to remain in the same area during the day 2nd (*Figure 43*b). During the 3rd day (*Figure 44*a) the dispersed condensate slick moves to the South, while on the 7thday (*Figure 44* b) high dispersed condensate ***with mean averaged concentration of ~100 bbl/km2*** moves towards ***s***outh of Netanya, with smaller quantities present at the Hadera desalination intake. The amount of the dispersed condensate which still remain at sea moves further South and continues to affect the near shore South of Netanya at the 10th day (*Figure 45*a). Similarly the same picture appears during the 20th day (*Figure 45*b).

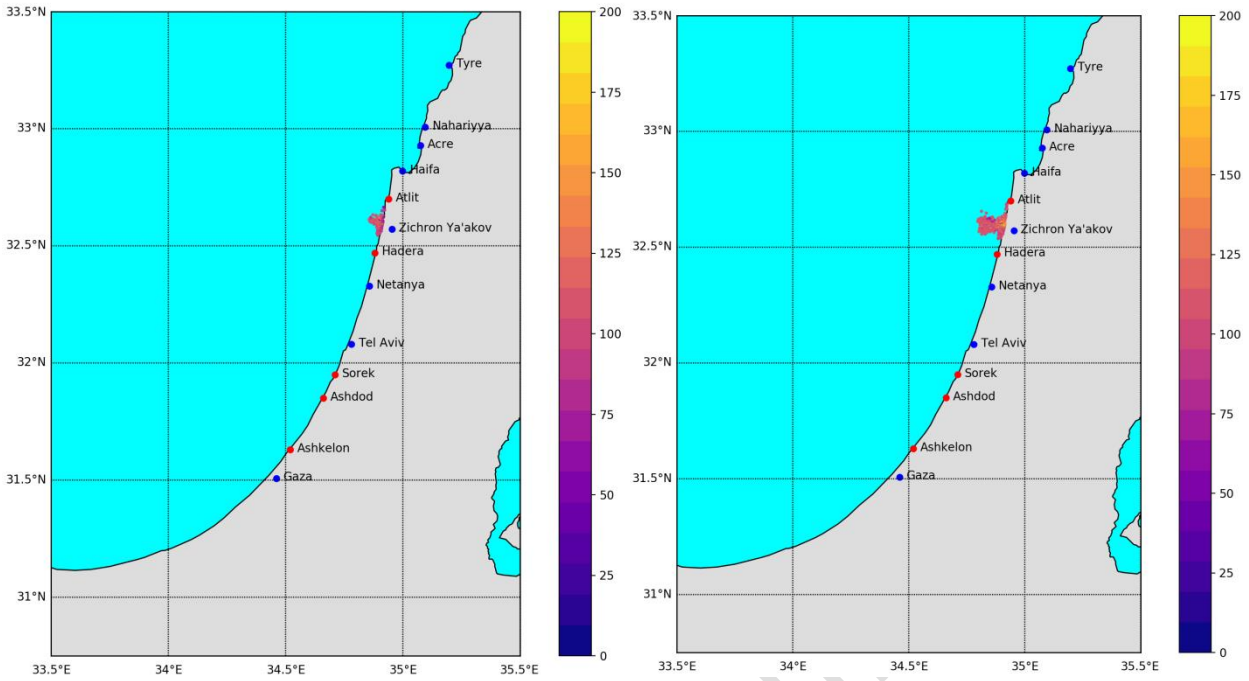

Figure 43: Mean averaged concentration of the dispersed condensate (bbls/km²)

Figure 43a (left): Mean averaged concentration of the dispersed condensate (bbls/km^2) from the pipe rupture on the 1st day from the spillage, October 2015-2018.

Figure 43b (right): Mean averaged concentration of the dispersed condensate (bbls/km^2) from the pipe rupture on the 2nd day from the spillage, October 2015-2018.

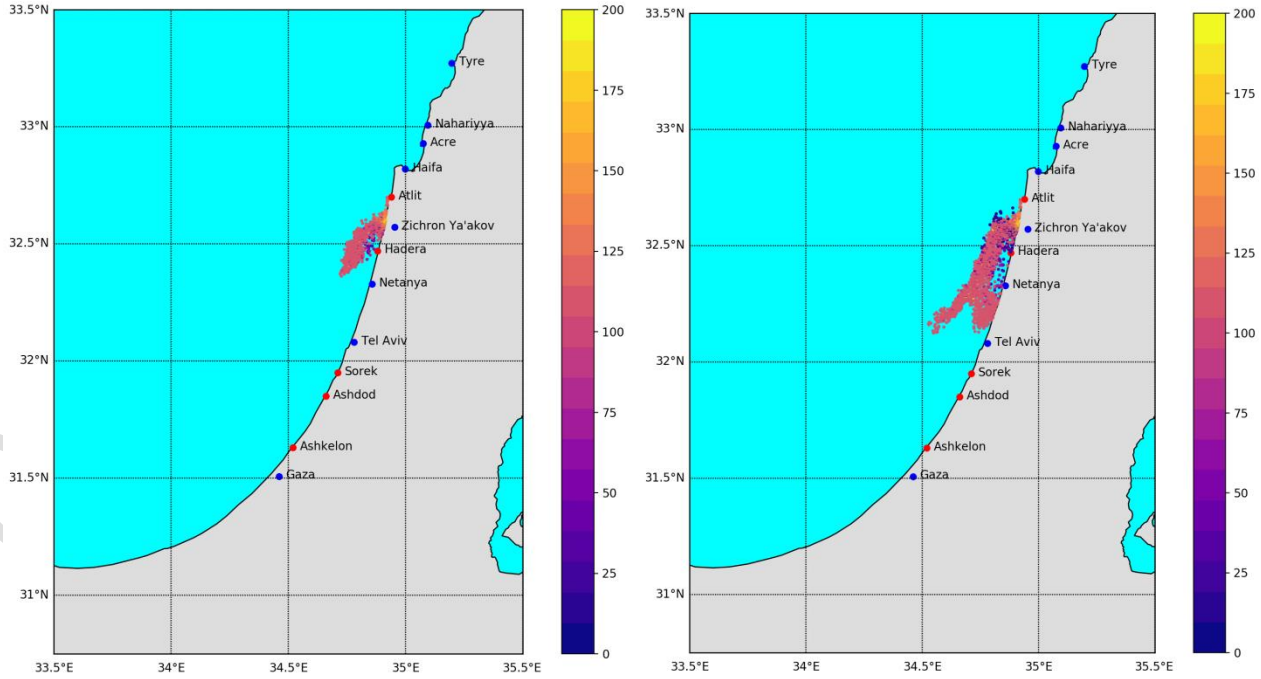

Figure 44: Mean averaged concentration of the dispersed condensate (bbls/km2)

Figure 44a (left): Mean averaged concentration of the dispersed condensate (bbls/km^2) from the pipe rupture on the 3rd day from the spillage, October 2015-2018.
Figure 44b (right): Mean averaged concentration of the dispersed condensate (bbls/km^2) from the pipe rupture on the 7th day from the spillage, October 2015-2018.

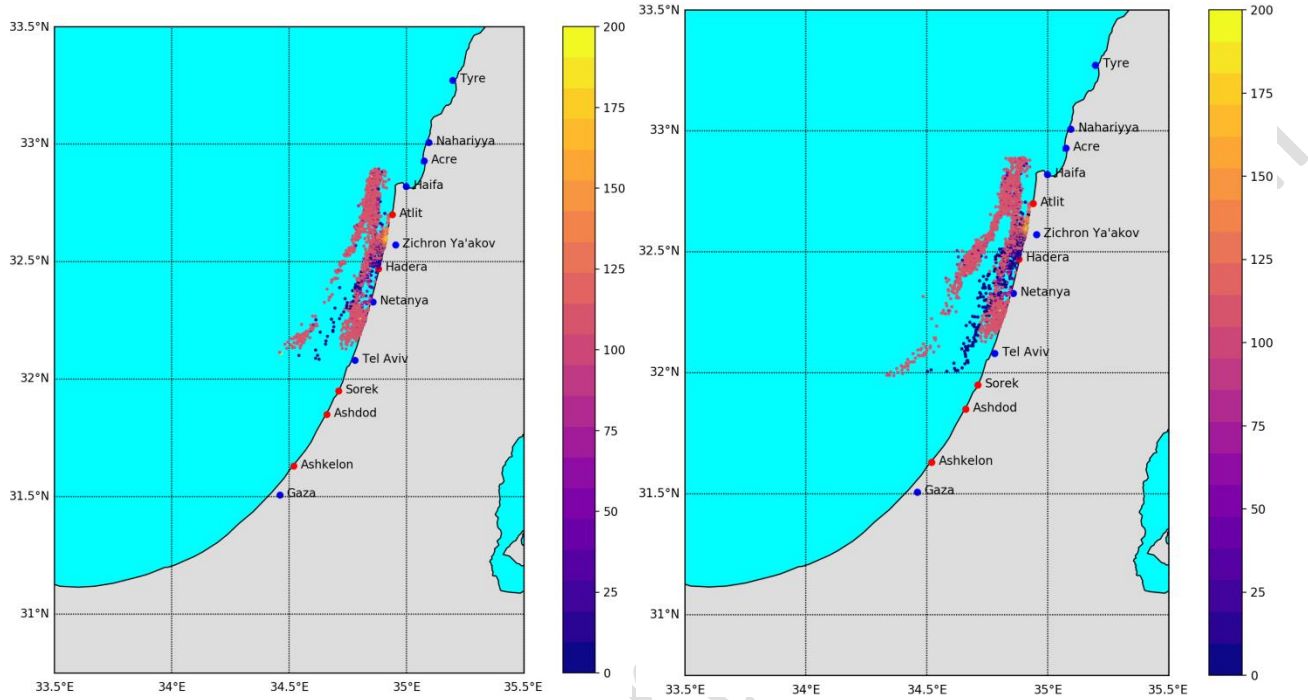

Figure 45: Mean averaged concentration of the dispersed condensate (bbls/km^2)
Figure 45a (left): Mean averaged concentration of the dispersed condensate (bbls/km^2) from the pipe rupture on the 3rd day from the spillage, October 2015-2018.
Figure 45b (right): Mean averaged concentration of the dispersed condensate (bbls/km^2) from the pipe rupture on the 7th day from the spillage, October 2015-2018.

5.6.4. Conclusions

1. There is as similarity in terms of the movement/pattern an beach deposition of the Condensate slick/discharge of the current simulation to the that of by Brenner to full extent and to a lesser degree with that of the Oscar model.
   It obvious that in terms of magnitude that of the current stimulation is much higher than that of the two others due to the bigger amount of condensate discharge.
2. It is clear that the Period in which the Hadera desalination will really impacted is during the transitional Period for the current stimulation and the previous ones.
3. In the Period where the desalination plant will be impacted the following preventive must be in placed
   3.1. Oil alarm sensors

3.2. Oil sorbent booms and oil mops as traditional inflated or solid booms will not work with the Condensate due to its physicochemical characteristics and its behavior at sea (Described in detailed in the Main Report)

3.3. The addition of analyses for the detection of Petroleum Hydrocarbons should be added to the existing continuous monitoring program of the desalinated water.

3.4. The provision of the shat down of the plan for a while must be consider in advance

3.5. The use of oil dispersant could not consider as preventive measure for the following reasons:

3.5.1. "Dispersant" means a mixture of surface active agents in one or more organic solvents, specifically formulated to enhance the dispersion of oil into the sea water column by reducing the interfacial tension between oil and water (IMO, 2011).

3.5.2. The addition of a mixture of surface active agents in one or more organic solvents which will result to the dispersion of condensate and transfer toxic hydrocarbon contamination into the sea water column, i.e . to the point of the desalination intake will possibly affect the R.O. membranes of the plant efficiency and at the same time increased the impact on the marine ecosystem.

3.5.3. The extent to which surface application of dispersants could affect the relative uptake into seafood and potential toxicity of oxygenated PAHs is unknown, although a recent study suggested that a relatively persistent PAH, chrysene, when oxygenated, may contribute to the developmental toxicity (heart, circulation, spine, and eye defects, among others, when exposure occurs during development) of weathered oil (Diamante, et al., 2017). The net risk is unclear (The Use of Dispersants in Marine Oil Spill Response, 2019).

3.5.4. Dispersants are generally used on surface films greater than 0.05 mm – 0.1mm thick (heavy fuels) which is considerably thicker than that of condensate films if such films occur as this is not always the case.

5.6.5. Mitigation and Preventive Measures

1. Use of permanent deployment of booms and bubble barriers are the standard practices to safe guard desalination plants from oil contamination. This practice might be useful in the case of heavy fuel oils but in the case of condensate and diesel oil this might be of ineffective due to their characteristics and behavior at sea of environment. They create oil slicks so thin (μm) and after weathering they were not create balls or oil emulsions in water.

Sorbent booms might be work better in the case of condensate.

2. The distance and exact point of the intake ports are very crucial. The distances from the shore should be at least 1000 meters. This distance safeguards the contamination of the plant from dissolved back to seawater in case of oil beaching. The intake ports must be at a enough high above sea bed i.e. 5 meters. This high avoid among others the intrusion of oil which sank on the bottom after weathering (This may applied only for heavy fuels).

The depth from the sea surface is also important. Ten to fifteen meters water depth is considered sufficient enough. In the case of condensate or diesel oil is of particular important, as their impact will be from the amount of oil dissolved in the water column and the amount of oil dispersed at the sea surface at the site of the sea water intake of the desalination plant.

In the case of the Hadera desalination plant the water intake fulfils the about requirement.

3. Oil spill detectors/ sensors. A remote hydrocarbon sensor for the detection of oil spill events or routine monitoring of hydrocarbons would be an ideal solution for the protection of the desalination. A product is spotted in the market. This autonomous row oil spill detect or scan be powered by solar panel.

4. Monitoring should be carried out for the quality of the intake sea water and the produced water of the Hadera desalination plant. The analysis among other should include: Mineral oils (FTIR), Total oil and grease (FTIR) in the case where there is an oil accident which might affect the desalination plant of Hadera. More specific analyses should be carried for intake and produced water for all Petroleum Hydrocarbons contained in the specific type of the spilled oil. The specific hydrocarbons contents of the condensate and diesel oil should be carried out. In previous section were mentioned the problems can put petroleum hydrocarbons on the membranes of the RO desalination plant and also on human health.

5.7. Evaporation

5.7.1. Additional reviewed reports

The following recent publication was submitted for preliminary review being relevant to Leviathan Platform operations (Broday, Dayan, Aharonov, Laufer, & Adel, 2019)[7]:

Being the evaporation from oil spilled condensate not covered by the above-mentioned publication, no critical review was performed under the Scope of the present document.

5.7.2. Additional international guidelines

In addition to the Community Exposure Guidelines (PACs) referenced in report [13], the following PACs set by USEPA are taken into consideration in the present supplementary report *Table 10*.

The above mentioned standards are relevant to hydrocarbon mixture and they are not related to specific hydrocarbons as those referenced in report [13] for BTEX and C5-C12 alkanes. It is further to be noted that gasoline and Jet fuel do not represent the VOC mixture resulting from the evaporation of condensate spill, and thus their use within this report is to be considered as merely indicative.

Table 10: PAC standardization

PAC Type	Compound	Exposure reference duration	mg/m³	Source
PAC1/AEGL1 (proposed**)	automotive gasoline (unleaded)	30 min; 1h; 4h; 8 hr	730	https://www.epa.gov/aegl
PAC2/AEGL2 (proposed**)	automotive gasoline (unleaded)	30 min; 1h; 4h; 8 hr	*7500	https://www.epa.gov/aegl
PAC1/AEGL1 (final)	Jet Fuels (JP-5 and JP-8)	30 min; 1h; 4h; 8 hr	290	https://www.epa.gov/aegl
PAC2/AEGL2 (final)	Jet Fuels (JP-5 and JP-8)	30 min; 1h; 4h; 8 hr	1100	https://www.epa.gov/aegl

Notes

Acute exposure guideline levels (AEGLs) describe the human health effects from once-in-a-lifetime, or rare, exposure to airborne chemicals.

AEGL "levels" are dictated by the severity of the toxic effects caused by the exposure, with Level 1 being the least and Level 3 being the most severe.

All levels are expressed as parts per million or milligrams per cubic meter (ppm or mg/m3) of a substance above which it is predicted that the general population could experience, including susceptible individuals:

- AEGL1: Notable discomfort, irritation, or certain asymptomatic non-sensory effects. However, the effects are not disabling and are transient and reversible upon cessation of exposure.
- AEGL2: Irreversible or other serious, long-lasting adverse health effects or an impaired ability to escape.
- AEGL3: Life-threatening health effects or death.

[7] *https://doi.org/10.1016/j.eiar.2019.106313*. http://www.sciencedirect.com/science/article/pii/S0195925519300800

* = > 10% LEL (Lower Explosive Limit) = 14,000ppm. Safety considerations against the hazard(s) of explosion(s) must be taken into account.

** Proposed AEGLs are established following review and consideration by the National Advisory Committee for AEGLs (NAC/AEGL) of Draft AEGLs. Proposed AEGLs are available for use by organizations while awaiting public comments and NRC/NAS peer review and publication of Final AEGLs. Changes to Proposed values and Technical Support Documents may occur before AEGLs become interim values.

5.7.3. Simulation setup

The air dispersion simulations of the evaporated hydrocarbons from pipe rupture were performed following the same procedure as applied in report number LSR-OR-ZY-04-08-2019-R-A [13]. The modeling suite CALMET/CALPUFF was initialized with WRF meteorological data (year 2018), considering two additional spill scenarios depicted in *Table 11*. The additional spill scenarios are numbered consecutively to the 4 meteorological scenarios already addressed in [13].

Both scenarios #5 and #6 are selected under condition of winds blowing from offshore towards the Israeli coast. Scenario #5 is representative of high wind speed (ranging between 5 and 10 m/s during the first 24 hours); Scenario #6 is representative of low wind speed conditions (ranging between 0-5 m/s during the first 24 hours).

Table 11: Meteorological data year 2018

# Scenario	Season condition	Spilled Liquid	Spill Start	wind speed (first 24h average) [m/s]	main wind direction °N	Spill reaching coast
#5	High wind winter	condensate	01/01/2018 h03	8.4	250	Y
#6	Low wind summer	condensate	30/07/2018 h03	2.6	237	Y

5.7.3.1. Secondary evaporation from the beach deposition

Differently from previous simulations [13], the contribution of the vapor emissions from shored oil was explicitly included in the model by the means of variable linear sources. The emission rates of such sources were calculated for each MEDSLIK modeling step and coastline impacted section, considering the quantity of beached oil, the time from the spill, and the following generic evaporation *Equation 2* developed by Fingas[8]

[8] Fingas, 2014. Oil and Petroleum Evaporation. Handbook of Oil Spill Science and Technology. Chapter 7 (Pages: 205-223). © 2015 John Wiley & Sons, Inc. Published 2015 by John Wiley & Sons, Inc.

Equation 2 $$\boldsymbol{Precentage_{evaporated} = [0.165(\%D) + 0.45(T - 15)ln(t)]}$$

Where

- D (percentage by weight distilled at 180°) was assumed equal to 45, to pretty fit the MEDSLIK evaporation curve, and
- T (Temperature) was selected for each spill case scenario (19.1°C for #5 and 28.5°C for #6).
- t is the exposure time (minutes) of the beached oil, calculated for each step and each coastline section

5.7.4. Results

For each modelled spill scenario, maximum estimated concentrations are below reported for peak-value locations (offshore and onshore) and each discrete receptor (inhabited coastal areas) identified in the study area.

The following isoconcentration contour maps are also provided for each scenario:

- Maximum 1h average of total VOCs (ug/m^3)
- Maximum 8h rolling average of Benzene (ug/m^3)
- Maximum 24h average of Benzene (ug/m^3)

Scenario #5, considering high wind conditions, results in onshore hourly and daily peak of VOC concentration equal to of 42.6 mg/m^3 (hourly peak) and 3.3 mg/m^3 (daily peak) respectively.

Scenario #6, considering low wind conditions, results in onshore hourly and daily peak of VOC concentration equal to of 229 mg/m^3 (hourly peak) and 6 mg/^{m3} (daily peak) respectively.

5.7.4.1. Scenario 5 Total VOC

Table 12: Summary results for VOC (Scenario 5)

Scenario: 5 Condensate spill starting 01/01/2018 h03					Max estimated concentrations (VOCs)		
ID Receptor	X	Y	Municipality	Description	1-Hours Average	8-Hours rolling average	24-Hours Average
	[m]	[m]			ug/m³	ug/m³	ug/m³
Peak offshore	679000	3608000	Regional Council Hof Ha'Carmel	Offshore (0.7km from coast)	4.25E+04		
	679500	3609000		Offshore (0.4km from coast)		2.62E+04	2.11E+04
Peak onshore				Onshore	4.26E+04	6.77E+03	3.30E+03
1	686292	3630232	Haifa	Haifa	8.32E+01	1.75E+01	5.85E+00
2	684802	3626634	Tirat Hacarmel	Tirat Karmel	1.27E+02	2.31E+01	7.69E+00
3	683393	3625542	Regional Council Hof Ha'Carmel	Ha Hotrim	4.01E+01	6.51E+00	2.17E+00
4	683757	3622812		Megadim	2.92E+02	4.88E+01	1.63E+01
5	682156	3618766		Atlit	4.52E+02	6.72E+01	2.24E+01
6	681126	3617469		Neve Yam	8.66E+01	1.18E+01	3.93E+00
7	683258	3615537		Geva Carmel	4.37E+02	1.56E+02	5.21E+01
8	682564	3613952		Tzrufa	8.81E+02	3.17E+02	1.06E+02
9	681297	3612680		Ha Bonim	2.34E+03	9.98E+02	3.33E+02
10	682401	3611923		Ein Ayala	1.76E+03	5.37E+02	1.87E+02
11	680371	3610033		Nahsholim	8.73E+03	3.44E+03	1.19E+03
12	680473	3609440		Dor	6.97E+03	1.59E+03	1.10E+03
13	680074	3603982		Ma'agan Michael	0.00E+00	0.00E+00	0.00E+00
14	679526	3601497	Giser A'Zarka	Jisraz Zarqa	0.00E+00	0.00E+00	0.00E+00
15	678898	3599589	Regional Council Hof Ha'Carmel	Caesarea	0.00E+00	0.00E+00	0.00E+00
16	677901	3596614		Sdot Yam	0.00E+00	0.00E+00	0.00E+00
17	680499	3590202	Hadera	Hadera	0.00E+00	0.00E+00	0.00E+00

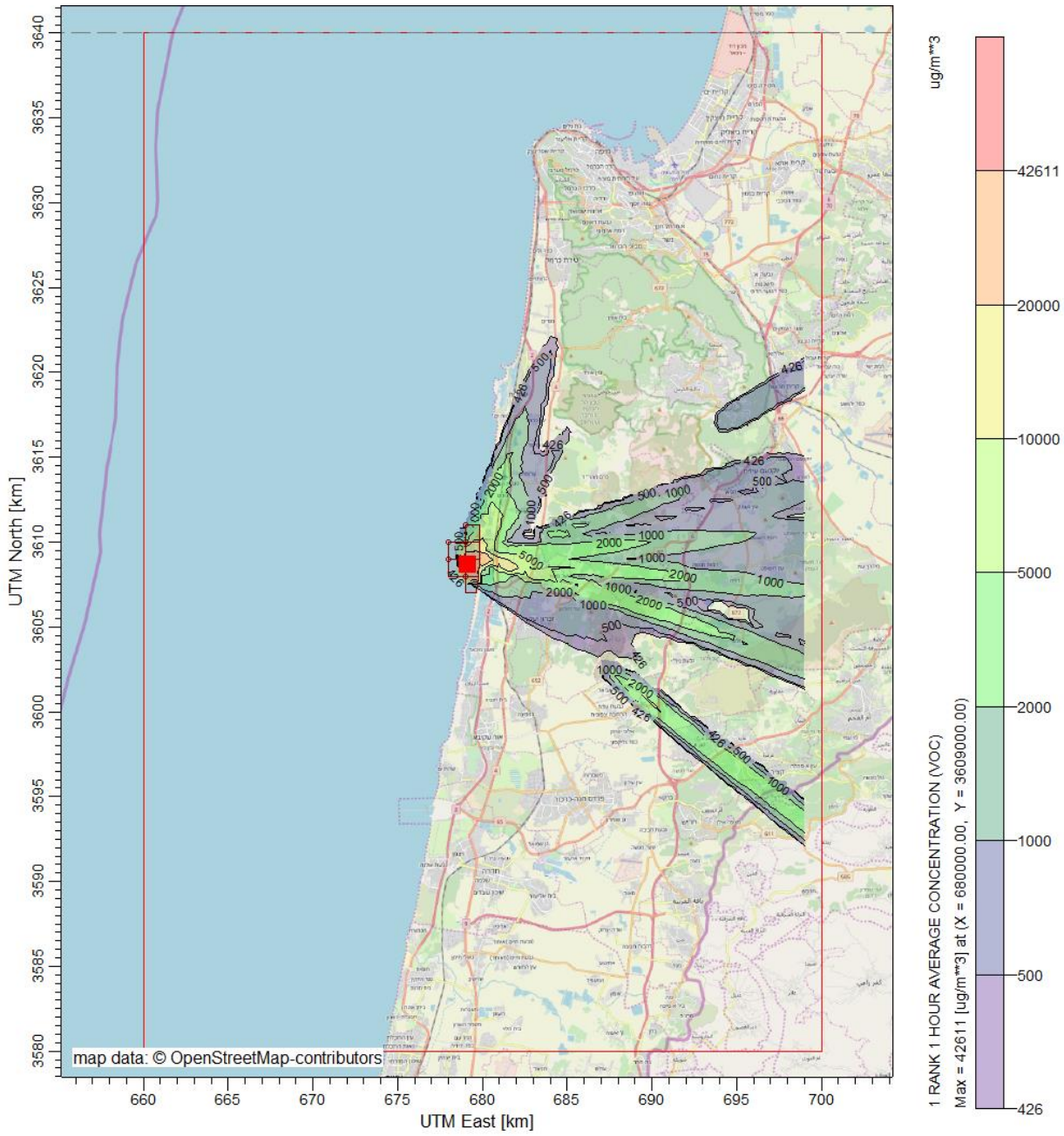

Figure 46: Scenario-5 condensate spill Maximum 1-Hr. average concentration VOCs

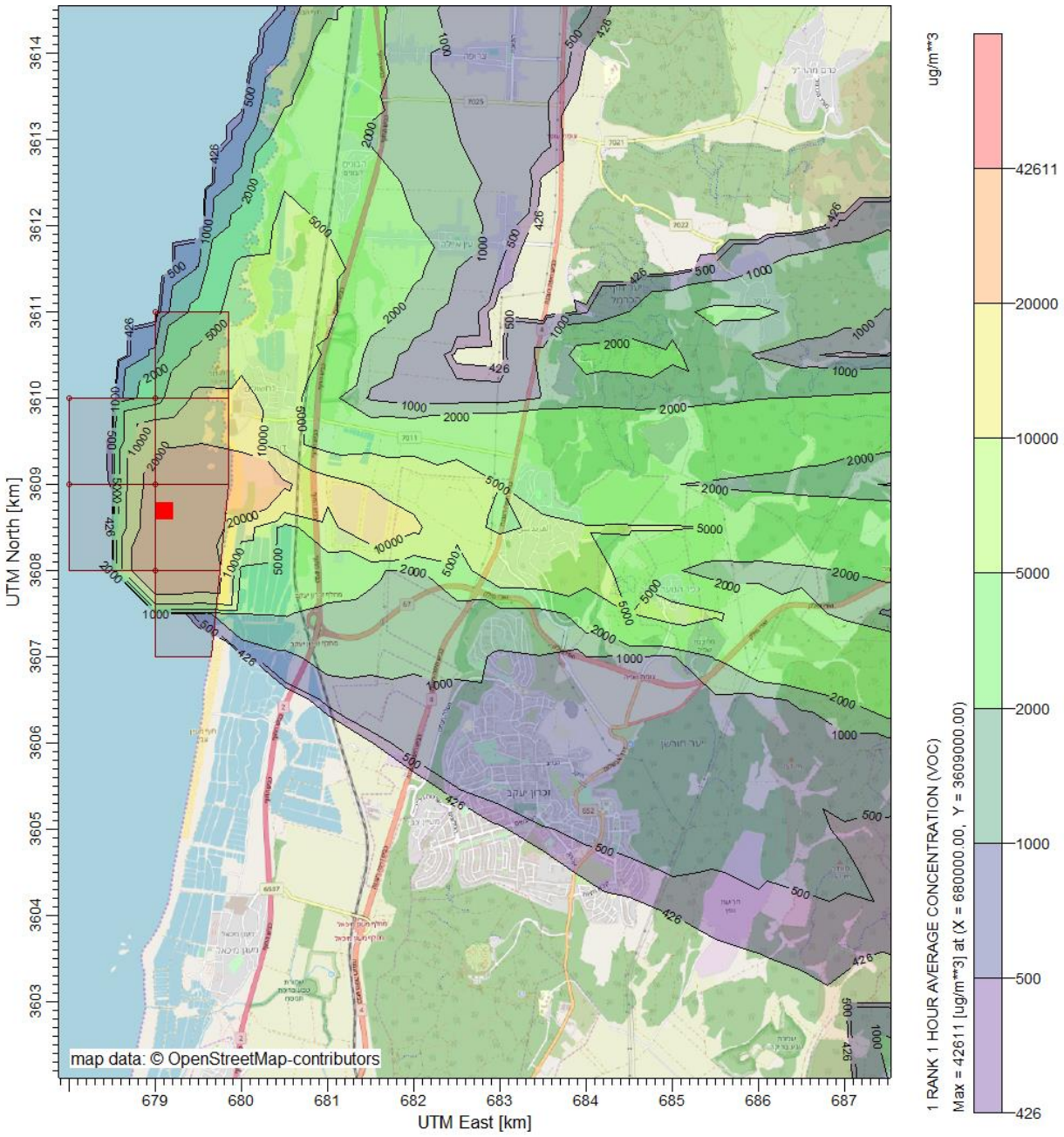

Figure 47: Scenario-5 condensate spill Maximum 1-Hr. average concentration VOCs (FOCUS on spillage area)

5.7.4.2. Scenario 5 Benzene

Table 13: Summary results for Benzene (Scenario 5)

Scenario: 5 Condensate spill starting 01/01/2018 h03					Max estimated concentrations (Benzene)		
ID Receptor	X	Y	Municipality	Description	1-Hours Average	8-Hours rolling average	24-Hours Average
	[m]	[m]			ug/m3	ug/m³	ug/m³
Peak offshore	679000	3608000	-	Offshore (0.7km from coast)	8.96E+02		
	679500	3609000		Offshore (0.4km from coast)		5.41E+02	4.48E+02
Peak onshore			Regional Council Hof Ha'Carmel	Onshore	2.50E+02	1.20E+02	7.10E+01
1	686292	3630232	Haifa	Haifa	1.59E+00	3.37E-01	1.12E-01
2	684802	3626634	Tirat Hacarmel	Tirat Karmel	2.44E+00	4.46E-01	1.49E-01
3	683393	3625542	Regional Council Hof Ha'Carmel	Ha Hotrim	7.75E-01	1.26E-01	4.21E-02
4	683757	3622812		Megadim	5.65E+00	9.44E-01	3.15E-01
5	682156	3618766		Atlit	8.79E+00	1.30E+00	4.35E-01
6	681126	3617469		Neve Yam	1.69E+00	2.29E-01	7.64E-02
7	683258	3615537		Geva Carmel	8.55E+00	3.00E+00	1.00E+00
8	682564	3613952		Tzrufa	1.72E+01	6.09E+00	2.03E+00
9	681297	3612680		Ha Bonim	4.57E+01	1.92E+01	6.41E+00
10	682401	3611923		Ein Ayala	3.45E+01	1.02E+01	3.56E+00
11	680371	3610033		Nahsholim	1.71E+02	6.64E+01	2.29E+01
12	680473	3609440		Dor	1.36E+02	3.09E+01	2.32E+01
13	680074	3603982		Ma'agan Michael	0.00E+00	0.00E+00	0.00E+00
14	679526	3601497	Giser A'Zarka	Jisraz Zarqa	0.00E+00	0.00E+00	0.00E+00
15	678898	3599589	Regional Council Hof Ha'Carmel	Caesarea	0.00E+00	0.00E+00	0.00E+00
16	677901	3596614		Sdot Yam	0.00E+00	0.00E+00	0.00E+00
17	680499	3590202	Hadera	Hadera	0.00E+00	0.00E+00	0.00E+00

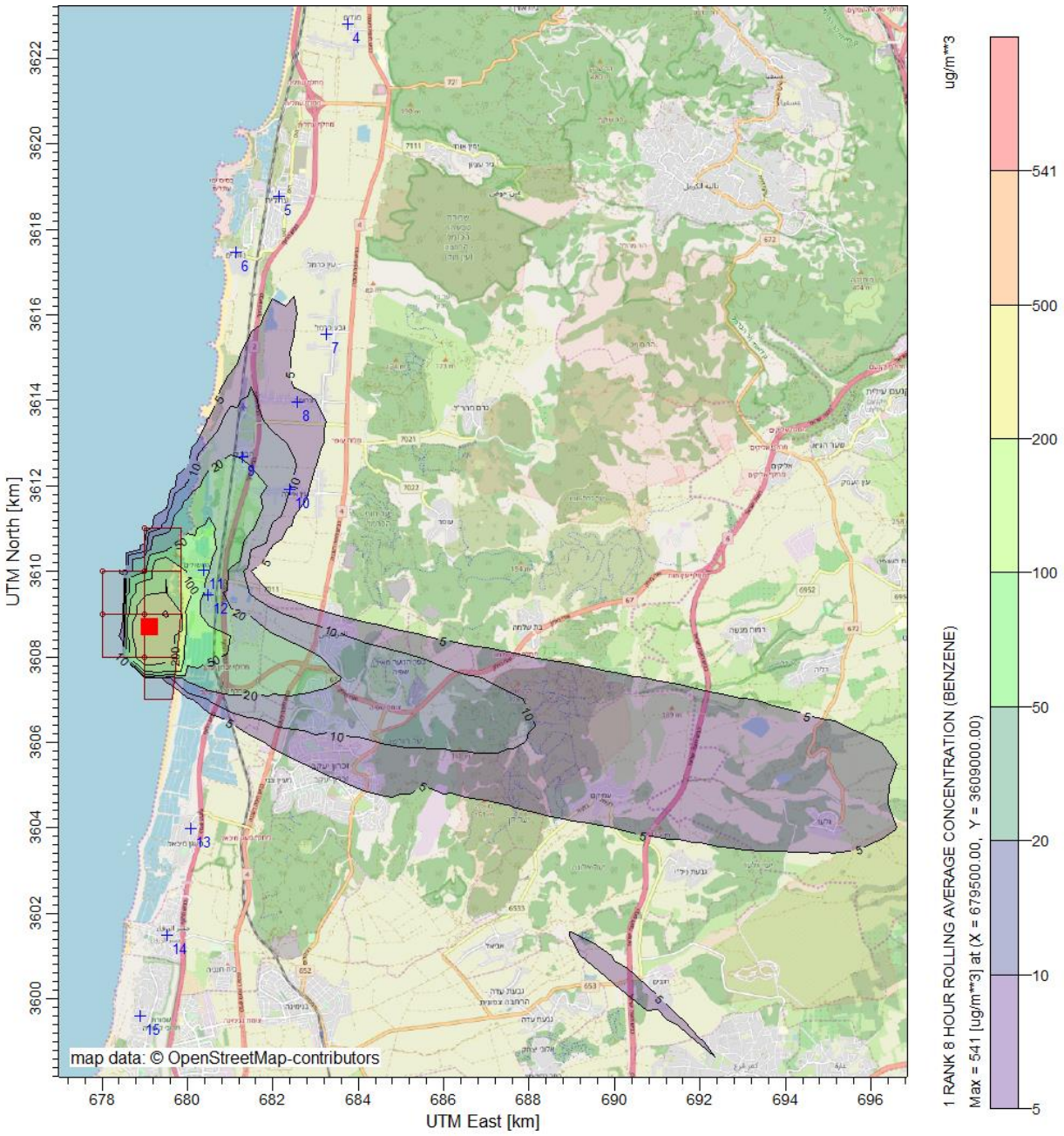

Figure 48: Scenario #5 Condensate spill - Maximum 8h-average concentration Benzene

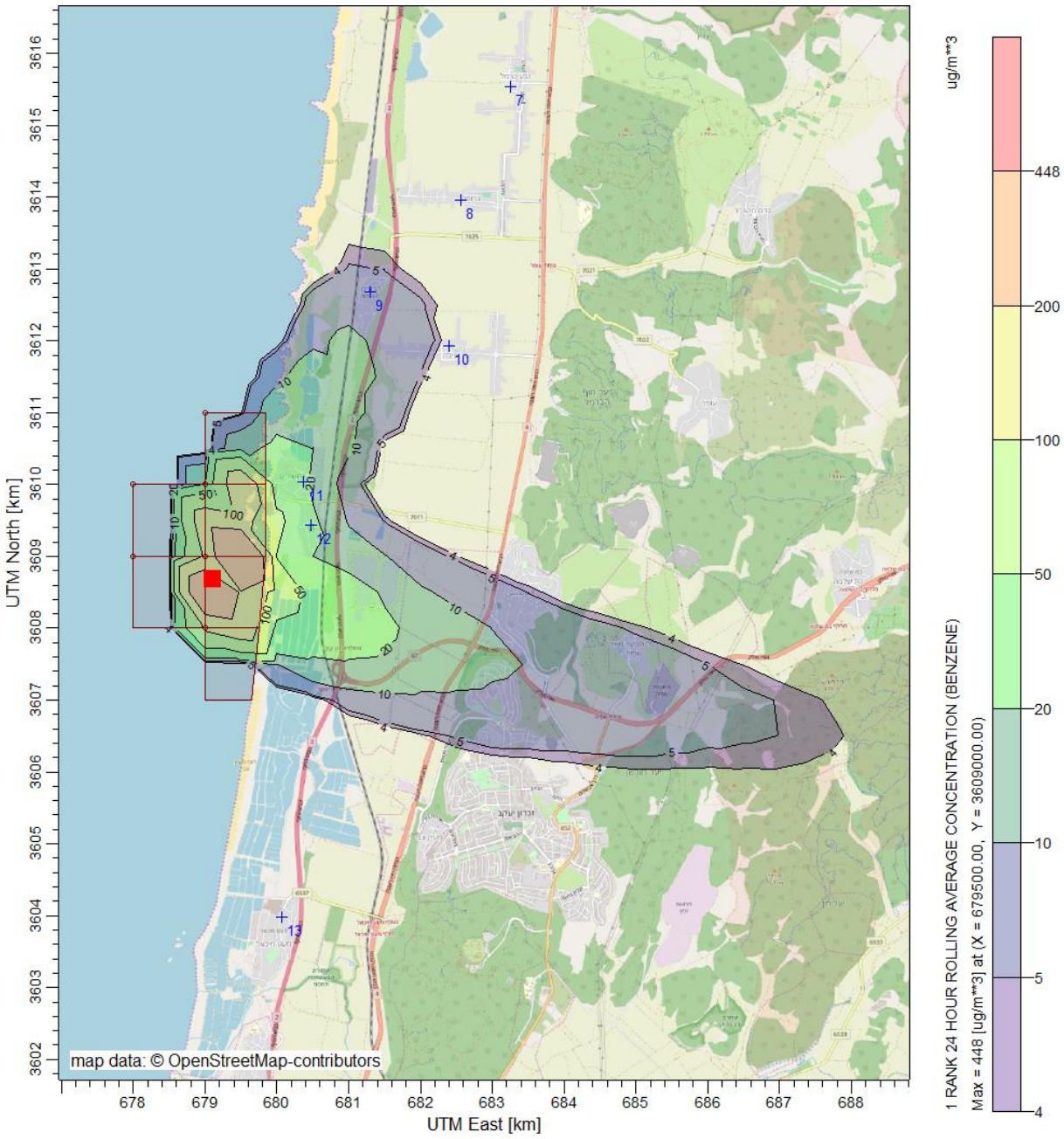

Figure 49: Scenario #5 Condensate spill - Maximum 24h-average concentration Benzene

5.7.4.3. Scenario 6 Total VOCs

Table 14: Summary results for VOCs (Scenario-6)

Scenario: 6 Condensate spill starting 30/07/2018 h03					Max estimated concentrations (VOCs)		
ID Receptor	X	Y	Municipality	Description	1-Hours Average	8-Hours rolling average	24-Hours Average
	[m]	[m]			ug/m³	ug/m³	ug/m³
Peak offshore	679500	3609000	Regional Council Hof Ha'Carmel	Offshore (0.4km from coast)	1.78E+05	1.06E+05	5.36E+04
Peak onshore				Onshore	2.29E+05	1.45E+05	5.99E+04
1	686292	3630232	Haifa	Haifa	8.78E+02	2.01E+02	6.71E+01
2	684802	3626634	Tirat Hacarmel	Tirat Karmel	2.01E+03	3.91E+02	1.30E+02
3	683393	3625542	Regional Council Hof Ha'Carmel	Ha Hotrim	3.50E+03	5.99E+02	2.00E+02
4	683757	3622812		Megadim	2.40E+03	4.83E+02	1.61E+02
5	682156	3618766		Atlit	3.13E+03	7.43E+02	2.55E+02
6	681126	3617469		Neve Yam	5.48E+03	1.16E+03	3.87E+02
7	683258	3615537		Geva Carmel	1.18E+03	4.14E+02	1.45E+02
8	682564	3613952		Tzrufa	1.67E+03	5.86E+02	2.54E+02
9	681297	3612680		Ha Bonim	3.54E+03	1.26E+03	5.57E+02
10	682401	3611923		Ein Ayala	1.02E+04	3.79E+03	1.62E+03
11	680371	3610033		Nahsholim	4.77E+04	3.06E+04	1.27E+04
12	680473	3609440		Dor	1.29E+05	9.78E+04	3.71E+04
13	680074	3603982		Ma'agan Michael	2.34E+03	8.90E+02	2.97E+02
14	679526	3601497	Giser A'Zarka	Jisraz Zarqa	1.07E+03	3.48E+02	1.16E+02
15	678898	3599589	Regional Council Hof Ha'Carmel	Caesarea	6.19E+02	1.95E+02	6.51E+01
16	677901	3596614		Sdot Yam	2.44E+02	8.45E+01	2.82E+01
17	680499	3590202	Hadera	Hadera	7.37E+01	2.75E+01	9.17E+00

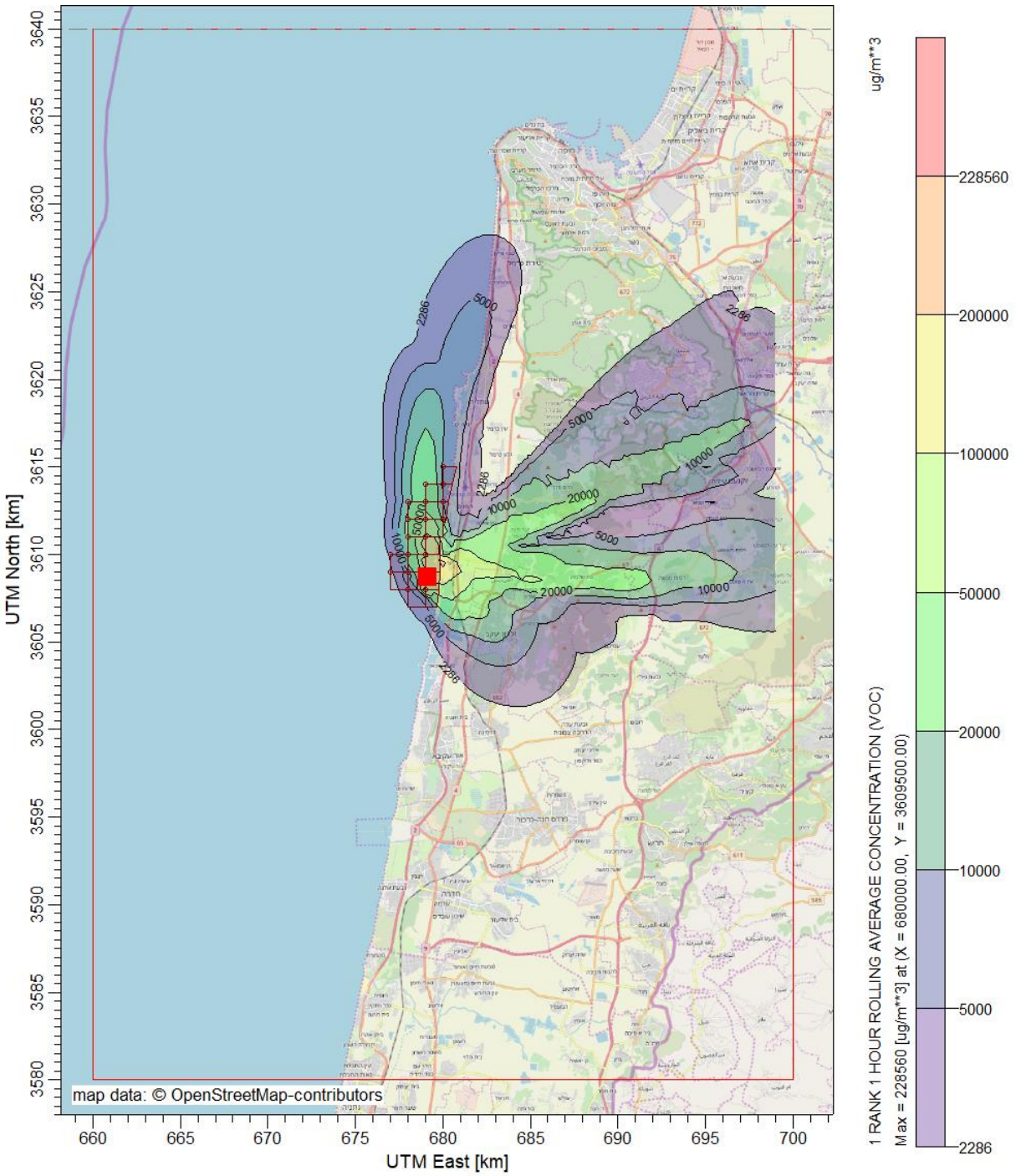

Figure 50: Scenario #6 Condensate spill - Maximum 1h-average concentration VOCs

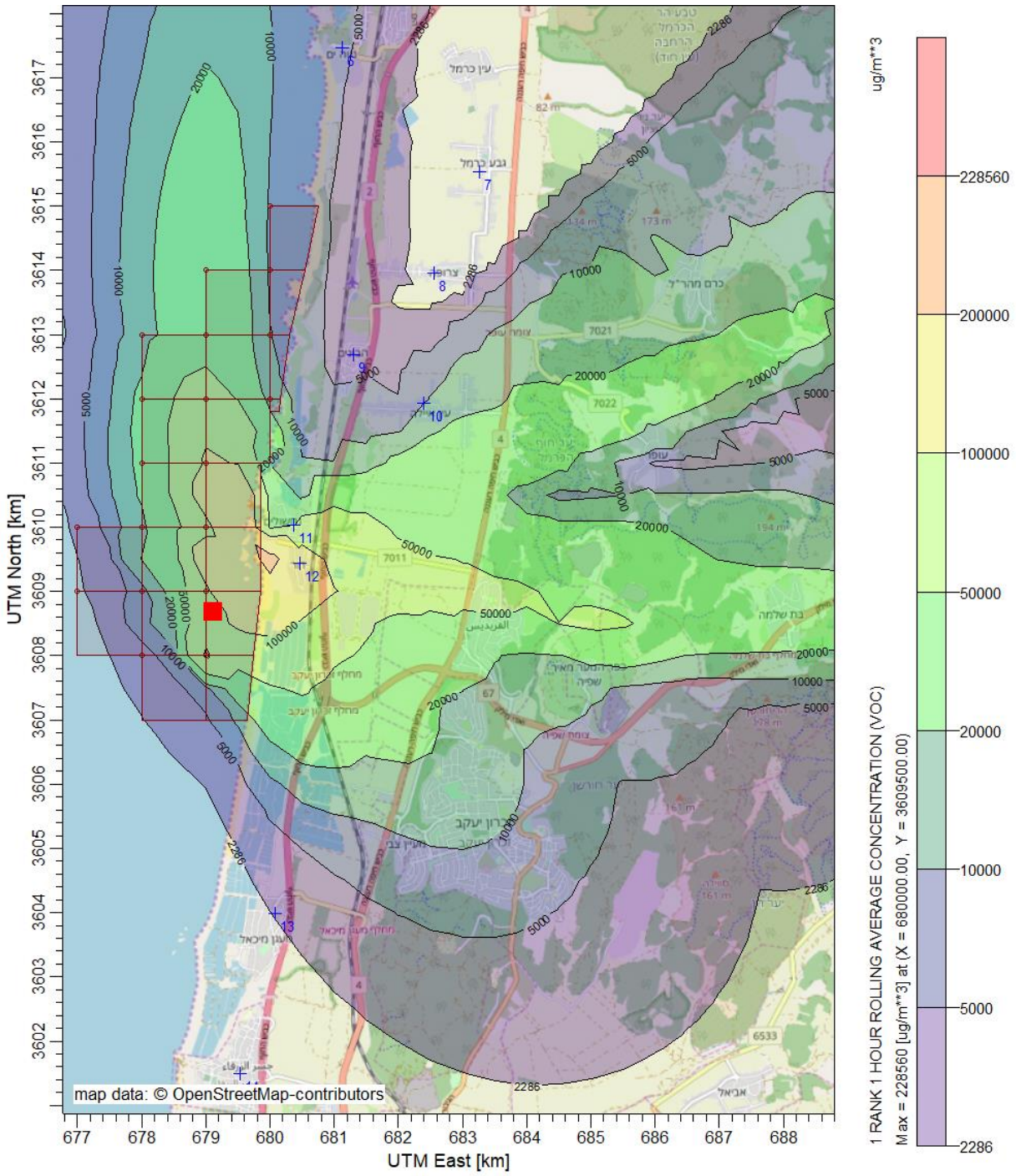

Figure 51: Scenario #6 Condensate spill - Maximum 1h-average concentration VOCs (FOCUS on spillage area)

5.7.4.4. Scenario 6 Total Benzene

Table 15: Summary results for Benzene (Scenario-6)

Scenario: 6 Condensate spill starting 30/07/2018 h03					Max estimated concentrations (Benzene)		
ID Receptor	X	Y	Municipality	Description	1-Hours Average	8-Hours rolling average	24-Hours Average
	[m]	[m]			ug/m³	ug/m³	ug/m³
Peak offshore	679500	3609000	Regional Council Hof Ha'Carmel	Offshore (0.4km from coast)	4.24E+03	2.53E+03	1.24E+03
Peak onshore				Onshore	3.73E+03	2.20E+03	8.84E+02
1	686292	3630232	Haifa	Haifa	2.11E+01	4.85E+00	1.62E+00
2	684802	3626634	Tirat Hacarmel	Tirat Karmel	4.86E+01	9.45E+00	3.15E+00
3	683393	3625542	Regional Council Hof Ha'Carmel	Ha Hotrim	8.47E+01	1.45E+01	4.83E+00
4	683757	3622812		Megadim	5.82E+01	1.18E+01	3.93E+00
5	682156	3618766		Atlit	8.17E+01	1.91E+01	6.36E+00
6	681126	3617469		Neve Yam	1.41E+02	2.92E+01	9.74E+00
7	683258	3615537		Geva Carmel	2.83E+01	1.02E+01	3.45E+00
8	682564	3613952		Tzrufa	3.34E+01	1.46E+01	5.00E+00
9	681297	3612680		Ha Bonim	8.21E+01	3.28E+01	1.15E+01
10	682401	3611923		Ein Ayala	7.22E+01	3.34E+01	1.87E+01
11	680371	3610033		Nahsholim	8.19E+02	5.09E+02	2.13E+02
12	680473	3609440		Dor	2.13E+03	1.34E+03	4.88E+02
13	680074	3603982		Ma'agan Michael	5.57E+01	2.12E+01	7.05E+00
14	679526	3601497	Giser A'Zarka	Jisraz Zarqa	2.54E+01	8.27E+00	2.76E+00
15	678898	3599589	Regional Council Hof Ha'Carmel	Caesarea	1.47E+01	4.64E+00	1.55E+00
16	677901	3596614		Sdot Yam	5.81E+00	2.01E+00	6.70E-01
17	680499	3590202	Hadera	Hadera	1.75E+00	6.53E-01	2.18E-01

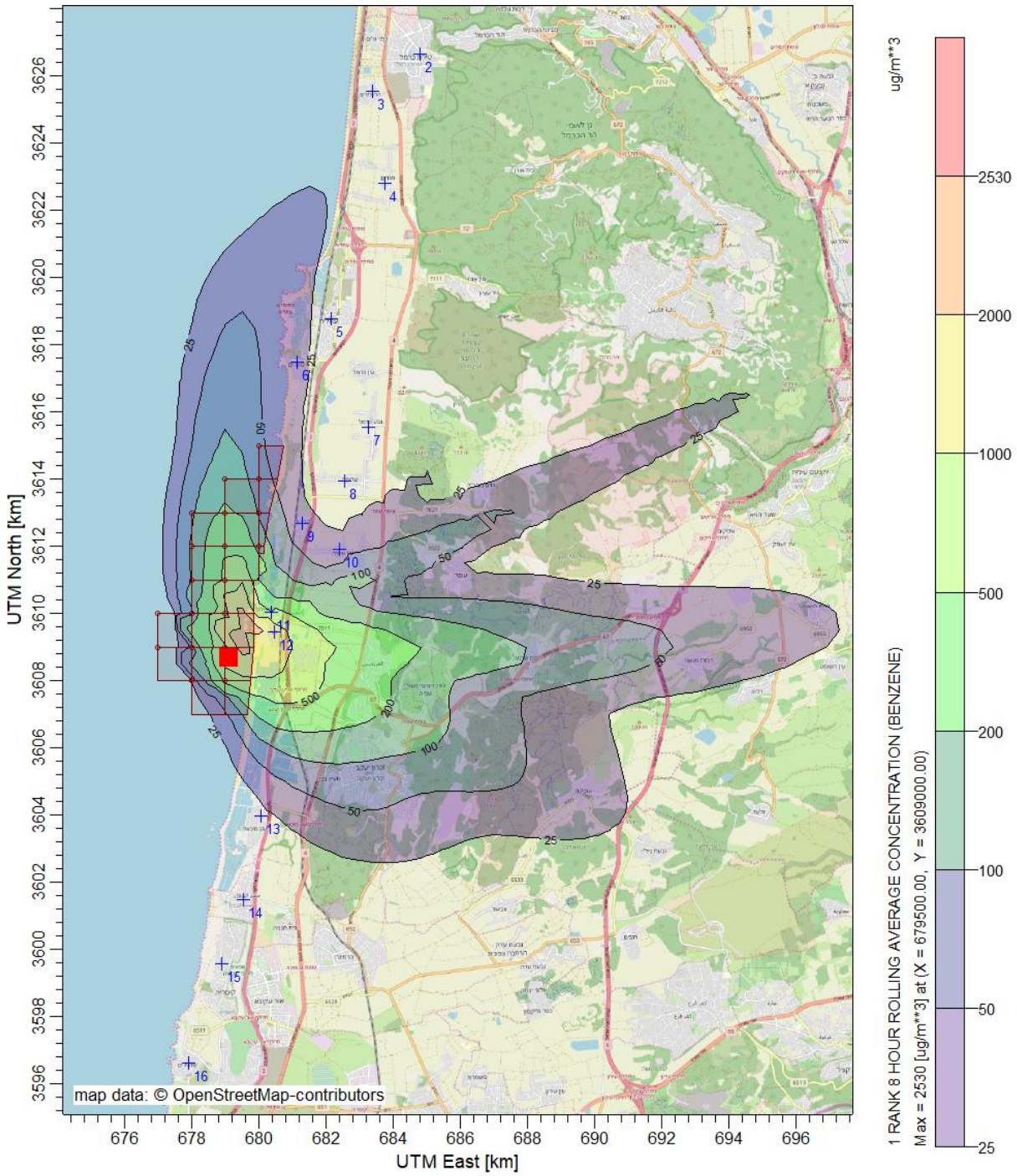

Figure 52: Scenario #6 Condensate spill - Maximum 8h-average concentration Benzene

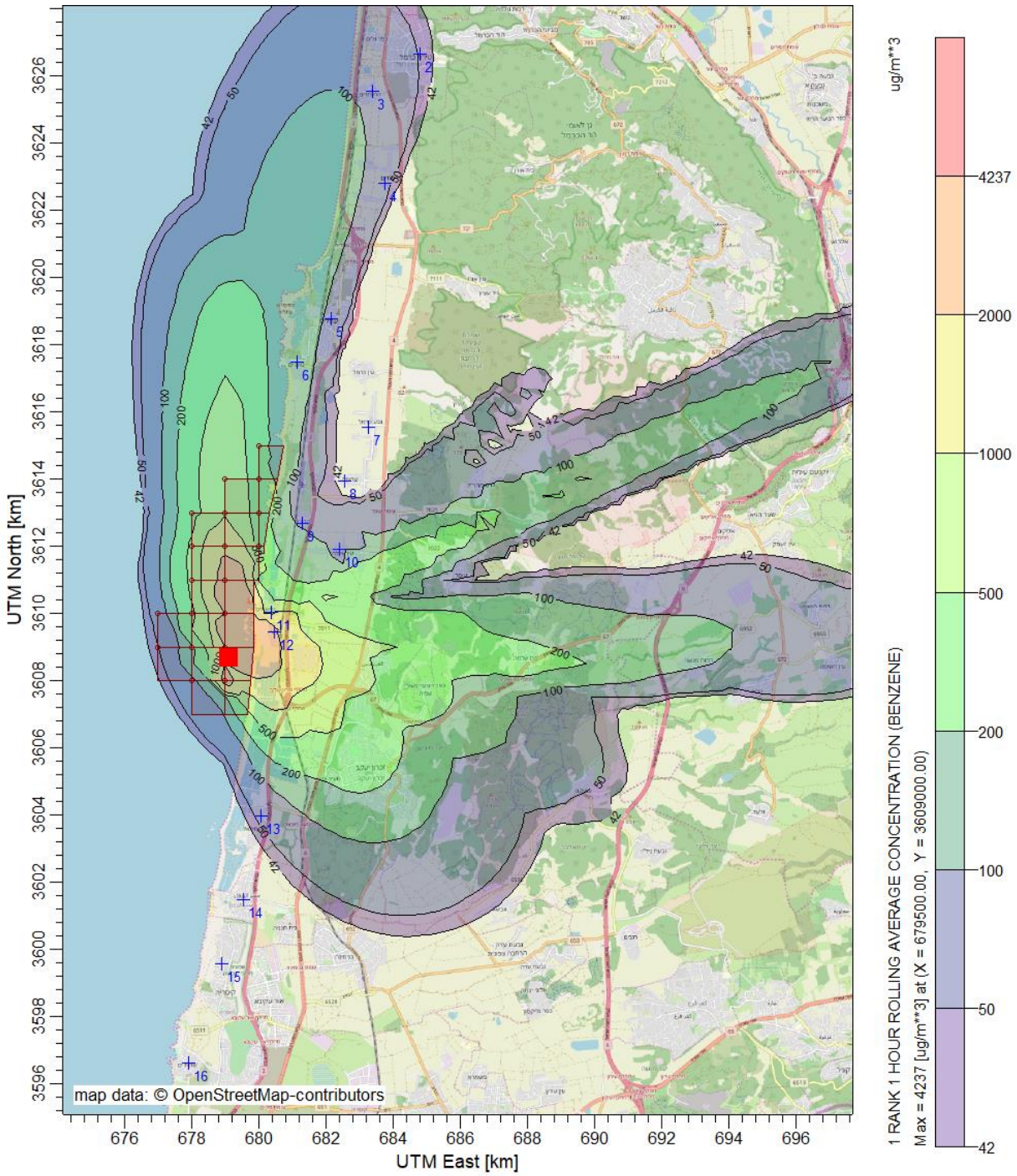

Figure 53: Scenario #6 Condensate spill - Maximum 24h-average concentration Benzene

5.7.5. Conclusion and comparison with reference threshold

In order to evaluate potential impacts on local air quality due to the hydrocarbon evaporation from an hypothetical condensate spill caused by pipeline rupture, a number of simulations have been run with the CALMET/CALPUFF modelling suite.

Each simulation was initialized with the hourly "oil-on-surface" and "oil-on-coast" outputs of the MEDSLIK experiments for selected spill start's dates. The same maximum spilled volumes are hence considered for the pipeline rupture case (3000 bbls).

Spill simulations cover 2 different wind and seasonal conditions, winter time with high wind (Scenario #5) and summer time with low velocity wind (Scenario #6)

Each spill scenario is applied respectively for simulate the dispersion of total VOCs and Benzene's hourly estimated emissions coming from MEDSLIK outputs and taking into consideration the contribution of shored oil as well.

Maximum 1h- 8h- and 24h-average onshore concentrations were compared with both Ambient Air Quality Values (as regulated by the National Clean Air Law) and international recognized thresholds for emergency condition (PACs defined by US DoE).

The following tables resumes the air dispersion results for each modelled scenario both for total VOCs and Benzene modelled species.

Table 16: Summary results for VOC Scenarios

# Scenario	Season condition	Spilled Liquid	av. wind speed (first 24h) m/s	Spill reaching coast	Max Tot VOCs (ug/m3)			
					Offshore		Onshore	
					1h	8h	1h	8h
Spill from pipeline rupture @1km from coast								
Sc5	High wind	condensate	8.4	Y	42'529	26'216	42'611	6'768
Sc6	Low wind	condensate	2.6	Y	178'150	105'980	228'560	144'550

Table 17: Summary results for Benzene Scenarios

# Scenario	Season condition	Spilled Liquid	av. wind speed (first 24h) m/s	Spill reaching coast	Max Benzene (1%) (ug/m3)				
					Offshore		Onshore		
					1h	8h	1h	8h	24h
Spill from pipeline rupture @1km from coast									
Sc5	High wind	condensate	8.4	Y	896	541	250	120	71
aSc6	Low wind	condensate	2.6	Y	4'237	2'530	3'728	2'200	884

The Regional Council Hof Ha'Carmel (Dor and Nahsholim) municipalities are the most affected areas by the vapor's cloud dispersion.

In case of massive near-shore spill caused by pipeline rupture, maximum onshore hourly concentrations of total VOCs range from 42.6 to 228.5 mg/m^3. This is approximately equal to the maximum offshore concentrations estimated for condensate spill occurring at Dor Platform, located 10km from the coast [13].

Precautionary assumed equal to 1%$_{w/w}$ of the spilled oil, Benzene maximum onshore hourly concentrations range from 250 to 3728 ug/m3 (0.25 and 3.8 mg/m^3 respectively).

During low-wind conditions (scenario #6), the vapor cloud is slightly dispersed during its travel from the spill location to the coast and high levels are anticipated on the nearby coastal receptors.

5.8. Regulation threshold violation

The following graphs are useful to compare the modelled results with the applicable thresholds. Results from the pipeline-rupture scenarios (Red-Cross) are superimposed on the values estimated from the previous platform-spill experiments [13].

Out of benzene (no PAC Violation expected), the other available PACs are not directly applicable to the (unknown) VOC mixture emitted during the spill.
Thus, we can't state if there will be or not a PAC violation of single VOC species, in case of massive spill from near coast pipeline rupture.
This cannot be excluded, mainly due to the lack of information of condensate VOC speciation.
The above clarification is clear evidently from the submitted conclusion of the evaporation in the supplementary report."
Moreover the following facts should be considered:

1. Condensate speciation for >C10 VOCs is unknown or at least was not disclosed to us for the needs of the supplementary report
2. PACs for Leviathan vapor mixture are not available in the literature.
3. Temptative comparison[9] of total-VOCs estimations with available single-VOC PACs could be highly cautionary.

[9] PACs are relevant to single substance or known mixtures (eg jet fuel). Compare total VOC concentrations of an unknown VOC mixture to a single substance PAC could lead to high underestimation or overestimation of the overall nuisance effect, depending on the toxicity of the selected compound and the actual composition of the mixture (and also the actual content of the selected compound in the mixture). Eg we have no evidence that c10-c11-c12 are representative of the overall condensate vapors. The formula "it cannot be excluded" is intrinsically cautionary. On the other hand a smoking gun cannot be identified.

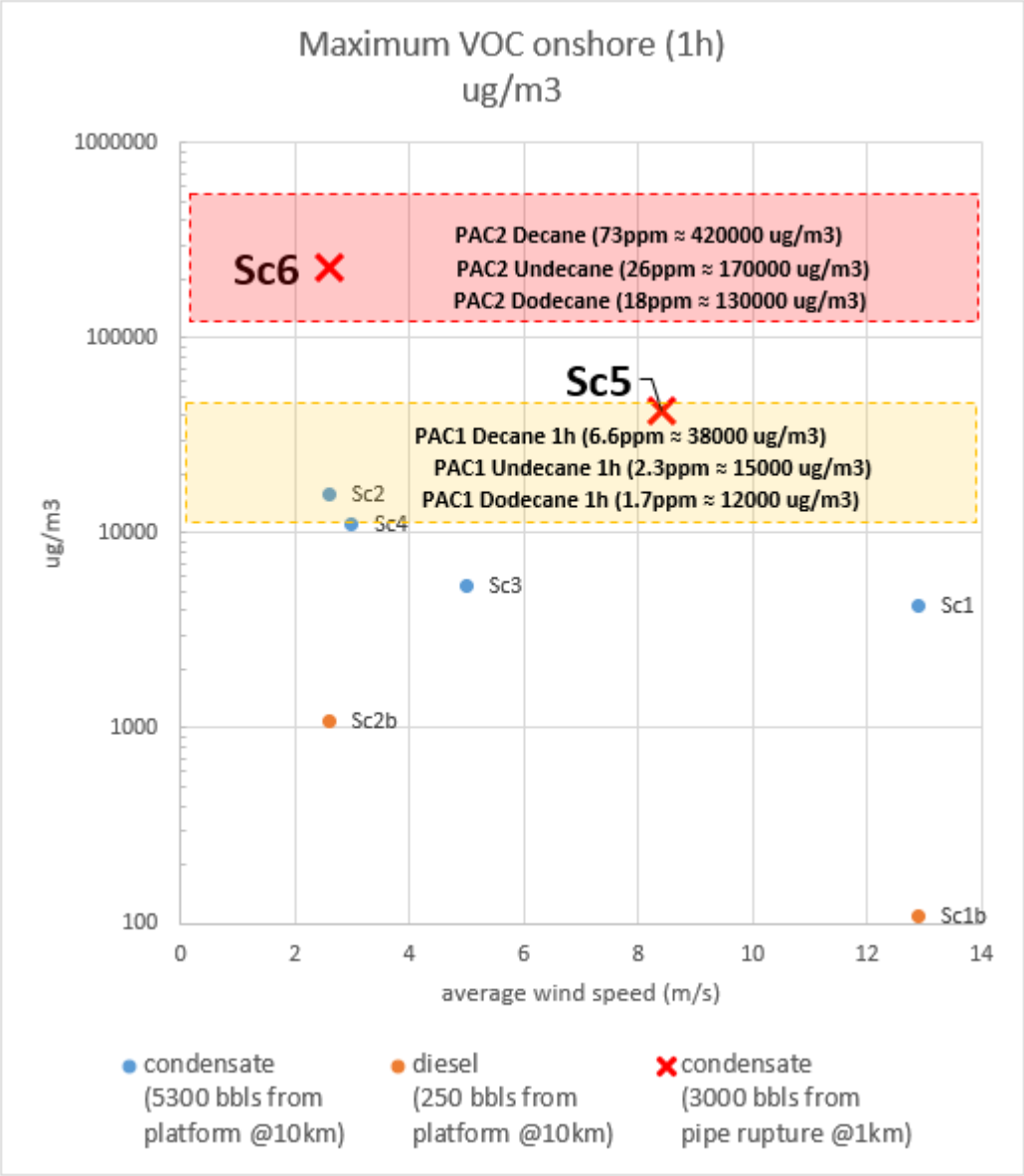

Figure 54: Comparison of estimated maximum onshore hourly concentrations for Total VOCs and emergency PACs thresholds for selected alkanes (C10-C12)

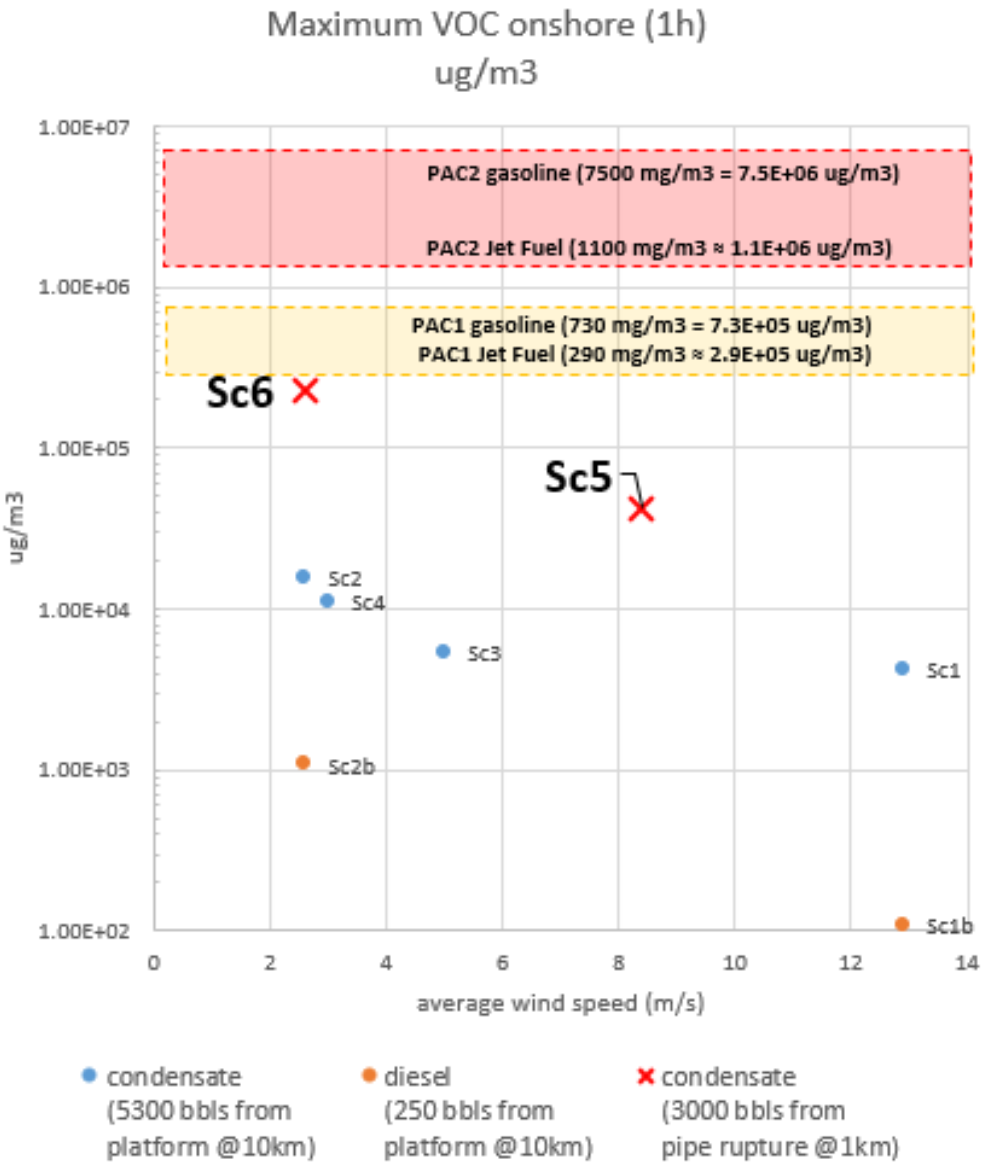

Figure 55: Comparison of estimated maximum onshore hourly concentrations for Total VOCs and available emergency PACs thresholds for hydrocarbon mixtures (automotive unleaded gasoline and jet fuels)

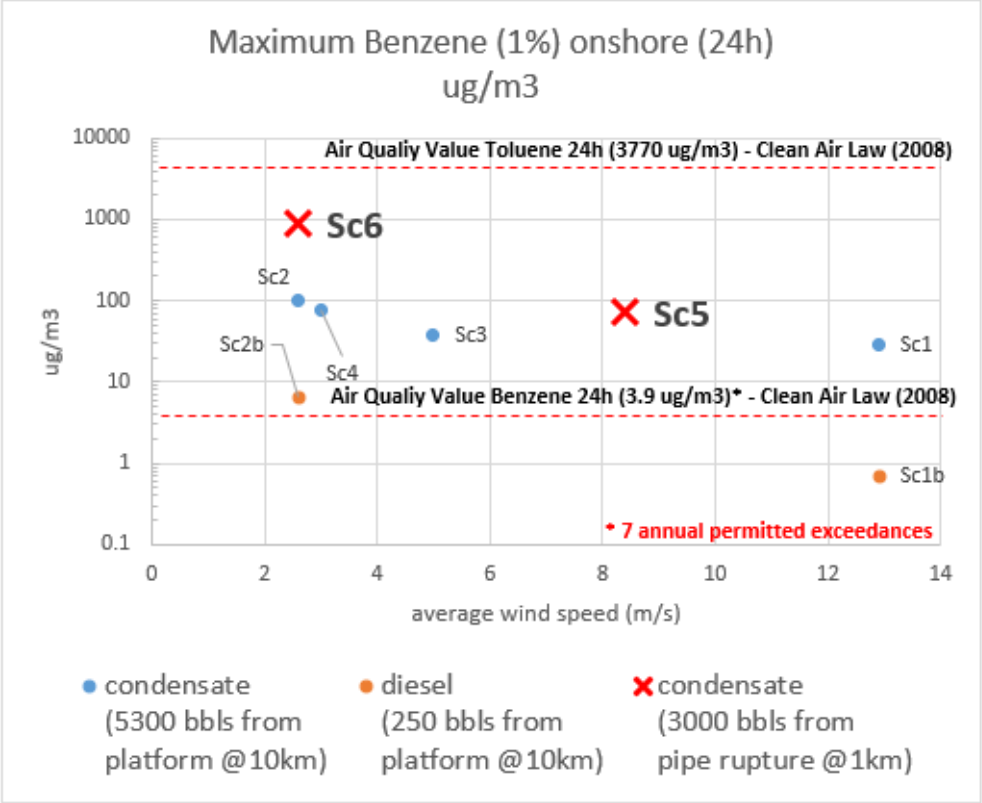

Figure 56: Comparison of estimated maximum onshore daily concentrations for Benzene and Israeli Air Quality Value for Benzene and Toluene

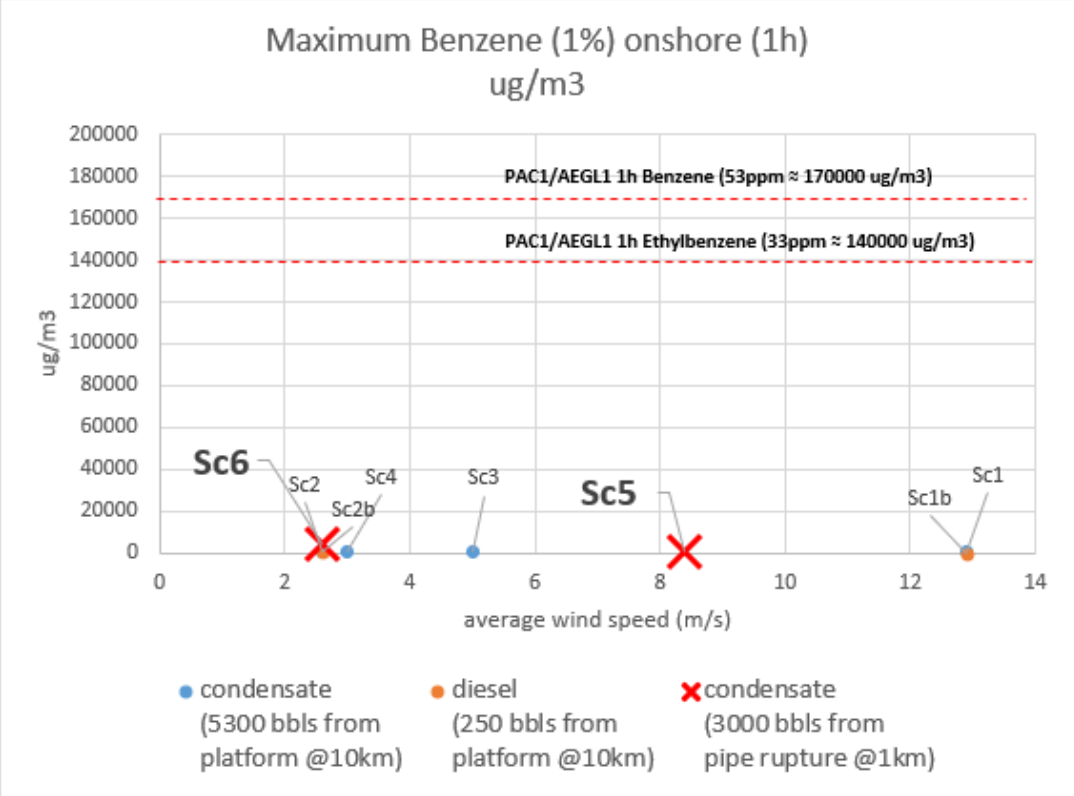

Figure 57: Comparison of estimated maximum onshore hourly concentrations for Benzene and emergency PACs thresholds for selected BTEX (Benzene and Ethylbenzene)

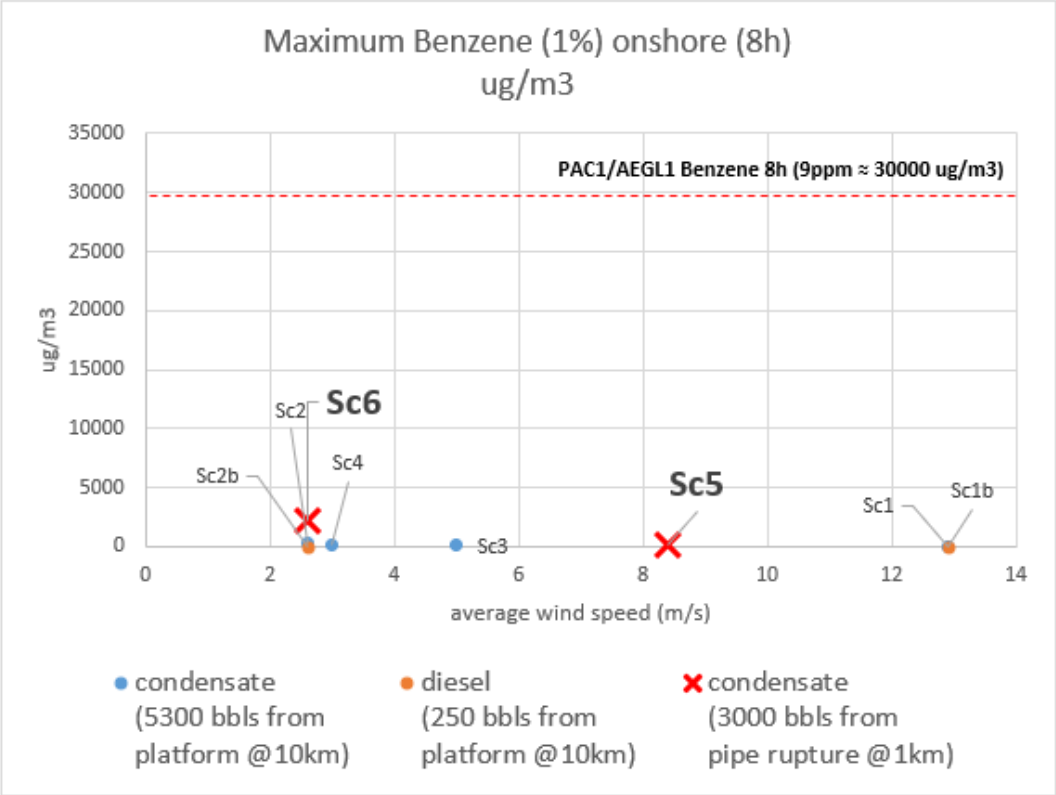

Figure 58: Comparison of estimated maximum onshore 8-hours concentrations for Benzene and emergency PACs thresholds for Benzene

Massive near coast condensate spills (3000 bbls) are likely to result into temporary exceedances of the 24-hours Ambient Air Quality Value of Benzene (3.9 ug/m3), but within the permitted number of exceedances by the National Regulation (maximum 3 days of exceedance, against 7 yearly permitted events).

On the other side, no exceedance of Acute Exposure Guidelines (PAC/AEGLs) are anticipated for Benzene and the other BTEXs, simulated levels being at least 1 order of magnitude lower than the relevant tier-1 thresholds (the lowest being: Benzene 8h: 9 ppm; Ethylbenzene 1h: 22 ppm) .

Low-wind conditions could result in high coastal concentrations of Total VOCs, with levels on the same order of magnitude of emergency public exposure guidelines (PAC2) for C10, C11 and C12 alkanes (respectively: 6.6 ppm, 2.3 ppm and 1.7 ppm). Tier-2 effects (irreversible or other serious, long-lasting, adverse health effects or an impaired ability to escape), cannot be excluded for the exposed population in case of massive condensate spill event such as those under study.

It is worth to be noted that no threshold level was found in literature for Total VOC. Due to the lack of data about the exact composition of the condensate, especially for hydrocarbons C>10 (90% v/v of the mixture), here the comparison is cautionary performed between Total VOC concentrations and single hydrocarbon (alkanes) PAC thresholds. This means that the comparison may be overly conservative, although the presence of other compounds[10] and of the overall mixture should also considered. For example, if the C10-C11-C12 Alkanes represent the 10% of the evaporated C>10 mixture, ground concentrations of this compounds could be roughly anticipated to be lower than relevant PAC1 and PAC2 thresholds.

Moreover, it should be noted that PACs are not directly applicable to releases of chemical mixtures such as those under study, as the potential additive, synergistic, or antagonistic effects that may result from exposures to multiple chemicals are not accounted for. Chemicals in combination may behave differently than when alone, and predicting the toxic potential of a mixture is often very difficult[11]. A chemical mixture methodology (CMM) should be used for estimating the potential health impact of exposures involving multiple chemicals[12].

To partially cover the gap, a tentative comparison with available PACs thresholds for hydrocarbons mixture (i.e. automotive unleaded gasoline and Jet Fuels) could be performed. Estimated maximum onshore concentrations of Total VOCs are lower than both PAC1 and PAC2 relevant thresholds, approaching PAC1 in low-wind conditions.

It should be noted that referenced PACs for gasoline and Jet Fuel mixtures are not directly applicable to actual (currently undefinable) mixtures such as those under study. The potential additive, synergistic, or antagonistic effects that may result from exposures to different hydrocarbon mixtures should be taken into account.

[10] S. Stout & Z. Wang (2017). Oil Spill Environmental Forensics Case Studies. Edited by Scott Stout, Zhendi Wang. Butterworth-Heinemann, 22 October 2017.

[11] Government of Alberta. (2017). *Protective Action Criteria: A Review of Their Derivation, Use, Advantages and Limitations*. Environmental Public Health Science Unit, Health Protection Branch, Public Health and Compliance Division, Alberta Health. Edmonton, Alberta.

[12] A chemical mixture methodology (CMM) has been developed by the US DOE SCAPA subcomitee for estimating the potential health impacts of exposures involving multiple chemicals. https://sp.eota.energy.gov/EM/SitePages/SCAPA-Home.aspx

5.9. Conclusions

The lack of detailed data about hydrocarbon speciation of potential spilled condensate does not allow to get a ultimate judgment on the harmfulness of VOC vapor mixture on potential exposed communities in case of Massive near coast condensate spills.

While maximum estimated onshore levels of Benzene are well below internationally recognized emergency thresholds (USEPA PACs/AEGLs) and maximum total VOCs do not reach available level-1 thresholds for hydrocarbon mixture (relevant to gasoline and jet fuels), the cautionary comparison of maximum onshore concentration of total VOCs with selected C10-C12 Alkanes threshold raise concerns, with onshore peaks on the same order of magnitude of level-2 emergency public exposure guidelines (PAC2).

Chemicals in combination may behave differently than when alone; predicting the toxic potential of a mixture is often very difficult[13]. A chemical mixture methodology (CMM) should be used for estimating the potential health impact of exposures involving multiple chemicals[14].

The speciation and concentration of airborne volatile compounds should be carefully monitored in case of spill. In the absence of additional data, a warning communication plan should also be activated in order to alert communities and minimize their exposure to vapor plumes in the area of major impact, especially in case of a near-coast spill with low-winds blowing towards coast.

[13] Government of Alberta. (2017). *Protective Action Criteria: A Review of Their Derivation, Use, Advantages and Limitations*. Environmental Public Health Science Unit, Health Protection Branch, Public Health and Compliance Division, Alberta Health. Edmonton, Alberta.

[14] A chemical mixture methodology (CMM) has been developed by the US DOE SCAPA subcomitee for estimating the potential health impacts of exposures involving multiple chemicals. https://sp.eota.energy.gov/EM/SitePages/SCAPA-Home.aspx

6. Grey Water Spillage

6.1. Definitions

Grey water is domestic sewage which originates from bathrooms and laundries and constitutes the largest flow of waste water. It includes the water from both tubs showers hand basins laundry tub, floor wastes and washing machines (E. Nolde, 1999).

Grey water contains significant amounts of nutrients particularly nitrogen and phosphorus. It is high in suspended solids, turbidity and oxygen demand.
The microbial quality of grey water is depended on the presence of faecal contamination. Washing machines bathroom sink shower and kitchen sink water contains 3.44x 10^6 number of faecal coliforms per 100ml (J. Ottosson, T. A. Stenstrom, 2003).

Viruses can also be found in grey water (Dixon A, Butter D, Fewkes A, 1999,).

The present of faecal pollution in grey water will give an indication that grey water contains etiological agents that can caused infections to humans (Dixon A, Butter D, Fewkes A, 1999,).

6.2. Simulation setup

6.2.1. Data

The quantities of grey water and product water including chemicals dissolved in it are described and listed in paragraph 3.9.2 Discharges to sea page 89. Chemicals permitted discharges are listed in Table 3.11 page 91 (*Table 18*) and flow rate quantities in Table 3.12 page 92 (*Table 19*) , applicable document [1] and official translation applicable document [3] paragraph 3.9.2 Discharges to sea page 89, Chemicals permitted discharges are listed in Table 3.11 page 91(*Table 18*) and flow rate quantities in Table 3.12 page 92 (*Table 19*). In addition discharge quantities and compositions are found in Annex 6.3 applicable document [1.1] Section 3.1 discharge quality Table 3-1 discharge quality page 249 and section 4.0 Discharge quantities page 250.

Table 18: Product water permitted discharges concentration thresholds [1] [3]

Parameter	Units	Average value	Maximum value
Produced water			
Mineral oil (FTIR)	mg/L		15
Total oil and grease (FTIR) – for the first 6 months run-in period.	mg/L	29	42
Total oil and grease (FTIR) - after the first 6 months	mg/L	15	21
BTEX	mg/L	5	
TOC – for the first 12 months run-in period	mg/L	2,100	10,000
TOC – after the first 12 months	mg/L	500[1]	
Total suspended solids (TSS) (105°C)	mg/L	30	100
Oil water separator (open drain)			
Mineral oil (FTIR)	mg/L		15
Total oil and grease (FTIR)	mg/L		30
Sanitary waste (Black Water)			
Free Chlorine	mg/L		0.3
Total suspended solids (TSS) (105°C)	mg/L		50
Total BOD	mg/L		50
Turbidity	NTU		50
Grey Water[2]			
Total suspended solids (TSS) (105°C)	mg/L		50
Total oil and grease (FTIR)	mg/L		50
Turbidity	NTU		50
All streams			
pH			6.0<pH<9.5

1. The value will be reviewed, in collaboration with the Ministry of Environmental Protection, 9 months after the commencement of production.
2. In case of grey water, we are dealing with target values rather than enforcement values.

Table 3.11: Permitted discharge concentration thresholds after treatment for the various water streams

Table 19: Product water and flow rate quantities [1] [3]

Current	Max. Daily flow (m^3)	Annual flow (m^3)	Notes
Production water	800	200,000	Calculated according to the gas characteristics from the reservoir and the gas production quantities
Open drain water and leachate	793	50,000	Calculated according to precipitation forecast and current operation
Sanitary waste_water	20	5,000	Calculated by the number of people expected on the platform (0.1 m^3 / person)
Grey water	20	6,000	Calculated by the number of people expected on the platform (0.13 m^3 / person)
Cooling water	85,200	21,000,000	Calculated according to pump capacity and operation
Brine	20	4,867	Calculated according to the data of the seawater desalination system on the platform
Extinguishing water	1,800	-	Calculated according to pump flow, working days and expected testing

Table 3.12: Maximum daily flow and expected annual flow rate (m^3)

Table 20: Discharge quality page 249 annex 6.3 [1.1] Section 3.1

Table 3-1 Discharge Quality

Parameter	Units	Average value	Maximum value
Produced water			
Mineral oil (FTIR)	mg/L		15
Total oil and grease (FTIR) – for the first 6 months run-in period.	mg/L	29	42
Total oil and grease (FTIR) – after the first 6 months	mg/L	15	21
BTEX	mg/L	5	
TOC – for the first 12 months run-in period	mg/L	2,100	10,000
TOC – after the first 12 months	mg/L	500(1)	
Total suspended solids (TSS) (105°C)	mg/L	30	100
Total nitrogen (TN)(2)			
Total phosphorus (TP)(2)			
Oil water separator (open drain)			
Mineral oil (FTIR)	mg/L		15
Total oil and grease (FTIR)	mg/L	29	42
Sanitary waste (Black Water)			
Free chlorine	mg/L		0.3
Floating solids (TSS) (105°C)	mg/L		50
Total BOD	mg/L		50
Turbidity	NTU		50
Gray Water(3)			
Floating solids (TSS) (105°C)	mg/L		50
Total oil and grease (FTIR)	mg/l		50
Turbidity	NTU		50
All streams			
pH			6.0<pH<9.5

Notes:

(1) Average target value will be 500 mg/l 12 months after Leviathan production begins. This 500 mg/l average value will be reassessed with the MOEP 9 months after Leviathan production begins and adjusted as necessary based on actual field data trends and production profiles.

(2) There is no enforceable specification for TN and TP. Specifications will be addressed with the MOEP once suitable and sufficient operating data is available after Leviathan start-up to accurately forecast a trend.

(3) Specifications for gray water discharge represent target values only, not enforceable limits.

Table 21: Discharge quantities page 250 annex 6.3 [1.1] Section 3.1

4.0 DISCHARGE QUANTITIES

Discharge quantities are estimated as follows:

Stream	BBL per day	M^3 per day
Produced water	up to 5,000	up to 800
Open drain	up to 3,500	up to 560
Sanitary waste	up to 125	up to 20
Gray water	up to 150	up to 24
Cooling water	up to 535,000	up to 85,200
Water maker brine	up to 125	up to 20

6.2.2. Model

6.2.2.1. Grey water simulation for accidental release from the Dor offshore platform

In order to map the grey water hazard, 104 scenarios were carried out during the current simulations using the MEDPOL general dispersion model, which is included as one of the MEDSLIK module. MEDPOL is a 3-dimentional pollutant convection-diffusion model and is designed to be user-friendly. In MEDPOL the transport of the pollutant cloud is governed by the sea currents. Direct wind forcing acts on parcels of pollutant on or near the surface. Convection and diffusion of the pollutant is modelled by a random walk model (Monte Carlo method). The effluent is modelled as a cloud of 20,000 Lagrangian parcels, each of which undergoes a convective displacement in accord to the sea currents and a random displacements in horizontal & vertical directions according to the diffusion parameters. The pollutant may or may not be conservative. If non-conservative the parameters of the half-life for its decay must be entered, or the present simulations the pollutant was considered conservative. MEDPOL has been used in the past in the frame of EU project, such as the MFSTEP for simulating the dispersion of nutrients from the coastal sea aquaculture cages, as well as in environmental studies to estimate the sand dispersion and deposition from the deepening of port facilities in Cyprus.

The scenarios corresponded to the numerical simulation of the dispersion of the continues leakage of the grey water originated from the Dor offshore platform located 10 km from the coastline, for 360h ahead. The procedure was repeated for 104 using a combination of ocean and atmospheric re-analyses conditions produced every 15 days from 01/01/2015 to 31/12/2018. The MEDPOL model, by ingesting ocean (i.e. CYCOFOS sea currents, as well as CYCOFOS waves) and atmospheric fields (i.e. SKIRON

winds at 10m) reproduces the three-dimensional dispersion of continues leakage of the grey water from the offshore platform in the marine environment. The grey water concentrations at five water layers (0-5m, 5-10m, 10, 20m, 20-40m and the total water column), are integrated in hourly basis with 100m spatial resolution. The ensemble experiment setup for the grey water leakage from the Dor offshore platform is summarized in the *Table 22*.

Table 22: Ensemble of the grey water leakage from the Dor offshore platform experiment setup summary

#	Parameter	Value
1.	Dor fixed platform coordinates	32º 35’ 55.76’’ N and 34º 48’ 21.55’’ E
2.	Type of leakage	grey water
3.	Spilled volume	20 m3/day
4.	Spill duration	continues
5.	Simulation length	360 hours
6.	Hydrodynamic fields	6- hourly CYCOFOS downscaled from CMEMS MFC Med at a horizontal resolution of 1.8km
7.	Wind fields	hourly, SKIRON at a horizontal resolution of 10km
8.	Wave fields	3-hourly, CYCOFOS at a horizontal resolution of 10km
9.	Horizontal turbulent diffusion	2 m^2/s

6.2.2.2. Overview of the grey water continues simulation outputs

1. An ensemble of 104 spills maps were simulated every 15 days for up to 15 days ahead, during the period of 2015-2018.
2. 360 hours simulation outputs were produced.

5 sets of maps at 24housr, 48 hours, 73 hours, 120 hours, 240hours and 360 hours were produced be-weekly: ensemble averaged concentrations at the water layers: 0-5m, 5-10m, 10-20m, 20-40, total water column.

6.3. Results

6.3.1. Results of the current model simulations for the grey water

6.3.1.1. Extreme winter storm conditions (December -January 2015-2018)

December 2015-2018

From the 1st day of the above period (*Figure 59*a) the extent of the grey water dispersion increased to the 5th day (*Figure 59*b; *Figure 60* a; b). The grey waters dispersed very close to the shoreline only after the 10th day (*Figure 61* a;b) transported at the coastal waters along the shoreline between Hadera and Nahariya with high concentrations at certain areas, particularly along the coastal waters of Atlit, Acre and Nahariya shoreline on the 15th day *Figure 61* b).

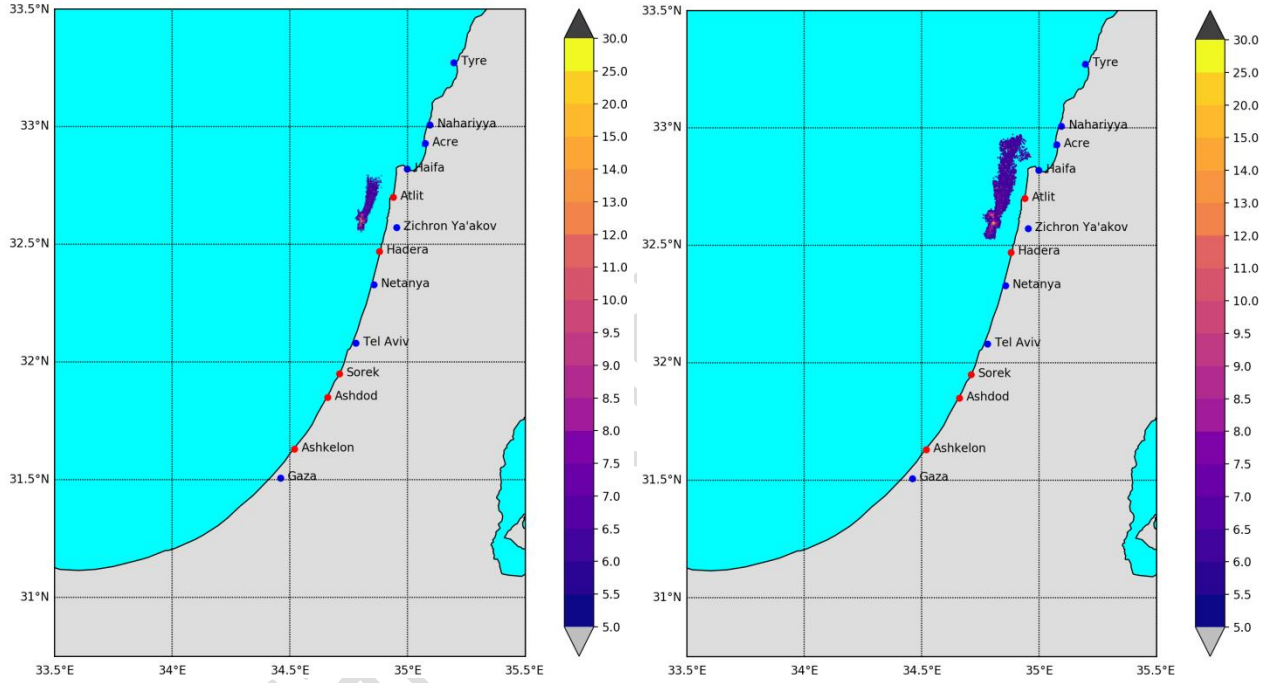

Figure 59: Mean averaged concentration of the grey water dispersed in the entire water column

Figure 59a (left): Mean averaged concentration of the grey water dispersed in the entire water column (m^3/km^2) from the offshore Dor platform on the 1 day from the spillage, December 2015-2018.

Figure 59b (right): Mean averaged concentration of the grey water dispersed in the entire water column (m^3/km^2) from the offshore Dor platform on the 2 day from the spillage, December 2015-2018.

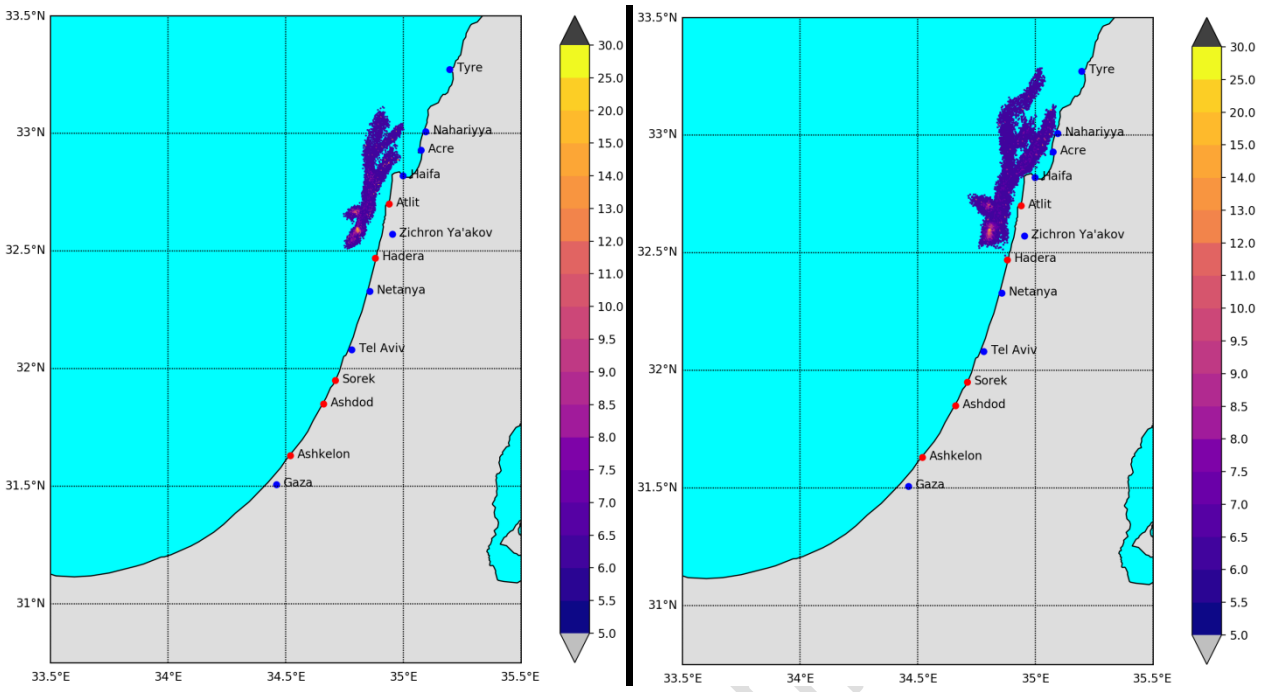

Figure 60: Mean averaged concentration of the grey water dispersed in the entire water column

Figure 60a (left):Mean averaged concentration of the grey water dispersed in the entire water column (m^3/km^2) from the offshore Dor platform on the 3rd day from the spillage, December 2015-2018.

Figure 60b(right):Mean averaged concentration of the grey water dispersed in the entire water column (m^3/km^2) from the offshore Dor platform on the 5th day from the spillage, December 2015-2018.

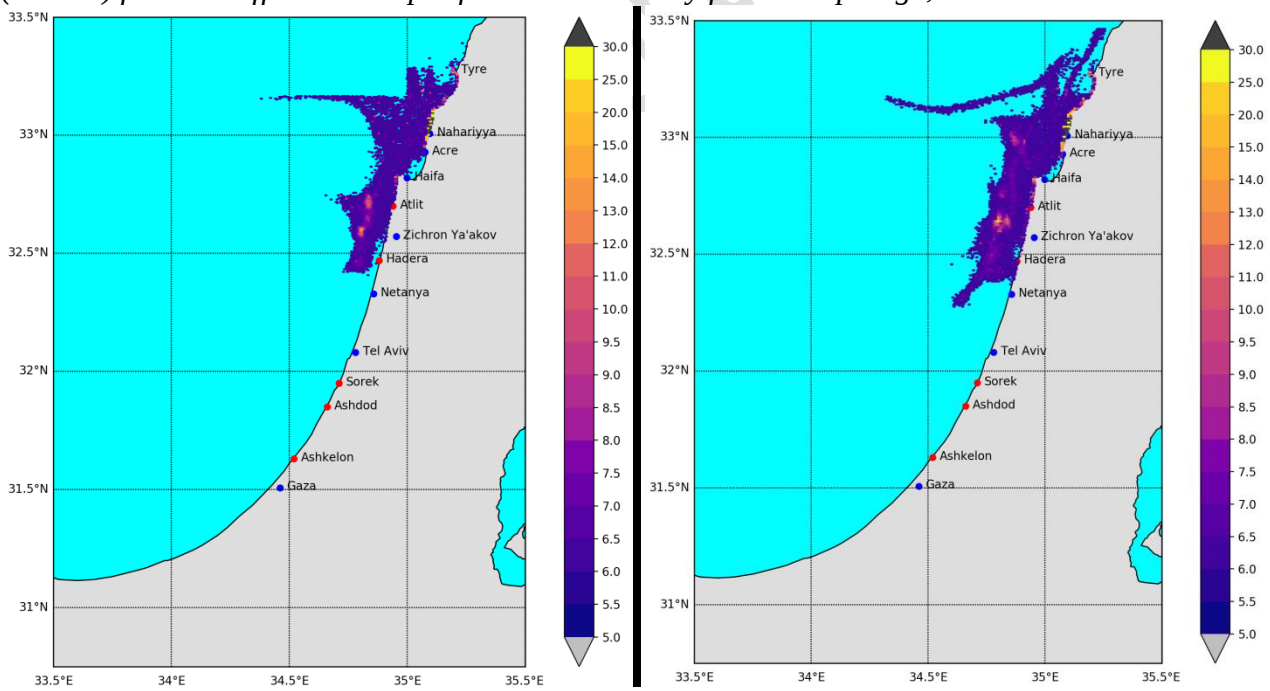

Figure 61: Mean averaged concentration of the grey water dispersed in the entire water column

Figure 61 a (left): Mean averaged concentration of the grey water dispersed in the entire water column (m^3/km^2) from the offshore Dor platform on the 10th day from the spillage, December 2015-2018.

Figure 61 b(right): Mean averaged concentration of the grey water dispersed in the entire water column (m^3/km^2) from the offshore Dor platform on the 15th day from the spillage, December 2015-2018.

January 2015-2018

During this period there is a general lower dispersion compared to the December period from the 1st day (*Figure 62* a) and the days after 2nd and 5th day (*Figure 62* b; *Figure 63*a, *Figure 63*b), for which higher concentrations of grey waters were simulated along the coastal waters of the Zichron-Ya'akov coastline. On the 10th day (*Figure 64*a) the grey water plume reaches the Nahariyya coastal waters with high concentrations between Zichron-Ya'akov to Atlit. On the day 15th (*Figure 64*b) the plume of the grey waters extended at the coastal waters along the shoreline between south of Hadera to Atlit and Shikmona with the highest concentrations of the grey water regardless of the season during the period 2015-2018 and between Acre and north of Nahariyya with high but lower concentrations than in the southern coastal sea areas.

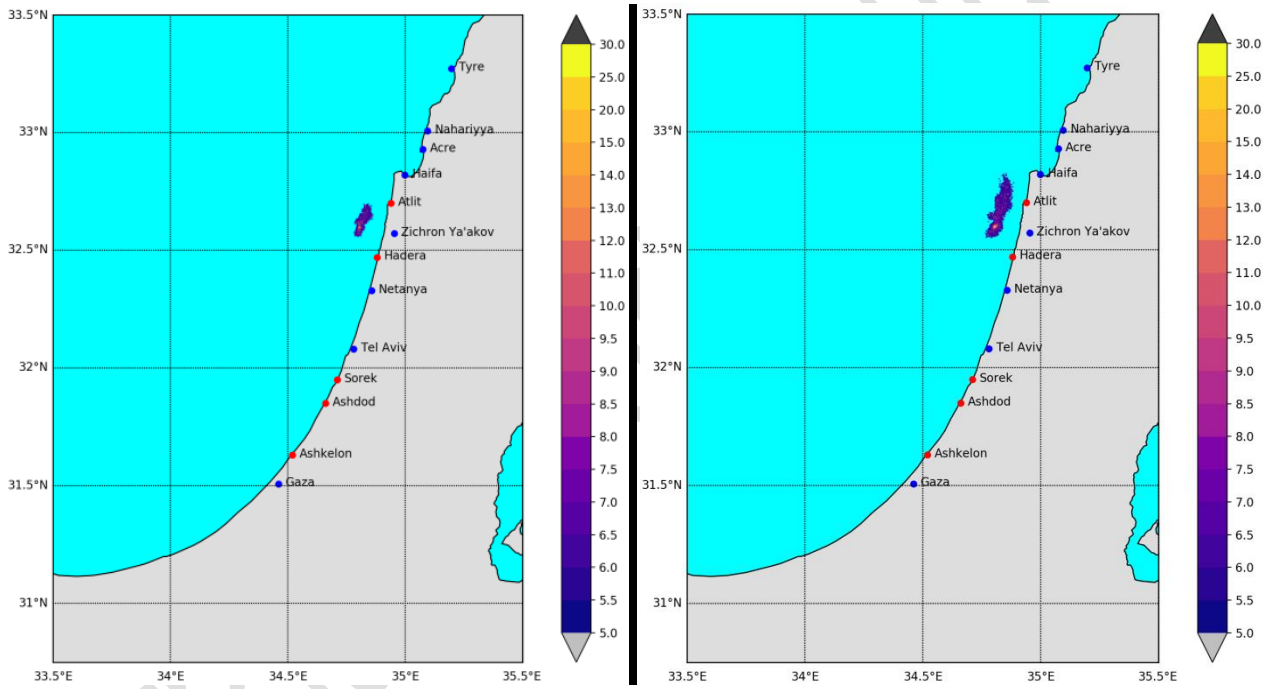

Figure 62: Mean averaged concentration of the grey water dispersed in the entire water column

Figure 62a (left): Mean averaged concentration of the grey water dispersed in the entire water column (m3/km2) from the offshore Dor platform on the 1 day from the spillage, January 2015-2018.
Figure 62b (right): Mean averaged concentration of the grey water dispersed in the entire water column (m3/km2) from the offshore Dor platform on the 2 day from the spillage, January 2015-2018.

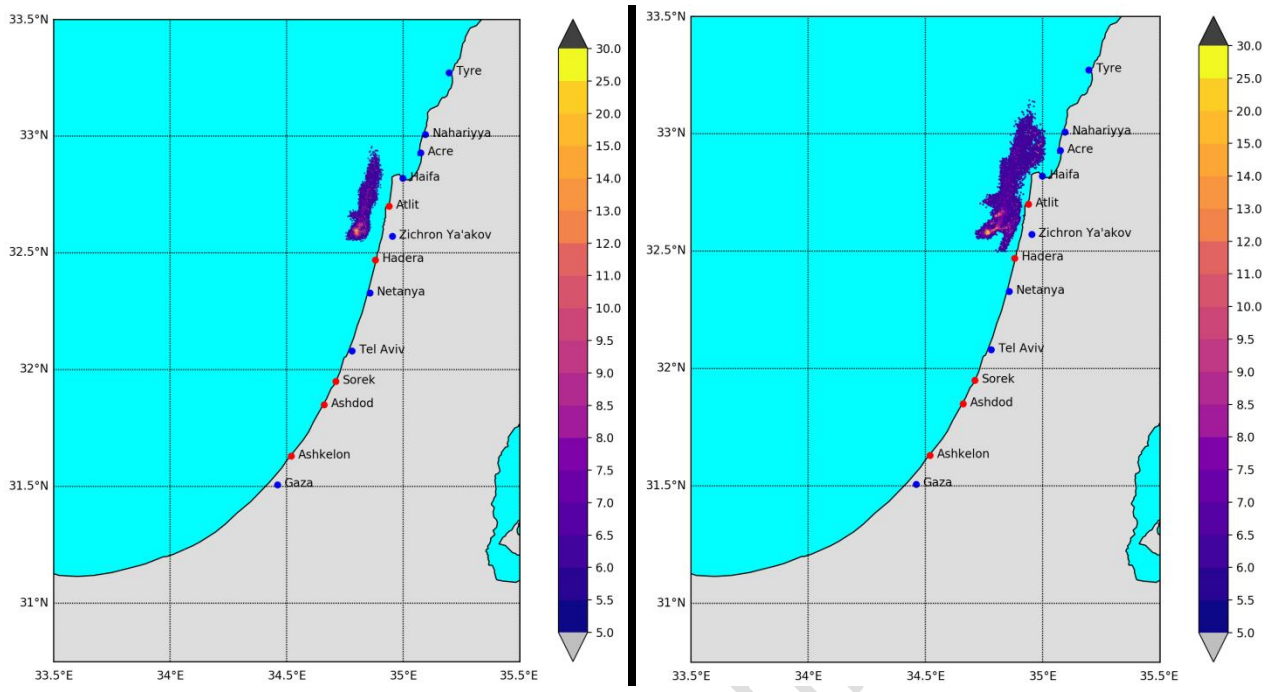

Figure 63: Mean averaged concentration of the grey water dispersed in the entire water column

Figure 63a (left): Mean averaged concentration of the grey water dispersed in the entire water column (m^3/km^2) from the offshore Dor platform on the 3rd day from the spillage, January 2015-2018.

Figure 63b (right): Mean averaged concentration of the grey water dispersed in the entire water column (m^3/km^2) from the offshore Dor platform on the 5th day from the spillage, January 2015-2018.

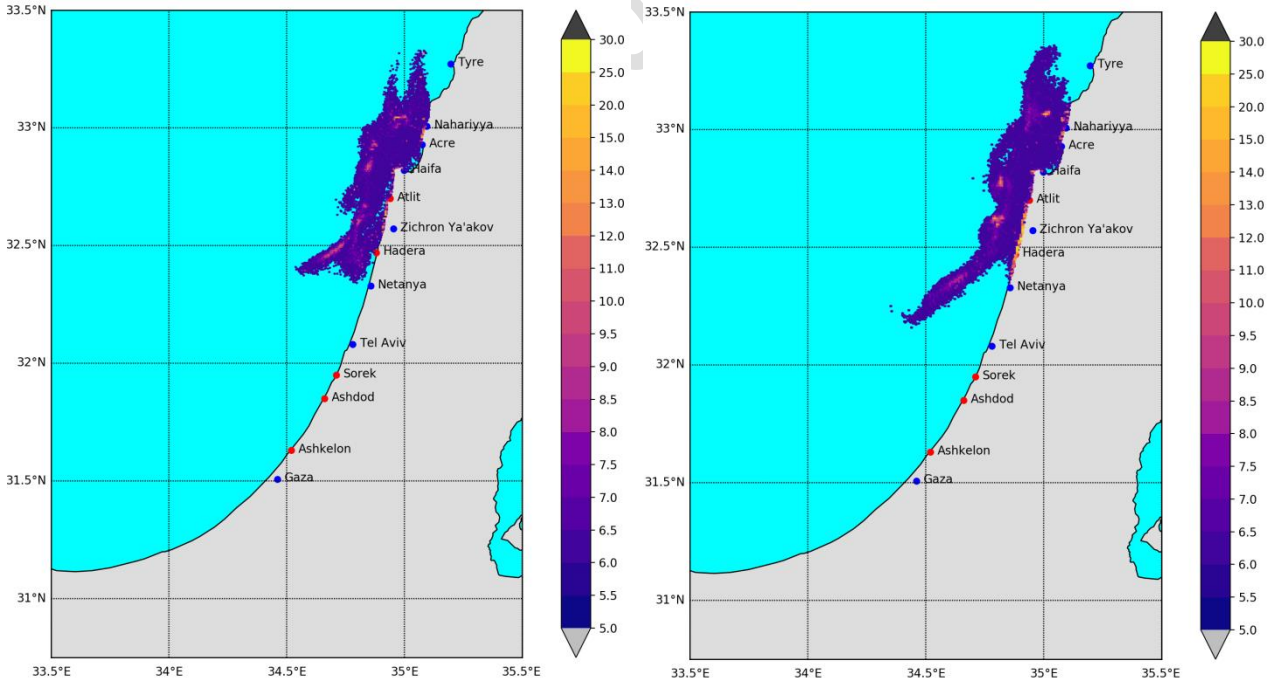

Figure 64: Mean averaged concentration of the grey water dispersed in the entire water column

Figure 64a(left): Mean averaged concentration of the of the grey water dispersed in the entire water column (m^3/km^2) from the offshore Dor platform on the 10th day from the spillage, January 2015-2018.
Figure 64b(right): Mean averaged concentration of the of the grey water dispersed in the entire water column (m^3/km^2) from the offshore Dor platform on the 15th day from the spillage, January 2015-2018.

6.3.1.2. Typical winter conditions (January-February 2015-2018)

During typical winter the grey water plume remains at sea offshore from the 1st to the 5th day (*Figure 65* a; b) and only after the 10th day (*Figure 66* a) came closer to coastal waters along the shoreline between Zichron-Ya'akov and Nahariya. On day 15th day (*Figure 66* b) the grey water plume reaches the coastal water along the shoreline between Atlit and Zichon-Ya'akov, but there were considerable higher concentration offshore.

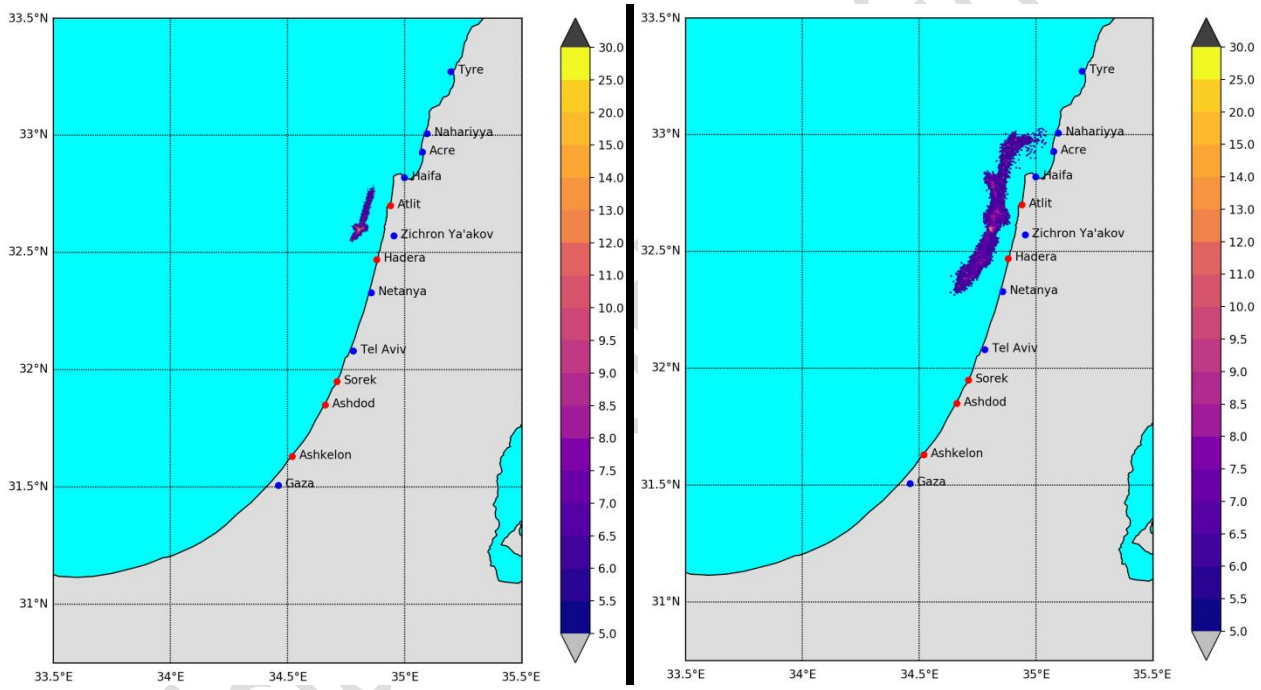

Figure 65: Mean averaged concentration of the grey water dispersed in the entire water column
Figure 65 a(left): Mean averaged concentration of the of the grey water dispersed in the entire water column (m^3/km^2) from the offshore Dor platform on the 1st day from the spillage, January - February 2015-2018.
Figure 65 b(right): Mean averaged concentration of the of the grey water dispersed in the entire water column (m^3/km^2) from the offshore Dor platform on the 5th day from the spillage, January-February 2015-2018.

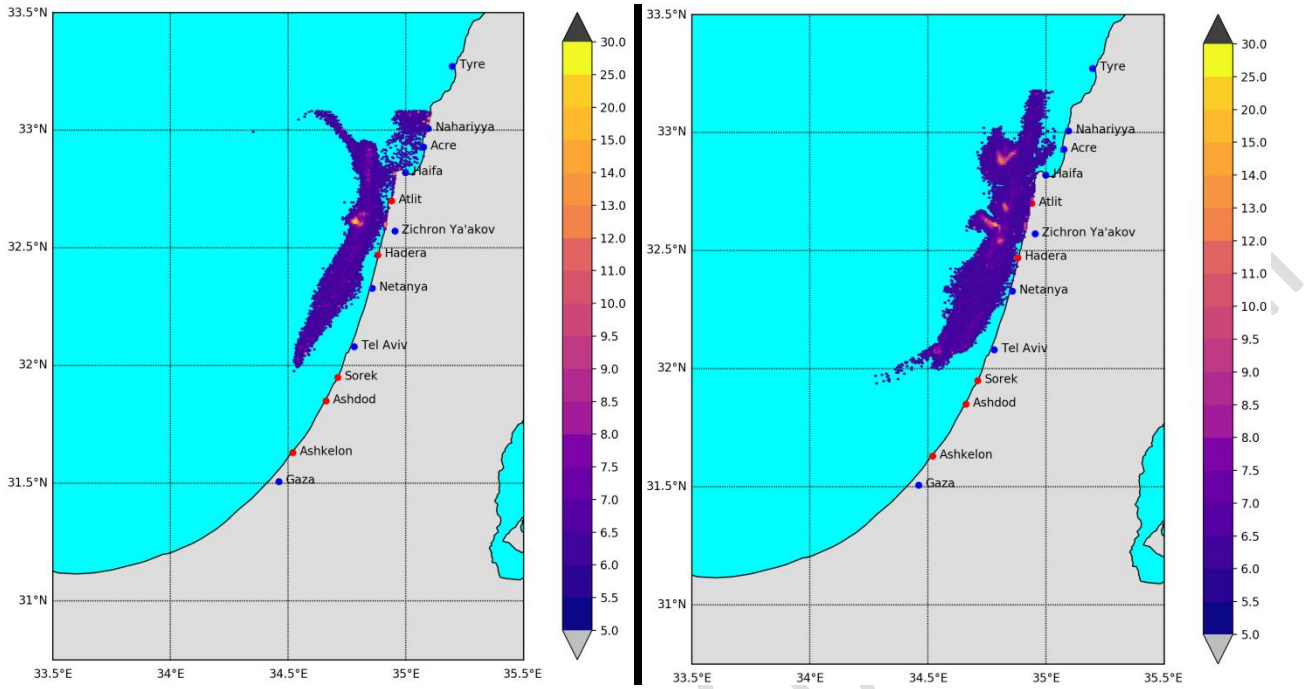

Figure 66: Mean averaged concentration of the grey water dispersed in the entire water column

Figure 66 a(left): Mean averaged concentration of the grey water dispersed in the entire water column (m^3/km^2) from the offshore Dor platform on the 10th day from the spillage, January-February 2015-2018.
Figure 66 b(right): Mean averaged concentration of the grey water dispersed in the entire water column (m^3/km^2) from the offshore Dor platform on the 15th day from the spillage, January-February 2015-2018.

6.3.1.3. Typical summer conditions (July-August 2015-2018)

July 2015-2018

The grey water plume dispersed from the 1st day to the 5th day (*Figure 67* a, b) away from the coastal waters, even until the 10th day (*Figure 68* a) does not reach close to the shore. Only on the 15th day (*Figure 68* b) the grey water plume came closer to coastal waters, along the shoreline of Acre and Nahariya, North of Haifa, with high grey water concentrations offshore. Similar patterns of the grey water plume dispersion (*Figure 69* a, *Figure 69* b *Figure 70*a, *Figure 70*b) were obtained also during August 2015-2018.

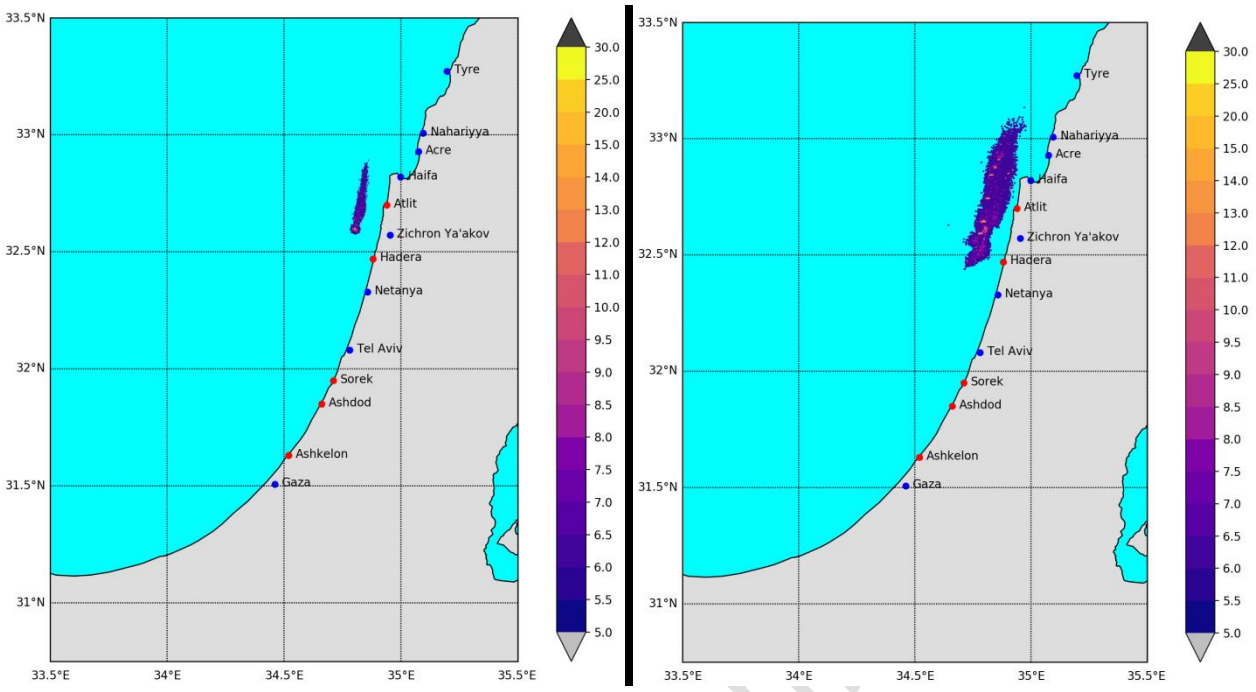

Figure 67: Mean averaged concentration of the grey water dispersed in the entire water column

Figure 67 a(left): Mean averaged concentration of the grey water dispersed in the entire water column (m^3/km^2) from the offshore Dor platform on the 1st day from the spillage, July 2015-2018.

Figure 67 b(right): Mean averaged concentration of the grey water dispersed in the entire water column (m^3/km^2) from the offshore Dor platform on the 5th day from the spillage, July 2015-2018.

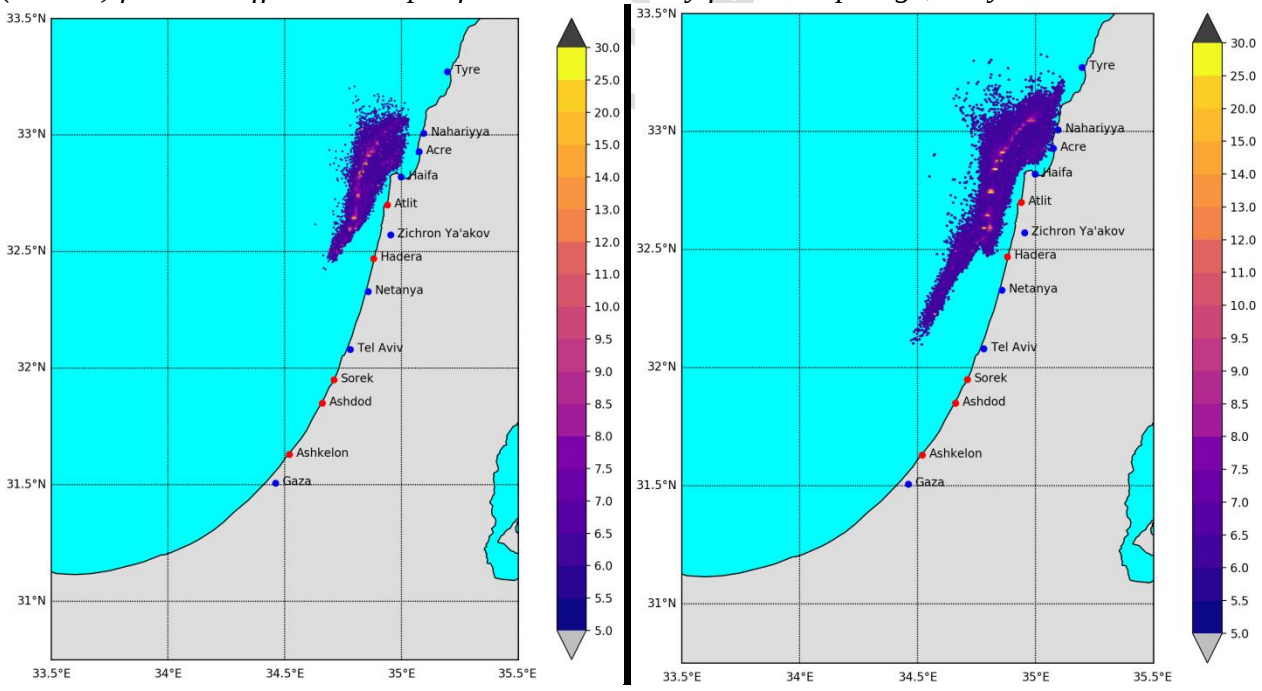

Figure 68: Mean averaged concentration of the grey water dispersed in the entire water column

Figure 68 a (left): Mean averaged concentration of the grey water dispersed in the entire water column (m^3/km^2) from the offshore Dor platform on the 10th day from the spillage, July 2015-2018.
Figure 68 b (right): Mean averaged concentration of the grey water dispersed in the entire water column (m^3/km^2) from the offshore Dor platform on the 15th day from the spillage, July 2015-2018.

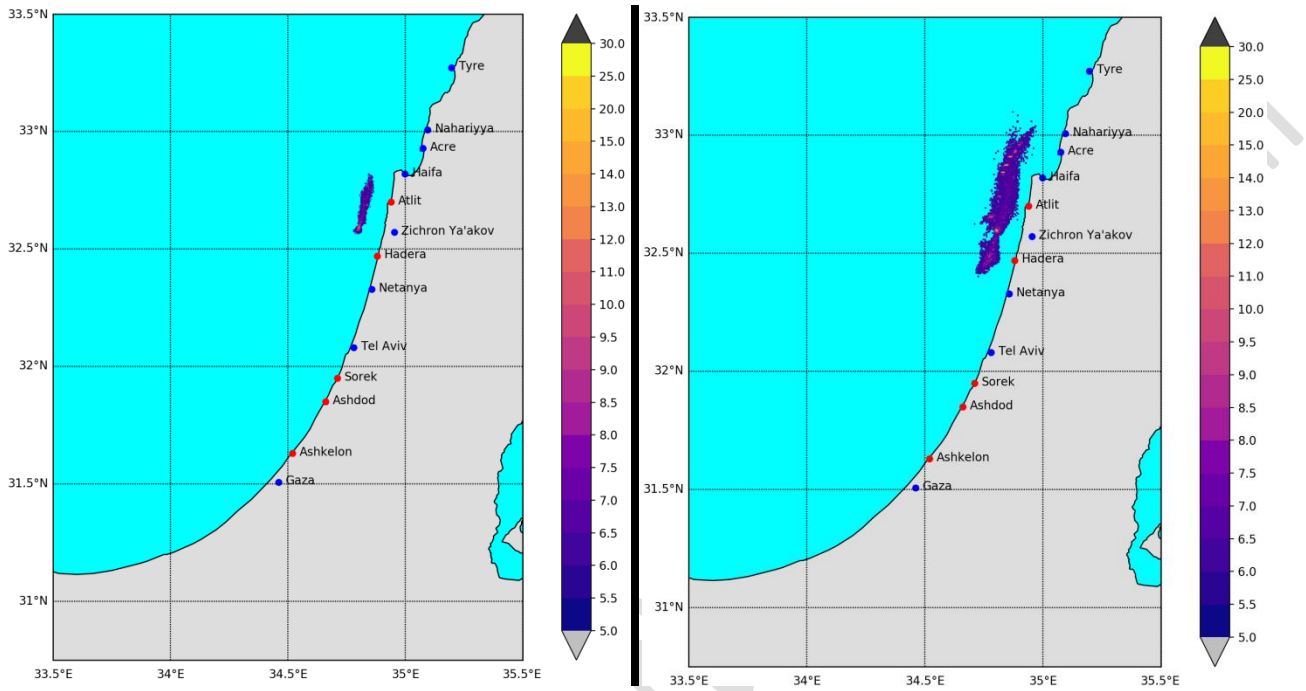

Figure 69: Mean averaged concentration of the grey water dispersed in the entire water column
Figure 69*a(left): Mean averaged concentration of the of the grey water dispersed in the entire water column (m^3/km^2) from the offshore Dor platform on the 1st day from the spillage, August 2015-2018.*
Figure 69*b(right): Mean averaged concentration of the of the grey water dispersed in the entire water column (m^3/km^2) from the offshore Dor platform on the 5th day from the spillage, August 2015-2018.*

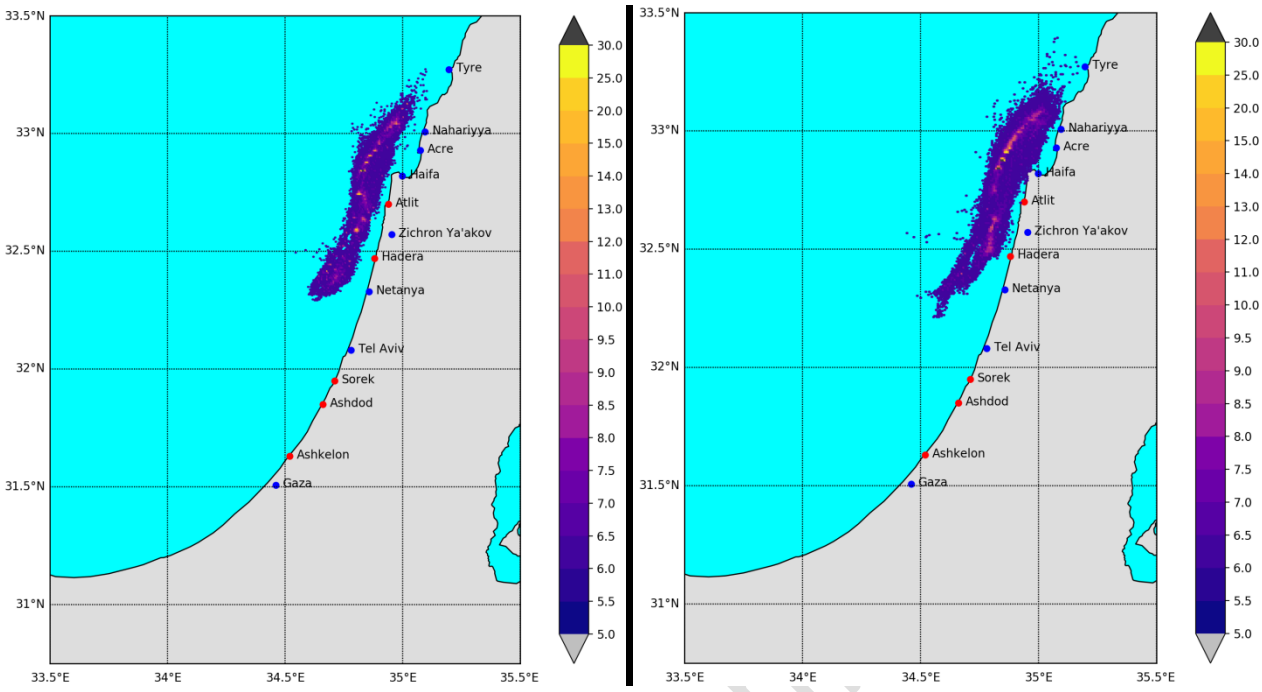

Figure 70: Mean averaged concentration of the grey water dispersed in the entire water column

Figure 70 a(left): Mean averaged concentration of the of the grey water dispersed in the entire water column (m^3/km2) from the offshore Dor platform on the 10th day from the spillage, August 2015-2018.
Figure 70b(right): Mean averaged concentration of the of the grey water dispersed in the entire water column (m^3/km^2) from the offshore Dor platform on the 15th day from the spillage, August 2015-2018.

6.3.1.4. Transition conditions (September-October 2015-2018)

September 2015-2018

The grey water plume dispersed slowly and covers a small sea area during the first three days (*Figure 71* a; b). On the day 5th (*Figure 72*a) the grey water dispersed further but it is still offshore. On day 10th (*Figure 72*b) very small quantity of grey water plume reaches the coastal water along the shoreline of the Zichron-Ya'akov, while on day 15th (*Figure 73*) the grey water from the Zichron-Ya'akov coastal waters extended towards the Atlil coastal waters. Higher grey water concentration were simulated offshore.

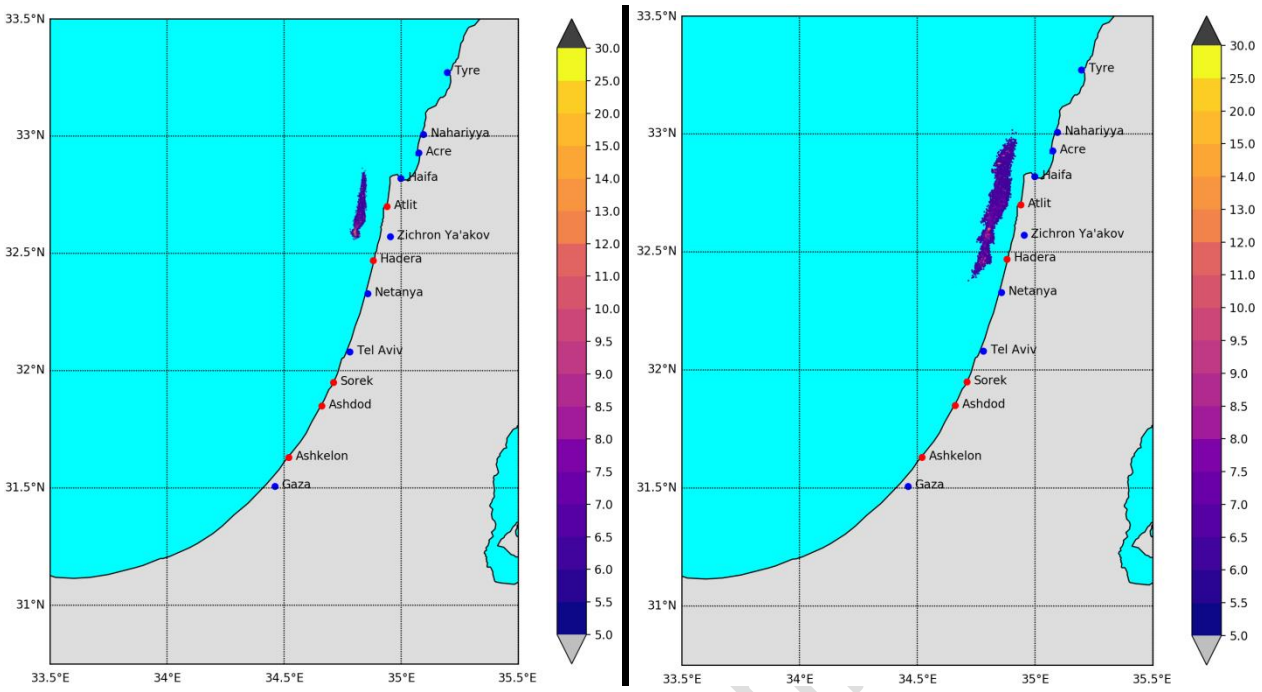

Figure 71: Mean averaged concentration of the grey water dispersed in the entire water column

Figure 71 a(left): Mean averaged concentration of the grey water dispersed in the entire water column (m^3/km^2) from the offshore Dor platform on the 1st day from the spillage, September 2015-2018.

Figure 71b(right): Mean averaged concentration of the grey water dispersed in the entire water column (m^3/km^2) from the offshore Dor platform on the 3rd day from the spillage, September 2015-2018.

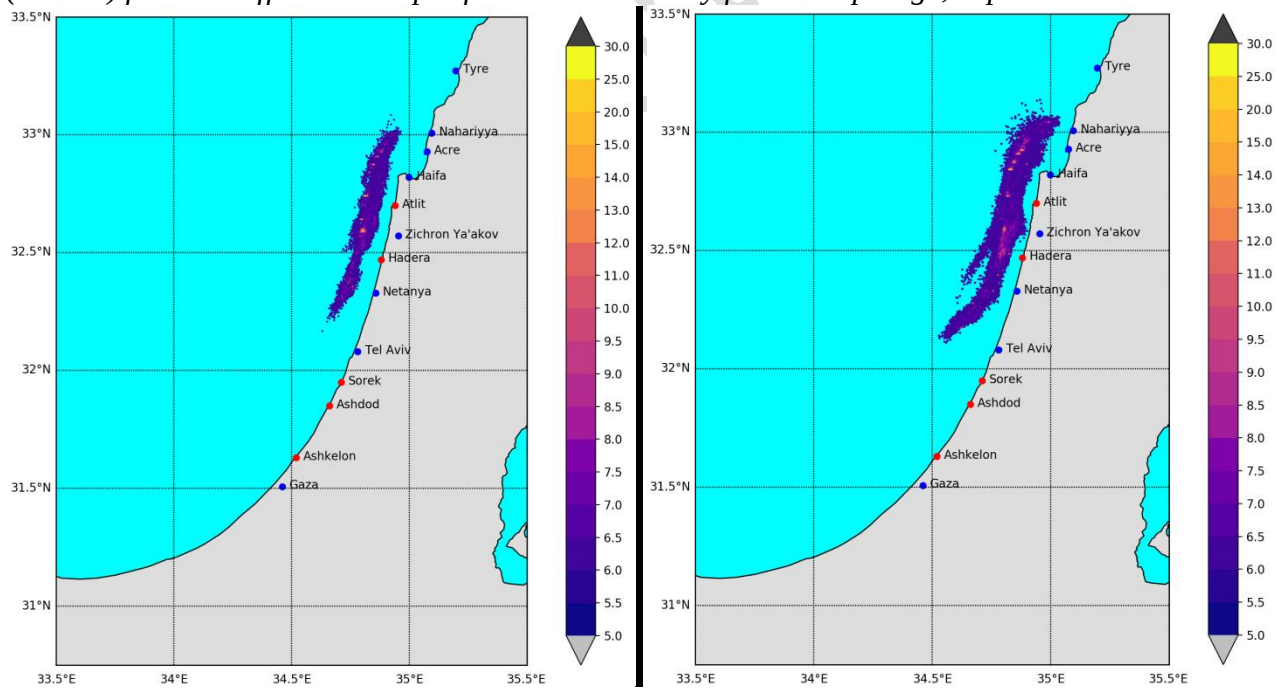

Figure 72: Mean averaged concentration of the grey water dispersed in the entire water column

Figure 72 a(left): Mean averaged concentration of the grey water dispersed in the entire water column (m^3/km^2) from the offshore Dor platform on the 5th day from the spillage, September 2015-2018. Figure 72 b(right): Mean averaged concentration of the grey water dispersed in the entire water column (m^3/km^2) from the offshore Dor platform on the 10th day from the spillage, September 2015-2018.

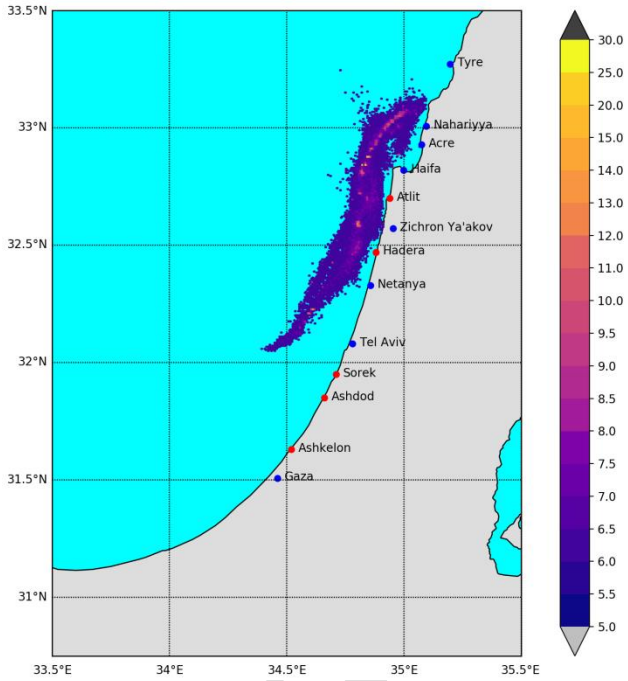

Figure 73: Mean averaged concentration of the grey water dispersed in the entire water column

Figure 73: Mean averaged concentration of the grey water dispersed in the entire water column (m^3/km^2) from the offshore Dor platform on the 15th day from the spillage, September 2015-2018.

October 2015-2018

During the first four days of the simulations during this period, the patterns of the grey water horizontal concentrations are very similar as those of the previously month, i.e. September, where until the 5th and the 10th day the plume did not reached the shoreline (*Figure 74* a; b). On the 15th day (*Figure 75*) the grey water reaches the coastal water along the shoreline between ZichronYa' akov and Atlit with higher concentrations at offshore.

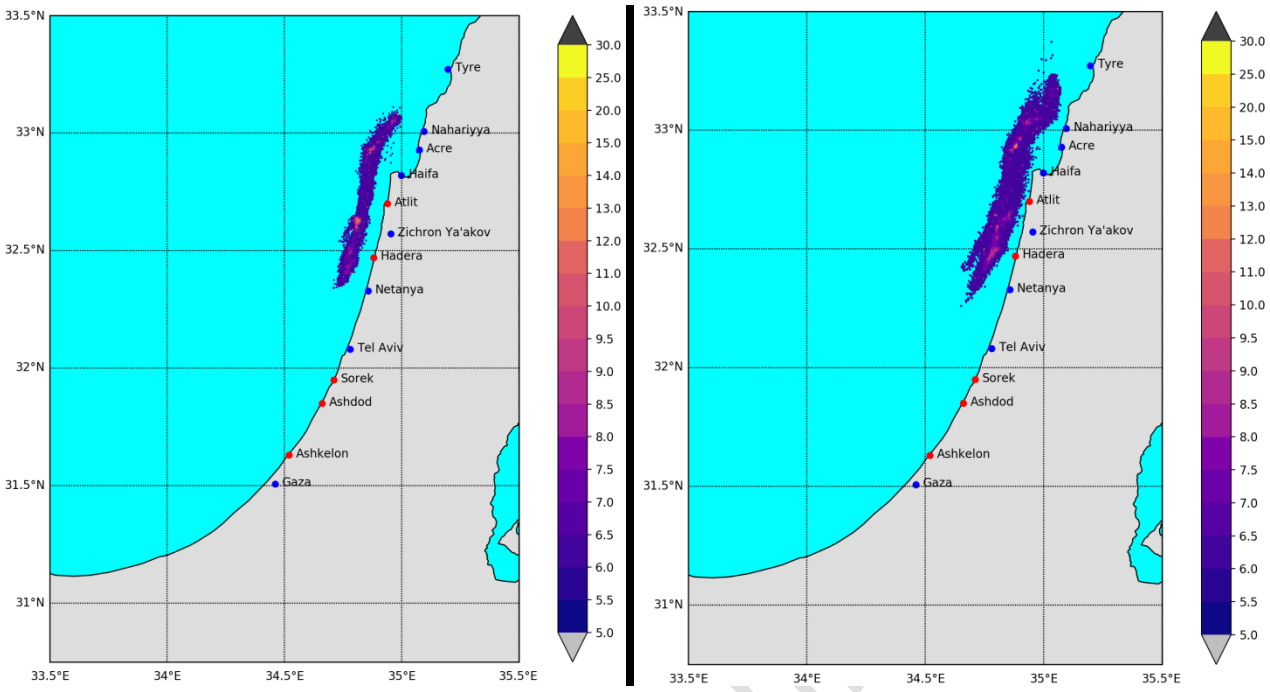

Figure 74: Mean averaged concentration of the grey water dispersed in the entire water column

Figure 74 a (left): Mean averaged concentration of the grey water dispersed in the entire water column (m^3/km^2) from the offshore Dor platform on the 5th day from the spillage, October 2015-2018.

Figure 74b (right): Mean averaged concentration of the grey water dispersed in the entire water column (m^3/km^2) from the offshore Dor platform on the 10th day from the spillage, October 2015-2018.

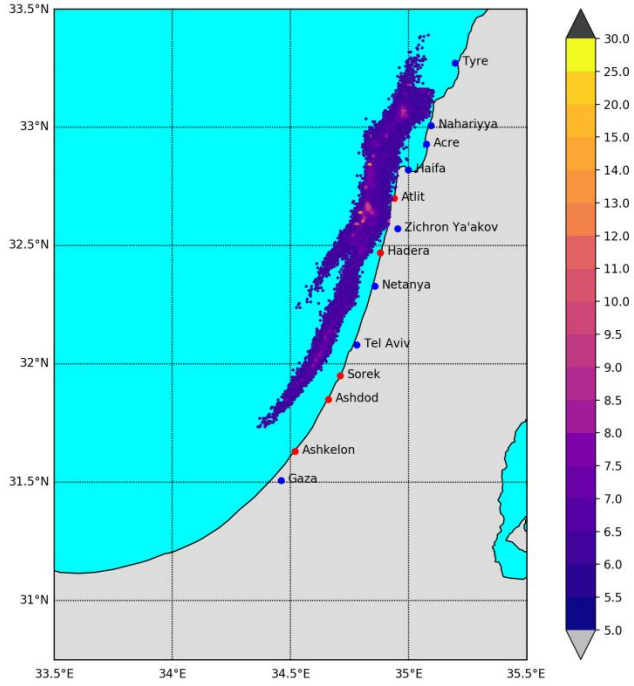

Figure 75: Mean averaged concentration of the grey water dispersed in the entire water column

Figure 75: Mean averaged concentration of the grey water dispersed in the entire water column (m^3/km^2) from the offshore Dor platform on the 15th day from the spillage, October 2015-2018.

6.3.2. Evaluation of Impacts

In assessing the impact of grey water two issues are elements should needed to be considered. The total suspended solids and nutrients and the bacterial load. Taking into accounts the rate of grey water discharge from the offshore platform is $20m^3$/day and the dispersion/dilution derived from the model simulations, the only impact to be considered it is the health impact at the coastal waters due to bacteriological contaminations. Most of human pathologies related to the use of marine waters for bathing purposes are caused by the presence of pathogens discharged in the ougmotic environment during faecal contamination episodes as in the case of grey water.

From the results of the simulation it seems that due to height dilation/dispersion of the grey water, any accidental discharge it will reach the shoreline after 10 to 15 days.

In assessing the bacteriological impact the time is very critical factor as the potentially infection microorganisms have a life time in sea water environment and sunlight, salinity and temperature are critical factors.

A review which considers the above factors and focuses in articles which refers to the survival of indicator organism or pathogens in the sea water lead to interesting results (Heather Murphy, 2017).

The following *Table 23* and *Table 24* (Heather Murphy, 2017) summarize the survival of bacteria, protozoa, bacteriophage and viruses in brackish or seawater under varying temperature and light conditions.

Table 23: Summary of the persistence of bacteria and indicator bacteria in saltwater or brackish water under different temperature and light conditions

Bacteria Type	T90 (Days)	T99 (Days)	Temperature (°C)	Light Source	References
Bacteriodales human marker[b]	1.77	NR	17	Light	Walters et al. 2009
Bacteriodales human marker[b]	8.72	NR	17	Dark	Walters et al. 2009
Bacteriodes HF183 DNA[b]	2.7	NR	14 to 18	Sunlight	Ahmed et al., 2014
Catellicoccusmarimammalium marker	0.56[d]	NR	8 to 12	Dark	Brown and Boehm, 2015
Clostridium perfringens	>1.3[d]	NR	22 to 24	Dark	Zhang et al. 2015
E.coli spp.	9 to 10.7	14	-2 to 0	Dark	Smith et al., 1994
E.coli spp.	1.7	NR	16.8	Sunlight	Ahmed et al., 2014
E.coli spp.	0.68 to 16.7[d]	NR	22 to 24	Dark	Zhang et al. 2015

Bacteria Type	T90 (Days)	T99 (Days)	Temperature (°C)	Light Source	References
E.coli spp.	NR	16 to 22	20 to 30	Nat. light cycle	Chandran et al., 2013
E. faecalis	NR	8 to 35	-2 to 0	Dark	Smith et al., 1994
Enterotoxigenic E. coli	NR	8.75	21	Nat. light cycle	Lothigius et al., 2010
Fecal enterococci	0.06 to 0.07[d]	NR	8 to 12	Nat. light cycle	Brown and Boehm, 2015
Fecal enterococci	0.27 to 0.40[d]	NR	8 to 12	Dark	Brown and Boehm, 2015
Fecal enterococci	1.04 to 1.d	NR	14 to 18	Sunlight	Ahmed et al., 2014; Walters et al. 2009
Fecal enterococci	1.32 to 5.56[d]	NR	22 to 24	Dark	Zhang et al. 2015
Fecal enterococci	0.28 to 1.46	NR	16 to 20	UV Radiation	Kay et al., 2005
Fecal enterococci	0.63 to 2.54	NR	16 to 20	Dark	Kay et al., 2005; Walters et al. 2009
Fecal enterococci (qPCR)[b]	0.19 to 0.44[d]	NR	8 to 12	Nat. light cycle	Brown and Boehm, 2015
Fecal enterococci (qPCR) [b]	> 0.4[d,e]	NR	8 to 12	Dark	Brown and Boehm, 2015
Fecal coliforms	0.88 to 2	NR	22 to 26	Fluorescent	Fujioka et al., 1981
Fecal coliforms	0.02 to 0.06	NR	22 to 26	Sunlight	Fujioka et al., 1981
Fecal streptococci	1.5 to 3.5	NR	22 to 26	Fluorescent	Fujioka et al., 1981
Fecal streptococci	0.04 to 0.13	NR	22 to 26	Sunlight	Fujioka et al., 1981
Salmonella typhimurium	4 to 11	17 to 22	-2 to 0	Dark	Smith et al., 1994
Salmonella enterica	0.02 to 0.03	NR	15	Light	Boehm et al., 2012
Salmonella enterica	47.9	NR	15	Dark	Boehm et al., 2012

Bacteria Type	T90 (Days)	T99 (Days)	Temperature (°C)	Light Source	References
Salmonella paratyphi	NR	15 to 16	20 to 30	Nat. light cycle	Chandran et al., 2013

[a] Unless specified otherwise, all data presented are from cultured organisms and were not monitored using molecular methods;
[b] Detected/ monitored using molecular methods;
[c]NR: Not Reported;
[d] Calculated from log_{10}/ day reduction values reported in the paper;
[e]Study also reported zero die-off (log_{10}/ day reduction = 0), *After Heather Murphy,2017Ref.No.4.*

The T90 of different types of Enterovirus are higher than 14 days or 15.7 and 16.4, while for a number of other types of virus have much lower values as it is shown on *Table 24*.

Table 24: Summary of the persistence of pathogenic and indicator organisms in saltwater or brackish water under different temperatures conditions

Specific Organism/ Pathogen	T90 (Days)	T99 (Days)	Temperature (°C)	Light Source	References
Enterovirus	>14	NR	17	Dark	Walters et al. 2009
Enterovirus	> 8	NR	17	Sunlight	Walters et al. 2009
Enterovirus (genome)[b]	16.4	NR	17	Dark	Walters et al. 2009
Enterovirus (genome) [b]	15.7	NR	17	Sunlight	Walters et al. 2009
Human Adenovirus- type 2	0.04	0.08	7	UVB Radiation	Carratalà et al., 2013
Human Adenovirus- qPCR[b]	9.40	NR	13 to 18	Sunlight	Ahmed et al., 2014
Human Adenovirus 40 & 41		77 to 85	15	Dark	Enriquez et al., 1994
Human Adenovirus- type 2	0.28	0.64	20	UVA Radiation	Carratalà et al., 2013
Human Adenovirus- type 2	0.34	0.67	37	Dark	Carratalà et al., 2013
Human Adenovirus- type 2	0.23	0.57	37	UVA Radiation	Carratalà et al., 2013
Norovirus GI by qPCR[c]	3.58	NR	9 to 11	Dark	Flannery et al., 2013

Specific Organism/ Pathogen	T90 (Days)	T99 (Days)	Temperature (°C)	Light Source	References
Norovirus GI by qPCR[c]	3.72	NR	9 to 11	Sunlight	Flannery et al., 2013
Norovirus GI by qPCR[c]	2.49	NR	16 to 18	Dark	Flannery et al., 2013
Norovirus GI by qPCR[c]	0.90	NR	16 to 18	Sunlight	Flannery et al., 2013
Norovirus GII by qPCR[c]	4.23	NR	9 to 11	Dark	Flannery et al., 2013
Norovirus GII by qPCR[c]	3.50	NR	9 to 11	Sunlight	Flannery et al., 2013
Norovirus GII by qPCR[c]	1.71	NR	16 to 18	Dark	Flannery et al., 2013
Norovirus GII by qPCR[c]	0.85	NR	16 to 18	Sunlight	Flannery et al., 2013
Poliovirus	NR	18	15	Dark	Enriquez et al., 1994
Poliovirus (naked genome)[c]	32.4	NR	17	Dark	Walters et al. 2009
Poliovirus (naked genome)[c]	22.3	NR	17	Sunlight	Walters et al. 2009

[a]Unless specified otherwise, all data presented are from cultured organisms and were not monitored using molecular methods;
[b]NR: Not Reported;
[c]Infectious after 60 days, *After Heather Murphy,2017,Ref.No 4*

As it is seen from *Table 23* the basic bacteria indicators *Faecal coliforms and Faecal streptococci* have a T90 of 1.5 to 2 days and 1.5 to 3.5 days respective, while for *Salmonella* species the T99 varies and are higher than 10 days.

The T90 of different types of Enterovirus are higher than 14 days or 15.7 and 16.4, while for a number of other types of virus have much lower values as it is shown on *Table 24*.

Taking in to account that in most of the season periods the grey water reaches the shoreline after 15 days and the days of bacterial survival there will be no real danger for bacterial contamination of the coastal waters.

During the Extreme Winter period, where the grey water reach the shoreline within 10 days this danger exist.

6.3.3. Deposition

Please see applicable document [13] (Main report) for all the analysis.

6.3.4. Desalination plants contamination

Microbial contamination of the sea area of the water intakes of the desalination plants is possible during *Extreme Winter Period*.

It is obvious that as the produced desalted water is used for drinking water the health impact from microbial contamination is related with its use.

The pre- treatment requirements as determined under the Israeli Public Health Regulations 2013: The sanitary quality of drinking water and drinking water facilities, diminish the risk to human health *Records Collection of Regulations Number 7262 June 26, 2013* (Department of Environmental Health Public Health Services Ministry of Health State of Israel, 2013).

The following provisions of the above regulations safeguard and extinguish the risk to human health.

Chapter B: Quality of Drinking water and Response to Deviations
Quality of drinking water
4 The following shall be applied for drinking water at all time: (1) It contains no coliform bacteria in 100 milliliters; (2) It contains no factor deviating in measure, concentration, value or Sum of ratios value of those detailed in Annex 1,2,5 or 6 to these regulations; (3) It has been treated in accordance with the provisions of these regulations.

Chapter C: Provisions for Water Sources and Production facilities
Approval of a drinking water source
9 (a) A Water supplier shall not supply water from a water source unless the Health Authority has approved the water source and in accordance with the conditions of such an approval, which shall contain, among others, provisions regarding the water treatment as stated in Regulation 17. (b) The Health Authority shall not approve a water source as stated in sub-regulation (a) if the water is unsuitable for use as raw water because of water contamination or concern for contamination.
Testing a drinking water source
10 (a) A supplier who produces water from a water source shall perform tests of the raw water in the production facility as detailed hereunder: (1) A full microbiological test and a turbidity test - once every three months; once water supply has been renewed from a production facility from which water has not been supplied for a period exceeding one month, the supplier shall perform a full microbiological test and a turbidity test prior to renewing the water supply as aforesaid; (2) A chemical test of all the factors specified in Annex 1 and 2, at a frequency as specified in Annex 3, according to the monitoring frequency group detailed in Annex 1 and 2 to these regulations; (3) Additional tests of such types and frequency required by the Health Authority, in case of concern for public health or for water contamination.

Chapter E: Water Treatment

Water treatment and monitoring in treatment facility

17 (a) A supplier shall operate a water treatment facility and shall monitor the water in a facility approved by the Health Authority and in accordance with the instructions of The Director, with regard to the types of production and treatment facilities, their capacity and their complexity. (b) A treatment facility shall be planned, established and operated in accordance with the Best Available Technology (BAT) as approved by The Director, with consideration of, among others, the effect of the facility on the environment. (c) In addition to sub-regulations (a) and (b) - (1) Raw water produced in an underground water facility in which a deviation has occurred as stated in Regulation 11(a)(2) or has been exposed to contamination, in the opinion of the Health Authority, shall be treated in a manner that ensures the removal of at least 3 orders of magnitude of viruses. (2) Raw water produced in a surface water facility shall be treated with a technology that will include at least filtration, and in a manner that ensures the removal of factors as detailed herein: (a) cryptosporidium - 2 orders of magnitude (99% removal); (b) giardia – 3 orders of magnitude (99.9% removal); (c) viruses - 4 orders of magnitude (99.99% removal); (d) Notwithstanding what is stated in sub-regulation (c), the Health Authority may demand the removal of higher orders of magnitude than stated in sub-regulation (c), when high concentrations of cryptosporidium or giardia have been found in the water source or when such concern exists. (e) A filtration treatment facility shall be designed for a turbidity level of between 0.1 - 0.3 Nephelometric Turbidity Units (NTU) upon leaving the facility (exit point), at the discretion of The Director. (f) Water turbidity shall be continuously analyzed at the exit point of each filtration unit and shall not exceed 0.3 NTU for 95% of the time on

a daily average, and in any event, a deviation from 0.3 NTU shall not persist for more than 30 consecutive minutes.

Desalination 18 (a) In addition to what has been stated in Regulations 10 and 17, where raw water is treated by desalination, it shall be monitored at sampling points and for factors as detailed in Annex 6 and shall meet the levels required as specified in Column E of that Annex.

11 (b) In a desalination facility producing more than 5,000 cubic meters of water per day, continuous conductivity monitoring meters shall be installed in a number that is appropriate for the structure of the facility and its complexity and in accordance with the instructions of the Health Authority. (c) A supplier who is desalinating water or is otherwise treating the water in a manner causing changes in acidity or alkalinity of the water, shall provide for the stabilization of the water by a method that shall assure that stabilization values of the water as specified in Column C in Annex 6 match the level required in Column E. (d) Notwithstanding what is stated in sub-regulation (c), The Director may approve stabilization of the water, in order to minimize corrosion of the pipe system, by another method .

Water disinfection

19 (a) A supplier shall not supply drinking water unless it contains at least one of the disinfectants specified in Column A of Table A in Annex 5, at a concentration which shall not be less than the concentration specified in Column B, and shall not exceed the concentration specified in Column C, both in the production facility and in the supply system, as the case may be. (b) Where drinking water contains more than one disinfectant of those specified in Table A of Annex 5, the minimal required residue shall be calculated according to the Sum of Ratios Value and shall not be less than 1 and the maximum required concentration shall be calculated according to the Sum of Ratios Value and shall not exceed 1. (c) The supplier shall monitor the concentration of disinfectant in the drinking water as detailed hereunder: (1) In a treatment facility where water disinfection is carried out - by continuous monitoring at the exit point from the facility; (2) In a water supply system - at the time of any microbiological test or by continuous monitoring; if the frequency of the microbiological sampling is only once monthly, the residual disinfectant shall be monitored on one further occasion in the middle of the month; (3) At the entrance to a water supply system serving a population larger than 50,000 residents - by continuous monitoring; such monitoring shall be carried out by the supplier transferring the water to another supplier. (d) The Director may approve the disinfection of water with a disinfectant, or by a technology, not specified in Table A of Annex 5, on such conditions as he finds appropriate, if he has found that the efficiency thereof is equivalent to those disinfectants specified in Table A of Annex 5. (e) A supplier shall plan the water supply system in a manner that shall reduce as much as possible the disinfection by-products in the drinking water; in any event, the maximum concentrations of byproducts specified in Column B of Table B in Annex 5 shall not exceed the values specified in Columns C, D and E. (f) The supplier shall monitor disinfection by-products at frequencies specified in Annex 5, in Tables C.1 to C.3, as the case may be. (g) A supplier shall notify the Health Authority, another supplier, if exists and the consumers, in advance, of any change in the method or in the level of disinfection of supplied water.

Further regulation refer the desalination intake contamination. The Public Health and the Environment World Health Organization report Section (Public Health, 2007) explains in chapter 1.8 contamination issues details (page 12 paragraph 1.8.2) ***"the petroleum and petroleum products"*** concerns. The molecular weight cut off for RO membrane performance is typically in the range of 100-300 Daltons for organic chemicals. RO membranes can remove larger molecules, however significant fouling would impede operations; small molecules pass through the membrane. Distillation processes can theoretically separate any substance by fractionation based upon boiling point differences, however distillation for desalination is not designed to be a fractionating system, thus substances with boiling points lower than water's would be carried over in the vapors and should be vented out. Paragraph 1.8.3 details the Disinfection and microbial control in drinking water. Recommendations. Spill risks are attributed also in section 2.7 page 23 concerning oil spills potential and standardization by the WHO guidelines standard (ProDes).

6.3.5. Conclusions

1. In assessing the impact of grey water two issues are elements should needed to be considered. The total suspended solids and nutrients and the bacterial load.

2. Taking in to account the small quantity of grey water discharged and the subsequent dilution there will be no impact from suspended solids on the feed water of the desalination plants and the coastal water quality in respect of these parameters.

3. Based on the results of the simulation of grey water discharged the grey water will reach shore only after 15 days for all tested periods with the exception during the extreme winter period that it will reach the shoreline within 10 days.

4. Considering the above mentioned and the short survival time TC 90 of most of the bacteria and viruses in the very saline and warm sea waters and high periods of sunshine, the risk of microbial pollution is restricted only during the extreme winter period.

5. Desalination feed water standards for microbial quality standards as defined in the Israeli Public Health Regulations of 2013 might be violated but the disaffection legally applied in all desalination plants under the these regulations where their produced water is used as drinking water will exclude any human heath impact.

7. Growth Impact to Four platforms in the Polygon

Figure 76 depicts the northern polygon as appears in page 19 figure 3.1 applicable document [18] and in applicable document [1] figure 2.3 page 18, also see *Figure 3* for the Dor offshore LPP platform in the northern polygon.

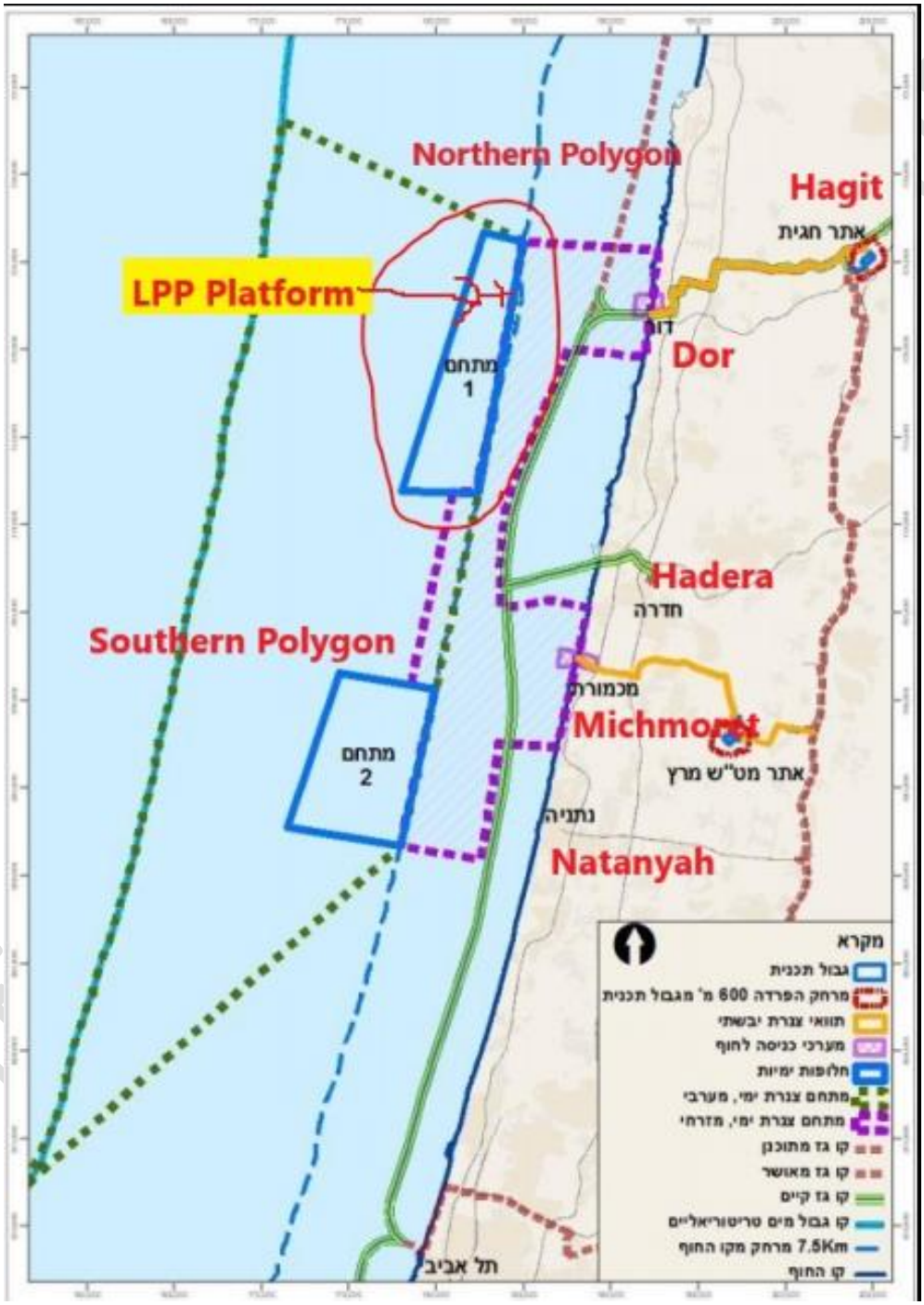

Figure 76: Northern Polygon map [18]

The northern polygon is lasts from the city of Hadera to the Dor village. It length is about 15Km and width of about 3.5Km over the sea-shelf of Israel. It is located 7.5Km from the shoreline. In the case licenses will be provided to increase the number of platforms within this polygon, then in an oil spill event occurring simultaneously in all the platforms within this polygon, would result higher risk to the shoreline and to the marine environment.

Assuming growth plan to four platform evenly distributed within the northern polygon, and assuming that all four platforms are equal to the Leviathan Dor LPP platform in terms of discharges, in case of an oil spill event, then larger beaching deposition at the shoreline will be expected. Additionally, in such malfunction event will result in a large scale of condensate evaporation, which might violate the PAC standards *Table 10*. If FSO is planned to anchor by the offshore platform as indicated by App Doc.[18] page 50 , page 63 section 3.4.1, or using submerged storage tanks as indicated in page 4, 22 and table 3.1.4-1 page 44 (which describes three tanks with total capacity of 20,000m^3) the spill event becomes severer by order of magnitudes.

Moreover in case of pipe-rupture in two, three or at all four platforms, then larger scale events are expected to occur with higher concentrations at the desalination plan intake.

Growth plan must account the short alert and readiness of a ***"Red-Team"*** to protect the environment. Hence it must have a base with all equipment such as a boat, helicopter, at the shoreline. Combating a spill event has to be well considered. Dispersants are often used however they are not good enough in Leviathan case (Cannot be used on shallow water[15], cannot be used 1-2 miles from shore or near national reserves, are not effective on 43 API condensate[16]. In general the majority of dispersants (chemical components) are used away from the coast, while the oil spill still is at sea. Within last years, in Cyprus was approved by the local response authorities the use in the coastal waters of an innovative like dispersant substance, they called it “water treatment”, like dispersant substance and it was demonstrated to be an efficient environmental friendly like dispersant for combating oil pollution at the very coastal waters, in marina and in ports. This innovative water treatment like dispersant substance is produced in Cyprus.

Continuous real time monitoring must be in place for seawater sensing, as well as for air contamination level monitoring. Further elaboration on monitoring levels is provided in chapter *9 Monitoring*

The expected air pollution from stack, flares and fugitive sources is to be increased in case of a malfunction. Hence real time monitoring stations must have triangulation abilities, wind measurement masts and online connection for streaming data directly to the environment protection hub.

[15] https://www.ukpandi.com/fileadmin/uploads/uk-pi/Knowledge_Base_-_International_Conventions/TIP%204%20Use%20of%20Dispersants%20to%20Treat%20Oil%20Spills.pdf
[16] https://www.nap.edu/read/11283/chapter/5#52

Good engineering practices suggest continuous monitoring on platforms as well as using monitoring buoys (Moroni, et al., 2016) with connection to online monitoring networks. Real time water pollution sensing must be a part of monitoring system.

The possible increase of the number of offshore platforms as part of the growth plan in the northern polygon will increase the likelihood of oil spill events. Furthermore, the deployment of offshore platforms close to each other in a relative small sea area, as the northern polygon, will increase the spillage rate in case of an accident from 2, 3 or from all four platforms. Therefore, to evaluate the impact to the marine environment and to the shoreline depositions from the possible increase of the platforms number in the northern polygon, a dedicated study is needed, implementing the same methodology applied in the present report, and in main report (App doc. [13]) in order to take into account the synergy of all the four platform to the marine and coastal resources.

8. Conclusions

8.1. Impact on the intake of the Hadera Desalination plan from the dispersed condensate

The current simulation shows that the dispersed condensate from the pipe rupture will impact the intake of the Hadera desalination plan during the transitional period.

In terms of magnitude of the dispersed condensate concentrations, those of the current stimulation are much higher than those of the two previous simulations (OSCAR and Brenner), due to the larger amount of the condensate discharge from the pipe rupture considered at the current simulation.

OSCAR and Brenner results did not provide any spatial and temporal distribution of the dispersed condensate from the pipe rupture, expect the fate parameters plots for each of the examined period in Brenner model domain and the peak value of the water column concentration of the condensate for each of the examined period in the OSCAR model domain. Therefore, the examination of OSCAR and Brenner results if will impact the intake of the Hadera desalination plan, is indirectly evaluated using the sea surface maps of the condensate concentration.

During the period defined to impact the Hadera desalination plant, the following preventive measures must be in place:

1. Oil spill alarm sensors
2. Oil spill sorbent booms and oil spill mops, because the traditional inflated or solid booms will not work with the condensate, due to its physicochemical characteristics and its behavior at sea (Described in detailed in the Main Report)
3. Include in the existing monitoring program of the desalinated water the parameters related to the detection of Petroleum Hydrocarbons.

The temporal shat down of the desalination plant in case of oil spill emergency should be considered

8.2. Grey water impact on the marine environment from the Dor offshore platform

1. The impact of grey water the parameters to be considered are the Total Suspended Solids (TSS), the nutrients (Nitrates and Phosphates) and bacterial load is discussed in (Oteng-Peprah, Acheampong, & deVries, 2018). Table 8.2 (see *Table 26*) of this paper is the physicochemical parameters of grey waters in low and high income countries comparison. Grey water characteristics, treatment systems reuse strategies and user perception a review is detailed. Concentration of TTS and Nutrients are shown too.

There are no references on the concentrations of these parameters for the grey water to be released from Dor platform. It is understood that concentrations levels of TSS, Nitrates and Phosphates are to be considered in this case, Israel is leveled as a high income and advanced country. Therefore it should be very close to the survey results of high income countries.

Applicable doc [19] entitled National Outline Plan NOP 37/H-Marine Environmental Impact Survey Chapters 3-5 page 233 Table 4.8.2 shows the dilutions factors. These factors are from the produced water dispersion model under various sea conditions and at different distances from the discharged point of produced water in the sea. As it can be seen from the table, dilutions factors are extremely high even in calm conditions and even in short distances from the discharge point. It is obvious that in the case of grey water it will be the same situation concerning the dilution.

Table 25: Dilution factors for produce water [19]

Table 4.8.2: Dilution factors obtained from the produced water dispersion model under various sea conditions and at different distances from the discharge point of produced water to the sea

Direction and distance from discharge point		Dilution factor		
Direction	Distance from discharge point (m)	Calm sea	Strong easterly wind	West to north-west summer wind
Down the current	250	13,200	72,700	32,200
	500	17,000	116,000	41,400
	1000	24,000	170,000	72,500
	1500	36,200	263,600	96,700
	2000	58,000	483,300	111,500
Perpendicular to the current	250	18,100	103,500	36,300
	500	72,500	966,700	96,700

2. In view of the above and the small quantity of the grey water the concentrations of TTS and nutrients (Nitrates and phosphates) will be minimal and they do not change the coastal water quality in this respect and thus there will be no impact on the desalination Plant.

3. According to simulation results of grey water discharged, the grey water will reach shore only after 15 days for all tested periods, with the exception during the extreme winter period that it will reach the shoreline within 10 days.

4. Considering the short survival time TC 90 of most of the bacteria and viruses in the very saline and warm sea waters and high periods of sunshine, the risk of microbial pollution is restricted only to during extreme winter period.

5. Desalination feed water standards for microbial quality standards as defined in the Israeli Public Health Regulations of 2013 might be violated but the disaffection legally applied in all desalination plants under the these regulations where their produced water is used as drinking water will exclude any human heath impact.

Table 26: Physicochemical characteristic of grey-water in low and high income countries

Table 2 Physicochemical characteristic of greywater s in low- and high-income countries

Parameter	Low-income countries				High-income countries			
	India[a]	Pakistan[b]	Niger[c]	Yemen[d]	USA[e]	UK[f]	Spain[g]	Germany[h]
pH	7.3-8.1	6.2	6.9	6	6.4	6.6–7.6	7.6	7.6
Turbidity (NTU)	–	–	85	619	31.1	26.5–164	20	29
EC (µS/m)	–	–	–	–	23	32.7	–	64.5
TSS (mg/L)	100–283	155	–	511	17	37–153	32	–
TDS (mg/L)	573	102	–	–	171	–	–	–
BOD_5 (mg/L)	100–188	56	106	518	86	39–155	–	59
COD (mg/L)	250–375	146	–	2000	–	96–587	151–177	109
Cl (mg/L)	53	–	–	–	–	–	–	–
Oil and grease (mg/L)	7	–	–	–	–	–	–	–
Nitrate (mg/L)	0.67	–	–	98	–	3.9	–	–
T. Nitrate (mg/L)	–	–	–	–	13.5	4.6–10.4	10–11	15.2
T. Phosp (mg/L)	0.012	–	–	–	4	0.4–09	–	1.6
FC (CFU)	–	–	–	1.9	–	–	–	1.4×10^5
E. coli (CFU)	–	–	–	–	5.4×10^5	$10–3.9 \times 10^6$	–	–
Ca (mg/L)	0.13	–	–	–	–	–	–	–
Mg (mg/L)	0.11	–	–	–	–	–	–	–
Na (mg/L)	32–50	–	–	–	–	–	–	–

[a] Parjane and Sane (2011)
[b] Pathan et al. (2011)
[c] Hu et al. (2011)
[d] Al-Mughalles et al. (2012)
[e] Jokerst et al. (2011)
[f] Birks and Hills (2007); Pidou et al. (2008)
[g] March and Gual (2007); March et al. (2004)
[h] Merz et al. (2007)

9. Monitoring

This section reviews and provides recommendations for air monitoring and sea water monitoring in three tiers in order to be fully responsive and alerted to spill events, as well as violations of emission of the offshore gas processing infrastructure. Such events are part of contingency plan to prevent any harmful to costal receptors, marine life and ecology balance as defined by the ministry of Energy of Israel[17]. The operator of the infrastructure is requested by the authorities to demonstrate means and measures to protect environment as described by a structured guidelines document (State of Israel Ministry of National Infrastructure, 2016). Hence the following monitoring levels are advised:

Tier-1: Continuous monitoring on platform for detection of NMVOC, BTEX, VOC, Benzene
Tier-2: On shore continuous monitoring for air quality using air sensors and dedicated equipment to alert thresholds violations.
Tier-3: Sea water continuous monitoring to detect spill events and contamination thresholds violations.

Operation and production of hydrocarbons requires awareness for the environmental risks, impacts and risk management measure plan which is associated with such offshore infrastructure (Corden, et al., 2016).

9.1. Tier-1: Continuous monitoring on platform

9.1.1. Introduction

This section summarizes the available solutions which are both technologically viable and regulatory approved for atmospheric pollutant emissions and ambient monitoring from the Leviathan near to shore condensate and gas processing platform.

Table 27 provides a summary of all monitoring means. The UK government had defined an Offshore Emissions Monitoring Guidance to be implemented on the platform (Government, UK, 2016). It can be understood that there is regulation to monitor offshore platforms and such infrastructure has to pass certifications.

[17] http://www.energy-sea.gov.il/English-Site/Pages/Data%20and%20Maps/Strategic-Environmental-Assessment-(SEA).aspx

9.1.2. Overall objectives of atmospheric emissions monitoring from gas and condensate processing platforms

Atmospheric emissions from gas and condensate processing on the Leviathan platform are anticipated to be detectable at coastal receptor locations in the vicinity of the platform. The monitoring of said emissions is required in order to meet three objectives:

1. To determine whether ambient air quality at receptor locations have been negatively impacted by platform emissions.
2. To enable sensitive populations to take preventive actions in the case of elevated ambient pollution levels at receptor locations.
3. To provide legal evidence and attribute responsibility of Israel clean air act infringements due to elevated pollutant levels at receptor locations above legal limits.

In order to meet these three objectives, it is necessary to perform continuous pollutant monitoring both on the platform and at receptor locations on the coast, in conjunction with meteorological data, in order to correlate detected ambient pollutant concentration rises at receptor locations with detected emission events from the platform. An appropriate system must therefore include the integration of both "on-platform" and "at receptor" pollutant data into a single coherent reporting solution.

9.1.3. Pollutants to be monitored

Gas and condensate processing platforms are known to produce significant atmospheric emissions of a number of different pollutants including, but not restricted to methane, non-methane volatile organic compounds (NMVOCs), nitrous oxides, and particulate emissions (Israel Ministry of Environmental Protection, 2017). The term TOC is also used and refers to the combination of both methane and NMVOCs. The broad category of NMVOCs include, but is not limited to Formaldehyde and the BTEX compounds, which are of particular interest, due to their known carcinogenic effects. The Israeli clean air act specifies legal limits on the ambient concentrations of formaldehyde, benzene and toluene, (Israel, 2016). The proposed solutions below will focus primarily on the BTEX compounds and benzene in particular due to its known carcinogenicity at very low ambient atmospheric concentrations (McMichael, 1988).

9.1.4. Mechanisms of atmospheric pollutant release from gas and condensate processing platforms

Gas and condensate processing are known to result in significant atmospheric emissions via two primary mechanisms, (i) flared and vented emissions and (ii) fugitive emissions.

9.1.4.1. Flared and vented emissions

The first mechanism is by release of gaseous biproducts of the separation process. Such releases may be further broken down into routine and non-routine emissions. On the Leviathan platform, the processing

train is designed to reroute the routine gaseous emissions, via a fuel gas recovery unit (FGRU) to a set of turbo-expanders which reuse the emissions in the treatment process. However, these turbo-expanders themselves produce emissions which are subsequently routed to the flare system on the platform. A number of other subsystems also route their emissions to the platform low pressure (LP) and high pressure (HP) flare systems. There is therefore a need to monitor the quantity and chemical identity of gases routed to the flare system. Such monitoring solutions are termed in-line monitoring solutions. In addition to the routine emissions described above, there are also non-routine emissions which result from either planned (e.g. maintenance related) or unplanned (e.g. safety pressure release) events. While by design, all such non-routine emission events should be routed to the FGRU or LP or HP flares, there is no historical precedent for a gas and condensate processing platform which does not produce cold vents to the atmosphere (Argonne Venting and Flaring Research Team, 2017) and the assertion that such will be the case on the Leviathan platform is unfounded. It should also be noted that the Leviathan expected production level of 12 billion cubic meters of natural gas per year in stage 1 (OffshoreEnergyToday, 2017) (And even more on stage 2) is considered very high compared with the vast majority of gas processing platforms worldwide, which further increases emission concerns.

9.1.4.2. Fugitive emissions

Fugitive emissions are emissions of gases or vapors from pressurized equipment due to leaks and other unintended or irregular releases of gases, in the gas and condensate process train. Fugitive emissions cannot be measured by in-line monitoring solutions and are usually estimated based on predetermined emission factors. Fence-line monitoring is the standard practice for facilities where fugitive emissions are anticipated to be substantial and the US EPA has mandated fence-line monitoring on all terrestrial oil and gas refining facilities. (EPA, Federal Register / Vol. 80, No. 230, 2015) .

9.1.5. On platform atmospheric emission monitoring solutions

This section will describe the available solutions to monitor atmospheric emissions on the gas and condensate processing platform. The solutions will be broken down into two categories; in-line emission monitoring and fence-line emission monitoring methods.

9.1.5.1. In-line emission monitoring on the platform

Current plans for the Leviathan platform, based on the draft emission permit is to monitor TOC only and rely on periodic calibration by manual sampling by the operator of the Benzene concentration in the flare gas. Such a methodology is not the best available technology and allows the operator the degree of freedom to pick and choose when to sample the flare gas, leaving the critical parameter of actual benzene emissions via the flare unknown. In-line continuous emission monitoring solutions are designed to quantitatively measure specific species such as Benzene routed via a pipeline to the flare. Specific solutions include:

9.1.5.1.1. Stack UV and FTIR-DOAS

This method is based on optical absorption in the ultra-violet or infra-red spectral range (EPA Handbook: Optical and Remote Sensing for Measurement and Monitoring of Emissions Flux of Gases and Particulate Matter, 2018). A number of specific systems are commercially available which sample by so called cross-stack methods. Two examples of such systems can be found at:

https://www.opsis.se/en/Products/Products-CEM-Process/Cross-stack-UV-IR-DOAS-Systems

http://cerexms.com/pdfs/UV3000_Product_Info.pdf

The Opsis solution has been approved by TÜV and MCERTS according to EN 15267 while the Cerexms solution has been qualified by the EPA for use on terrestrial petroleum refineries, according to a company spokesperson.

9.1.5.1.2. Periodic sampling of stack emissions

This method relies on the periodic manual extraction of samples by the operator from the emission train leading to the flare for further characterization at a remote certified laboratory. While this method guarantees high fidelity analysis of the sample, it enables only infrequent sampling at predetermined times, diminishing credibility of the results as observed by skeptical third parties.

9.1.5.1.1. Multistream Sampling

An effective alternative to a gas chromatograph GC is to use online mass spectrometry, which provides fast, multi-component gas analysis. One mass spectrometer (MS) can provide total plant coverage; our Sentinel PRO monitors a single sample point for benzene, toluene, ethyl benzene and xylenes (BTEX) in just 12 seconds, including stream settling time. Therefore, 60 sample points can be monitored in just 12 minutes, assuming all points are assigned equal priority. If some sample points are more important than others (because of a higher level of personnel activity or a higher risk of leaks) these can be assigned higher levels of priority, ensuring they are monitored more frequently.

The MS is required to monitor a wide range of volatile organics in air; if this data is to be used as part of a site monitoring strategy it must be accurate and reliable. The MS uses electron ionization to both ionize and fragment the molecules. Each molecule produces a unique "fragmentation pattern," which can be used to identify and quantify the numerous gas components in a typical chemical plant atmosphere. The result of all the various fragmentation and isotope possibilities that exist for all the volatile organics present in a typical plant environment is a complex composite spectrum. As an example, *Figure 77* shows the mass spectra fragmentation patterns of benzene, toluene, ethyl benzene and o-xylene from the National Institute of Standards and Technology (NIST) library[18]. *Figure 78* depicts the rapid multistream sampler (RMS) concept which enables continuous monitoring of stacks and vents on the offshore-platform and process the in office within the accommodation control section of the platform and relaying

[18] https://webbook.nist.gov/chemistry/

the results to an online central computer of the environmental protection stations. Further information can be found at Thermofisher web:

http://tools.thermofisher.com/content/sfs/brochures/EPM-Product-Drying-Mass-Spec_Apps_Note.pdf

https://assets.thermofisher.com/TFS-Assets/LSG/Application-Notes/epm-AN-Sentinel-VOCs.pdf

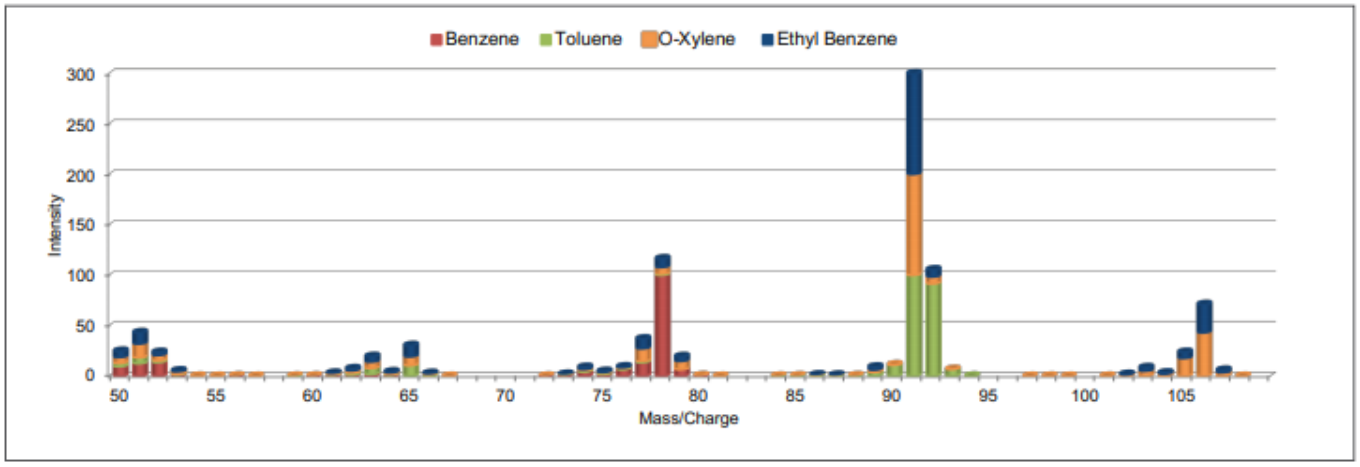

Figure 77: Composite mass spectrum of benzene, toluene, ethyl benzene and o-xylenes (NIST)

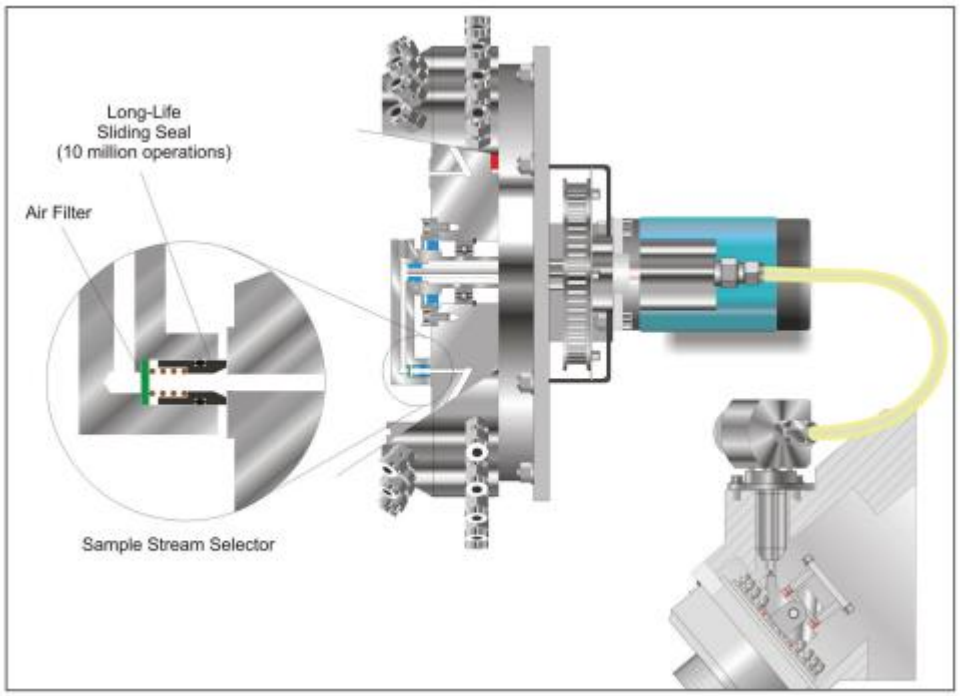

Figure 78: Rapid Multistream Sampler (RMS) cross section

APPLICATION SUMMARY – MONITORING BENZENE, TOLUENE, ETHYL BENZENE AND XYLENE IN AMBIENT AIR

The application is for ambient air multi-point monitoring of ppm levels of Benzene, Toluene, Ethyl Benzene and Xylene.

ANALYSIS SPECIFICATION

Compound being monitored	Benzene	Toluene	Ethyl Benzene	Xylene (combined ortho-, meta- and para-)
Mol Wt	78	92	106	106
Formula	C6H6	C7H8	C8H10	C8H10
Sentinel PRO Lower detection limit (LDL)	≤0.005 ppm	≤0.005 ppm	≤0.005 ppm	≤0.005 ppm
Sentinel PRO Upper detection limit (UDL)	50 ppm	50 ppm	50 ppm	50 ppm

Note Upper Detection Limits can be increased at the expense of the Lower Detection Limits by adjusting the detector gain. The Lower Detection Limit values shown refer to detection in the absence of any interfering components, i.e. in pure air.

Analysis time per point with stream settling will be approximately 12 seconds. Therefore, for example with 30 sample points or 60 sample points, the total cycle time to monitor all points would be either 6 minutes or 12 minutes respectively.

Figure 79: Rapid Multistream Sampler (RMS) detection range

9.1.6. Fence-line and multipoint emission monitoring on the platform

A number of technical solutions are available for fence-line monitoring of atmospheric emissions on a near to shore gas and condensate processing platform. Such systems can be deployed on the western edge of the platform with light-source and detection systems either separated or collocated utilizing retro or standard reflector solutions. The advantage of fence-line monitoring versus in-line monitoring is that it can also detect fugitive emissions that were not released via the flare. The disadvantage is that fence-line systems are not fool proof and do not always detect all emissions from a given source as they cannot cover all emission trajectories, depending on wind direction. Three methods will be presented here:

9.1.6.1. UV and FTIR DOAS

These systems are "line of sight" and enable the detection of pollutants along an optical path between a light source and a detector. A number of such systems are operational in terrestrial fence-line applications in the Haifa bay and in Petach Tikva. The DOAS (Differential Optical Absorption Spectroscopy) system can be configured to monitor NO, NO2, SO2, O3, BTX, NH3, CO, CO2, HF, H2O, CH4, Hg, HCl, among other gaseous compounds. The OPSIS UV DOAS system is approved according to TUV EN 15267 with a monitoring range of 0-10 μg/m3. The system is ETV verified by the U.S. EPA and MCERTS certified by the UK environmental agency. The system is described at this website below. An FTIR based fence-line monitoring solution is also available from Atmosfir:

https://www.opsis.se/en/Products/Products-AQM/Open-path-UV-IR-DOAS-Systems

https://www.atmosfir.net/d-fenceline

9.1.6.2. Optical Gas Imaging

Optical gas imaging (OGI) relies on the detection by imaging of emitted gas clouds in the atmosphere which are invisible in the visible light range but visible in the infra-red spectral range. Such a device can be implemented in a fence-line monitoring scenario by viewing the sky in a broad field of view on the western side of the platform. Page 35861 of EPA rule 40 CFR Part 60, [EPA–HQ–OAR–2010–0505; FRL–9944–75– OAR], RIN 2060–AS30, Oil and Natural Gas Sector: Emission Standards for New, Reconstructed and Modified Sources specifies that OGI is a work practice standard for the visualization of fugitive emissions. The disadvantage of these methods is that they cannot provide quantitative analysis or provide selective identification of specific VOC species. Nonetheless, these solutions enable spatially resolved imaging capabilities not achievable with alternatives. There are two major vendors of OGI solutions for the oil and gas industry, specifically

https://www.flir.eu/instruments/optical-gas-imaging/

https://www.opgal.com/gas-leak-detection-cameras/

Both are EPA 0000a certified.

9.1.6.3. Multipoint Ambient Pollutant Monitor

A process mass spectrometer analyzer relies on well-established principles of gas analysis to quantitatively measure the composition of ambient atmospheric samples which can be pumped from multiple locations on the platform to a central pollutant monitoring device. The advantage of such a system is the ability to sample at multiple locations on the fence-line of the platform, however the disadvantages are the retrofit costs and logistics of the pipelines required to transfer ambient gas samples to the analyzer. An example of a process mass spectrometer is shown in the link below:

Prima PRO Process Mass Spectrometer (Thermo Scientific™)

9.1.6.4. Passive tube sampling

This method of fence-line monitoring is based on EPA Method 325A—Volatile Organic Compounds from Fugitive and Area (US Environmental Protection Agency, 2015) and describes collection of volatile organic compounds (VOCs) at or inside a facility property boundary or from fugitive and area emission sources using passive (diffusive) tube samplers (PS). The concentration of airborne VOCs at or near these potential fugitive- or area-emission sources may be determined using this method in combination with Method 325B. Companion Method 325B (Sampler Preparation and Analysis) describes preparation of sampling tubes, shipment and storage of

exposed sampling tubes, and analysis of sampling tubes collected using either this passive sampling procedure or alternative active (pumped) sampling method. This method is not recommended because it enables only infrequent sampling at predetermined times, diminishing credibility of the results by skeptical third parties.

9.1.7. Ambient atmospheric pollutant monitoring

9.1.7.1. Ambient pollution monitoring at receptor locations

In order to meet all three objectives specified in section *9.1.3* above, continuous ambient air quality monitoring concomitant with meteorological monitoring is required at a number of receptor locations on the coast. A number of solutions which meet regulatory requirements are available for to meet this objective, as follows.

9.1.7.2. Gas chromatography and photo-ionization detection

These two technologies typically go hand in hand to enable very low detection limit continuous ambient air quality monitoring of BTEX components at receptor locations. The system draws a sample of ambient air which represents only the immediate vicinity of the sampling system. A number of regulatory accredited systems are available, which are QAL1 certified by the TUV following EN 14662-3 for benzene monitoring, including:

Envea VOC72M – VOC (BTEX) ANALYZER

AMA GC 5000 BTX FID for Benzene

Chromatotec airmoVOC

9.1.7.3. Ambient air sampling canisters

EPA Compendium Method TO-17 is a method of determination of volatile organic compounds in ambient air using active sampling onto sorbent tubes. This method is not recommended for pollutant monitoring at receptor locations due to the logistics and cost of frequent servicing and the inability to monitor continuously.

9.1.8. Data logging and Data publication

All monitored data should be made available in real time and should be logged into a central repository which allows the correlation of events recorded on the platform with ambient concentration events measured on the coastline. A dedicated SW platform is required in order to compile and make available in the public domain all recorded data. An example of such a system can be found at the webpage below.

http://www.envitech.co.il/Content/Images/UserFiles/file/EnvidasFW_EnvitechEurope.pdf

Table 27: Monitoring methods summary

Monitoring Solution	Monitoring Category	Benzene minimum detection limit*	Enclosure rating	Regulatory Standard
OPSIS UV & FTIR DOAS	In-line emission monitoring	Implementation dependent	TBD	TÜV and MCERTS EN 15267
CEREXMS UV3000 DOAS	In-line emission monitoring	15 PPB (20 meter folded path)	NEMA 4X	TBD
OPSIS BENZENE FENCE-LINE MONITORING	Fence-line monitoring	Implementation dependent	TBD	TÜV QAL1 MCERTS, AR500 Benzene
ATMOSFIR D-FENCE-LINE	Fence-line monitoring	3 PPB	TBD	TBD
FLIR GFx320	Fence-line monitoring	Qualitative nmVOC only	ATEX/IECEx	EPA OOOa
OPGAL EyeCGas® 24/7	Fence-line monitoring	Qualitative nmVOC only	IP66	EPA OOOa
PRIMA PRO MASS SPECTROMETER	Fence-line monitoring	10 PPB	ATEX Zone 1	TBD
ENVEA VOC72M	Ambient pollutant monitor	0.02 PPB	TBD	TÜV QAL1 EN 14662-3 Benzene
AMA GC 5000	Ambient pollutant monitor	0.02 PPB	TBD	TÜV QAL1 EN 15267-1&3 Benzene
CHROMATOTEC AIRMVOC	Ambient pollutant monitor	0.02 PPB	TBD	TÜV & MCERTS A21022 Benzene

*Benzene minimum detection limit requirements vary according to monitoring category; requirements are implementation dependent rough order of magnitude requirements are ~ 20 PPB for in -line, 5-10 PPB for fence-line and 0.1 PPB for ambient monitoring.

9.2. Tier-2: Continuous monitoring on shore

Tier -2 on-shore monitoring station is the second line for detection emissions conveyed by wind towards onshore receptors. Such stations are located along the coastline. Therefore this stations alert VOC, BTEX, Benzene levels as thy cover any wind regime. Having a single monitoring station is not sufficient. On the other hand such stations alone do not guarantee emission event on platform. This is because of wind regime that might carry the particles towards west in case of eastern wind.

Air monitoring station requirements are defined by the EPA (EPA, QA Handbook Vol II, Section 6.0). Such station must be connected to a network and continuously report measurements to the Ministry of Environmental Protection server. Monitoring station must have a mast with wind meter and air sensor.

9.3. Tier- 3: Oil spill monitoring

9.3.1. Overview

While a number of technologies have been demonstrated to be effective, the most mature and readily available solution is microwave (X-band) radar monitoring of the sea surface from the processing platform. A commercially available solution is the Miros system which is known to the Israel Ministry of Environmental Protection. An important alternative which should be carefully considered is satellite based X-band synthetic aperture radar (SAR) monitoring of oil spills which has been demonstrated using commercially available satellites. IAI's TecSAR satellite is likely to be technically capable of performing oil spill monitoring.

9.3.2. Overall objectives of oil spill monitoring from gas and condensate processing platforms and associated vessels

Spill response to released hydrocarbons now includes remote sensing as an essential component to the overall solution. The public expectation is that oil spill extent and location are precisely mapped. The monitoring of said releases is required in order to meet six objectives (Fingas & Brown, 2017):

4. slick detection and surveillance;
5. oil spill mapping for both tactical and strategic countermeasures;
6. gathering of legal evidence;
7. law enforcement such as regarding ship discharge;
8. direct support for oil spill countermeasures;
9. slick trajectory determination.

In order to meet these objectives, a range of technological alternatives are available and are in ubiquitous use in a number of regions worldwide (Vaišis & Pilžis, 2016), (Harahsheh, 2016).

9.3.3. Events to be monitored

Gas and condensate processing platforms and their support vessels have an extensive history of oil and condensate spills. The International tanker Owners Pollution Federation (ITOPF) maintains a database of oil spills from tankers, combined carriers and barges. Excluding acts of war, this database includes data for over 10,000 incidents, varying from a single barrel up to almost 300,000 metric tons released in a tanker collision. However, the three largest oil spills in history were all related to oil and gas activity, (Roser, 2016), the most infamous being the Deepwater Horizon oil spill which released an estimated 500,000 metric tons (On Scene Coordinator Report Deep Water Horizon Oil Spill, 2011). Encouragingly, there is a strong downward trend in this data since the inception of record keeping in the 70s, however the location of the Leviathan gas platform only 9.5 kms off the coast of Maayan Zvi beach. More pragmatically, large oil spills have received widespread media attention, while small and micro oil spills are usually only acknowledged by the authorities and local citizens who are directly or indirectly affected by these pollution events. However, small oil spills represent the vast majority of oil and condensate pollution events (Moroni, Pieri, & Tampucci, 2019). Considering the close proximity of the Leviathan gas processing platform to a number of coastal marine nature reserves, attention should be given to the implementation of an oil spill monitoring system that can identify even the smallest spills.

9.3.4. Mechanisms of oil and condensate release from gas and condensate processing platforms

In addition to routine release of produced water back into the sea, there are a number of non-routine risks which may result in significant condensate or diesel release into the Mediterranean Sea in the vicinity of the Israeli coast. These risk factors include operator error, ballast release by service vessels, impact of a heavy object on a submerged pipeline, and terror and paramilitary attacks.

9.3.5. On platform oil spill monitoring solutions

This section will describe the available solutions to monitor oil spills from the platform itself. Such a solution is highly efficient as it can provide immediate feedback and enable the fastest response to an oil spill event.

9.3.5.1. Pipeline pressure monitoring

The online monitoring of condensate pipeline pressure can provide the operator with information regarding the occurrence of a pipeline leak or rupture and subsequent oil spill. However, such methods suffer from a number of drawbacks, including lack of exact spill location information and ability to detect only larger oil spills, typically above 100 m^3 (Smaradottir, 2018).

9.3.5.2. Radar monitoring on the platform

The presence of oil or condensate on the water surface modifies the reflectance behavior of electromagnetic radiation in multiple spectral bands. One well established solution is based on

microwave reflectance in the X-band (wavelengths around 2.5 cm). Oil on the sea attenuates capillary waves, and the sea clutter from radar imagery. Oil is then shown as a "dark" spot or a region of sea clutter absence (Marzialetti & Laneve, 2016). This method requires the installation of a dedicated downward facing radar system on the processing platform. Overall, X-band is superior to other bands, but C-band radar and even L-band radar, to a degree, can provide useful oil spill data (Marzialetti & Laneve, 2016). Limitations of this method include radar scatter from high seas to the extent that detection is not possible inside the wave troughs. The range of the system depends on site specific factors like radar and camera mounting height, radar properties and wind conditions. Minimum wind speeds of 1.5 m/s (~3 knots) are required for detectability, and a maximum wind speed of 6–10 m/s (up to 20 knots) will again hamper radar detection (Leifer I., 2012). The Miros OSD surveillance will typically be used for surveillance of "small to medium sized" oil spills that is not detected by other systems. The OSD system is both radar and IR based and will give superior situational awareness, and the possibility to guide a recovery operation to the areas of "combatable oil" providing a more efficient oil recovery operation rather than relying on pipeline pressure drops to detect only larger oil spills, (Smaradottir, 2018). A typical implementation is shown in the figure below. The size of the scanned area depends on the radar band - for X-band radars in short pulse range it is 2 to 4 km and in medium pulse is 4 - 7 km range. To the authors' knowledge the Miros system is known to the Israel MoEP, who have been in dialogue with the Norwegian solution provider, see *Figure 80*. Estimated cost of the system is 40,000 - 100,000 GB pounds including day and night cameras depending on whether the system includes its own inertial guidance and stabilization gimbal.

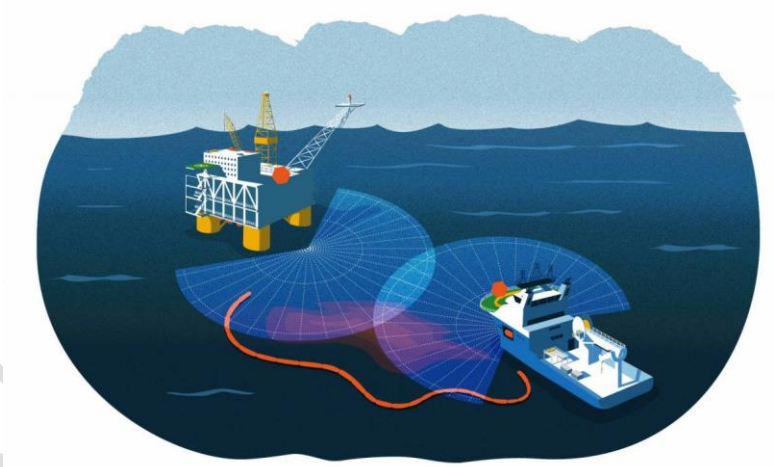

Figure 80: Miros oil spill detection implementation example.

More information can be found at Miros OSD - Oil Spill Detection System.

9.3.5.3. Infrared thermal imaging

Thin oil and diesel surface films tend to look darker than water in the long-wave IR band and lighter than water in the mid-wave IR band, making long-wave IR the preferred band-pass for oil spill detection in the IR. Furthermore, such long-wave thermal IR (8 – 12 μm wavelength) scenes are always intrinsically lit by IR emission from the scene itself, and therefore do not require illumination at night, and have an appearance that changes very little between day and night (FLIR, 2012). Two suppliers provide solutions, specifically:

FLIR Oil Spill Detection

Controp Oil Spill Detection

It is worth noting that this is the same thermal imaging technology that has been recommended for fence-line monitoring on the platform for the detection of invisible methane and NMVOC emissions.

9.3.5.4. Combined surveillance station

This solution integrations both of the previous solutions of an X-band oil spill radar system and an IR camera into a comprehensive oil spill surveillance solution. An example system is:

Furuno Finland FFSS-400 surveillance station

9.3.6. Remote oil spill monitoring solutions

9.3.6.1. Oil spill monitoring buoys

A common method to detect oil spills by floating buoys is by the use of an illumination beam of pulsed UV LED light to excite the oil molecules that have appeared in the studied water area, and induce their fluorescence. Laser fluorosensors use the phenomenon that oil aromatic compounds interact with ultraviolet light, absorb the light energy, and release the extra energy as visible light (Brown, 2017). The absorption and emission wavelengths are unique to oil. A photo-detector collects the resulting returning signal for further analysis and is immediately processed by the on board software to determine the presence of an oil slick. While the sensitivity of this method is high, the disadvantage of the system is the lack of spatial information and the ability to monitor only a single square meter of water surface area in the vicinity of the buoy. A supplier of such solutions is:

OSIL Oil Spill Monitoring Buoys

9.3.6.2. Marine vessel based oil spill monitoring

Marine vessel based spill monitoring is the most established method currently in use. The method typically employs visual identification of oil and condensate spills by trained personnel on board. However, this method suffers from a number of significant drawbacks. Firstly, it requires the vessel to be on location in the vicinity of the spill, within visual range and with appropriate scene illumination

geometry. Secondly, it is practical only in daylight hours. The second issue can be substantially mitigated by the use of a mounted X-band radar monitoring solution as described in section *9.3.5.2* above. However, the mounting of such a system on a marine vessel entails the additional expense of a stabilized gimbal to allow proper tracking of the oil slick. As shown in Figure 80**:** above, a vessel mounted monitoring system can be used in conjunction with a coastal or platform mounted system.

9.3.6.3. Aircraft based oil spill monitoring

Significant experience in aircraft-based oil spill monitoring was gained during the Deepwater Horizon disaster (Leifer I., 2012). The approach used in this event was near infrared, imaging spectroscopy data from the AVIRIS (Airborne Visual/InfraRed Imaging Spectrometer) instrument on the NASA ER-2 stratospheric airplane. Such a system requires retrofitting of an aircraft - a very significant capital expense which is probably unrealistic versus other alternatives describe in this paper.

9.3.6.4. Satellite based oil spill monitoring

A large number of near-earth orbit satellites have in principle capabilities for detecting, quantifying and tracking the progress of oil slicks. There is a range of spectral bands used by satellites to monitor oil slicks. Near infrared (NIR) bands with wavelengths of 0.75–1.4 μm, have only a short time record in oil spills. NIR bands on the MODIS and MERIS satellites have been used in research applications (Bulgarelli & Djavidnia, 2012) for oil spill monitoring, but they do not as yet appear to be in commercial use. The above mentioned Multi-spectral satellites provide various wavelength data for earth observation. Oil detection in the visible wavelength region depends on weather conditions, oil types, and view angles and the barriers to visual imagery are cloud cover and sun glint. Therefore, at this time the most promising method of space-based oil spill monitoring appears to be by SAR in the X-band, technologically similar to the method described in section 9.3.5.2 above. A number of satellites are currently in service which are potential candidates for this method of oil spill monitoring, as shown in *Table 28* below. According to this table, Israel Aircraft Industries operates a satellite named TecSAR, launched in 2008. This satellite has an X-band synthetic aperture radar (SAR) sensor which is in principle capable of oil spill identification and tracking as performed by other similar satellites such as the Kompsat 5 satellite described in this publication (Harahsheh, 2016).

Table 28: Satellite-borne synthetic aperture radar (SAR) sensors—current and future. Adapted from (Fingas & Brown, 2017)

Satellite	Launch Date	Owner/Operator	Band	Polarization
ERS-1	1991 (end 2000)	European Space Agency	C	
ERS-2	1995 (end 2011)	European Space Agency	C	VV
RADARSAT-1	1995 (end 2013)	Canadian Space Agency	C	HH
RADARSAT-2	2007	Canadian Space Agency	C	
ENVISAT (ASAR)	2002 (end 2012)	European Space Agency	C	HH, VV, Cross pol
ALOS (PALSAR)	2006 (end 2011)	Japan Aerospace Exploration Agency	L	
TerraSAR-X	2007	German Aerospace Centre	X	
Tandem -X	2010	German Aerospace Centre	X	
Cosmo Skymed-1/2	2007, 2010	Italian Space Agency	X	
TecSAR	***2008***	***Israel Aerospace Industries***	***X***	
Kompsat-5	2013	Korean Space Agency	X	
Sentinel-1	2013	European Space Agency	C	
RADARSAT-Constellation (3-satellites)	2018	Canadian Space Agency	C	

9.3.7. Operational oil spill prediction model coupled with monitoring systems

The increasing activities related to shipping and hydrocarbon industry in the Mediterranean Sea, particularly in its eastern region, show the necessity for having in place a reliable, well-tested operational oil spill modelling system to help response agencies in mitigating any accident, by providing oil spill predictions within an hour from the emergency warning. European (EMSA-CSN), regional (REMPEC) and national response agencies, civil protection teams, academia, industrial and NGO stakeholders have been working in tandem to develop, improve and operate oil spill models for predicting real and or potential oil spills (Alves T, et al., 2016) (Coppini, et al., 2011) (Zodiatis, Lardner, Solovyov, Panayidou, & De Dominicis, 2012) (De Dominicis, Pinardi, Zodiatis, & Lardner, MEDSLIK-II, a Lagrangian marine surface oil spill model for short term forecasting, Part 1: theory, 2013) (Lardner & Zodiatis, Modelling oil plumes from subsurface spills, 2017). They have recognized a strong influence of variable oceanographic and weather conditions on the movement of oil spills in the entire Eastern Mediterranean Sea. After modelling real and hypothetical oil spills in key hydrocarbon exploration areas, and shipping lanes in the Eastern Mediterranean Levantine region, (Alves T, et al., 2016), (Alves T. , et al., 2015) (Goldman, Biton, Brokovich, Kark, & Levin, 2015) (Brenner, 2015) confirmed that the variability of weather and oceanographic conditions have a crucial effect on oil slick movement (advection), and oil spill characteristics (weathering processes) through time and space.

With the development and implementation of operational oceanography in the Mediterranean Sea, as one of the CMEMS regions, and the provision of satellite SAR images detecting possible oil slicks, it is now possible to obtain near real-time operational oil spill modeling predictions within 1 hour from the oil spill warning. The successfully implementation of EC projects addressing the oil spill modeling in the

Mediterranean, particularly MEDESS-4MS www.medess4ms.eu, resulted in the harmonization of the input/output information for the needs of oil spill modeling, setting in this way the "basic standards" for oil spill models in the region.

Technological advances provided by geo-information systems, such as the use of satellite Synthetic Aperture Radar (SAR) and Automatic Identification System (AIS), made possible the detection of oil slicks and of the sources responsible for oil leakages on the sea (*Figure 81*).

At present, the coupling of satellite remote sensing systems with oil spill models constitute an effective monitoring and forecasting tool (*Figure 82*) (Klemas, 2010), (Liu Y. , Weisberg, Hu, & Zheng, 2011), (Liu, MacFadyen, Ji, & Weisberg, 2011), (Liu Y. , Weisberg, Hu, & Zheng, 2011), (De Dominicis, Pinardi, Zodiatis, & Archetti, MEDSLIK-II, a Lagrangian marine surface oil spill model for short-term forecasting – Part 2: Numerical simulations and validations, 2013). From SAR images collected during the period spanning 1999–2004, up to 2544 possible oil spills were detected in the Eastern Mediterranean (Topouzelis, Muellenhoff, Ferraro, & Bulgarelli, 2006). Similarly, in the NE part of the Eastern Mediterranean Levantine region, more than 1200 possible oil spills were detected from 2007 to 2011 (Zodiatis, Lardner, Solovyov, Panayidou, & De Dominicis, 2012). The majority of SAR-detected oil slicks as of recently followed main shipping routes in the Levantine region, and were the result of routine operations such as degassing, deballasting and other actions involving illegal discharges of oil, in violation of the EU Directive 2005/35 (*Figure 81*). Possible oil spillages from the offshore exploration of the hydrocarbon in the Levantine nowadays can be monitored using SAR data, which can be coupled with a well-established and tested oil spill model to predict the oil spill advection and weathering of the spilled oil from the offshore platform within an hour from the oil spill warning.

A common practice for assisting the national and regional contingency plans during emergencies is to have in place together with monitoring systems dedicated tools providing operationally, on a routine basis, high-resolution met-ocean information of the main parameters (sea currents, winds, waves, sea surface temperature, sea water density) affecting the advection and the weathering of the oil spills (Zodiatis, Lardner, Solovyov, Panayidou, & De Dominicis, 2012). The use of this information by oil spill models provides the capability for operational forecasting or hindcast predictions of oil spill advection and weathering (*Figure 82*) (Zodiatis, et al., Numerical Modeling of Oil Pollution in the Eastern Mediterranean Sea Part I, 2018), allowing the agencies in charge to combat oil pollution, and the decision-makers to promptly respond to oil pollution crises.

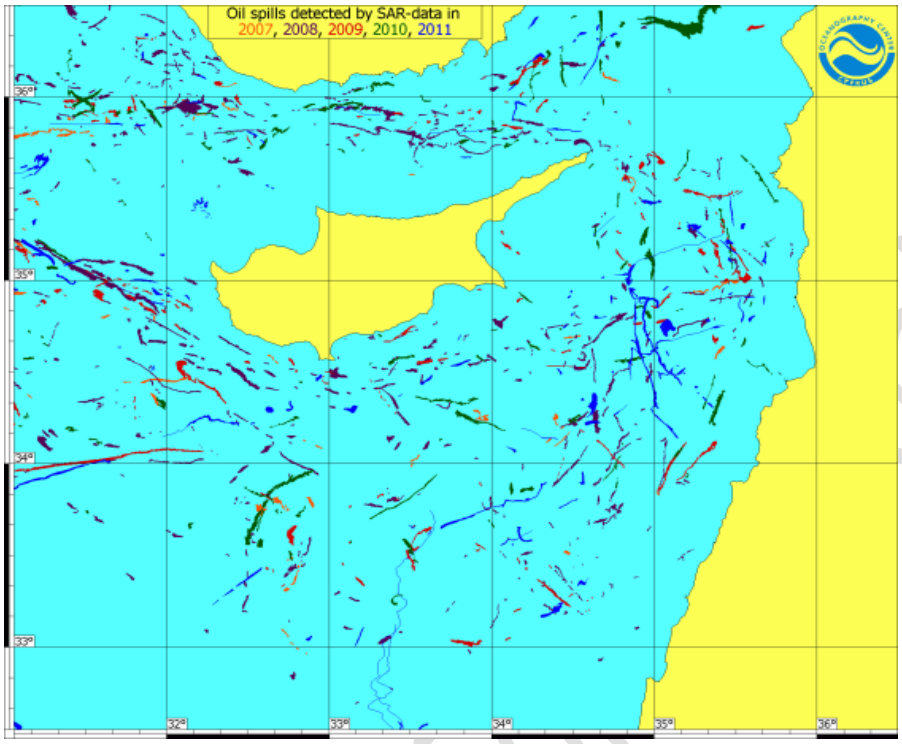

Figure 81: Possible oil spills detected in the NE Levantine Region during the period spanning 2007 to 2011 (Zodiatis, Lardner, Solovyov, Panayidou, & De Dominicis, 2012)

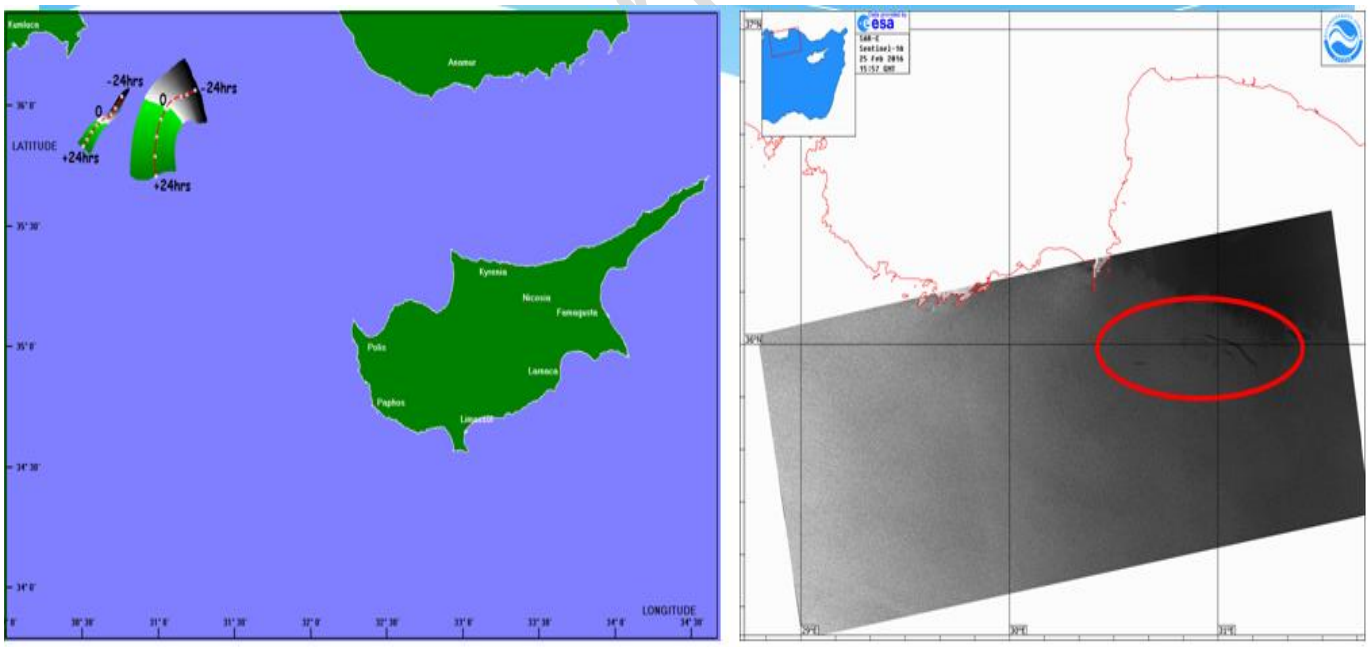

Figure 82: Example of the detection of oil slicks using ESA Sentinel SAR data and MEDSLIK 24hourly forward and backtracking predictions (date: 25/2/2016). White: initial oil slick position: 0h (date/time of observation), Dark green: forecast +24 hours, Black: backtracking -24 hours (Zodiatis, et al., Numerical Modeling of Oil Pollution in the Eastern Mediterranean Sea, 2017)**.**

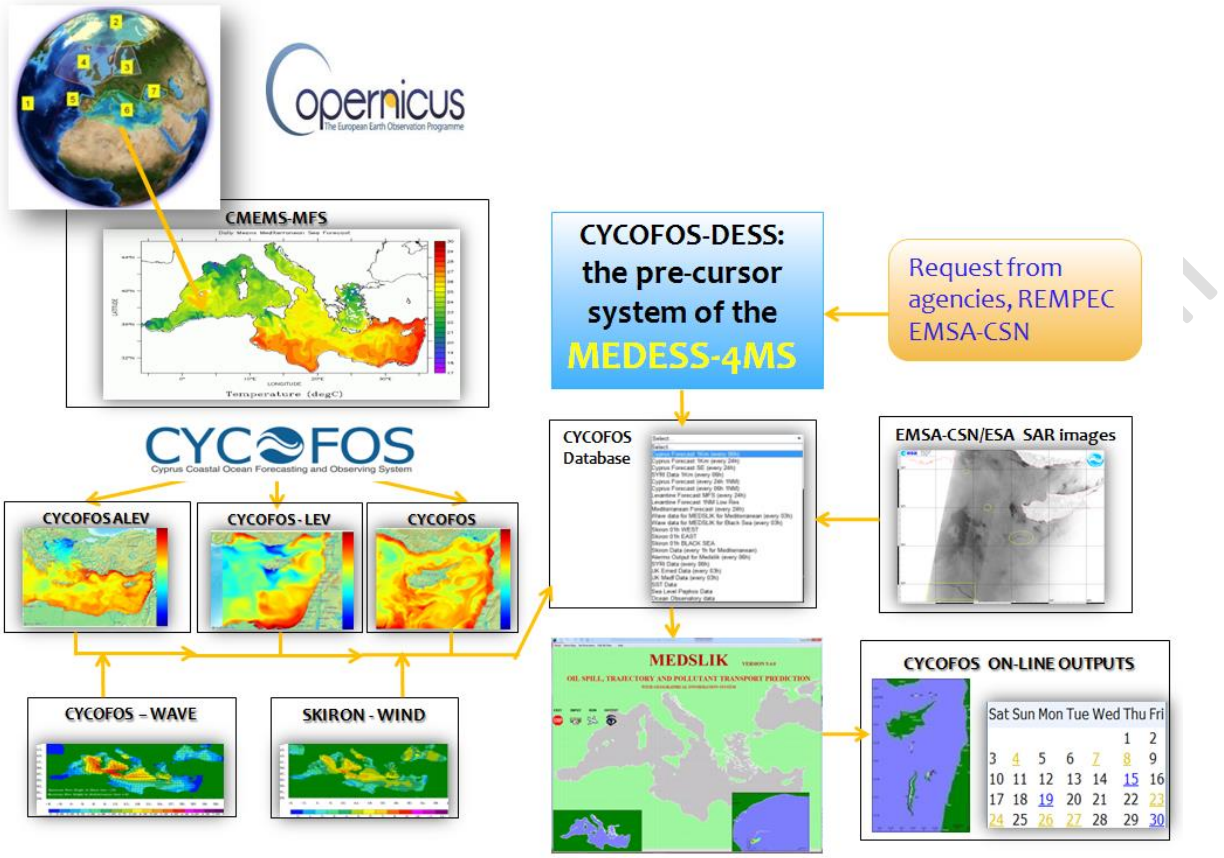

Figure 83: The MEDSLIK oil spill model uses regional CMEMS MED MFC and the downscaled CYCOFOS met-ocean data, and can incorporate emergencies warnings from the Mediterranean and European response agencies such as REMPEC and EMSA-CSN. The MEDSLIK oil spill prediction system was used as the precursor service to build the MEDESS-4MS multi model oil spill prediction service for the entire Mediterranean Sea (Zodiatis, et al., Numerical Modeling of Oil Pollution in the Eastern Mediterranean Sea, 2017)**.**

The Lebanon oil pollution crisis as an example for the operational oil spill prediction and remote satellite monitoring systems

A large oil spill occurred in mid-July 2006 at the Jiyeh power plant, located 30 km south of Beirut, Lebanon. The amount of oil spilt was reported as between 15000 and 20000 tons, and the type of oil as heavy fuel with an API of about 20. The spill took the form of a continuous leakage of oil from the power plant, starting at 0800 hours on 13 July 2006 (Coppini, et al., 2011), (Lardner, Zodiatis, Hayes, & Pinardi). The operational current forecast for mid July 2006 from the CYCOFOS forecasting system (*Figure 83*), which has a resolution of 1 km, showed a northerly flow parallel to and close to the coasts of Lebanon and Syria. Flow velocities were in the range of 20 to 30 cm/s. It turned out that these features persisted for the next two months, apart from the occasional development of eddies behind various headlands. The SKIRON wind forecast showed winds in the vicinity of the spill that varied in direction between South-West and South. This same wind pattern remained steady for most of the ensuing two months, with the wind strength varying generally between 2 and 7 m/s.

The oil spill predictions extracted from the MEDSLIK model were consistent with satellite observations (SAR and MODIS): The oil moved northwards by the currents and winds, while very large amounts were deposited on the coast adjacent to the Jieh power station, and between there and South Beirut. Some of these coastal deposits were subsequently washed back into the water and moved northwards. To the north of Beirut, MEDSLIK predicted a significant coastal impact between Beirut and Chekka, and both north and south of Tartus, with a relatively smaller coastal impact almost as far north as Latakia (*Figure 84*). These predictions are borne out by the satellite images.

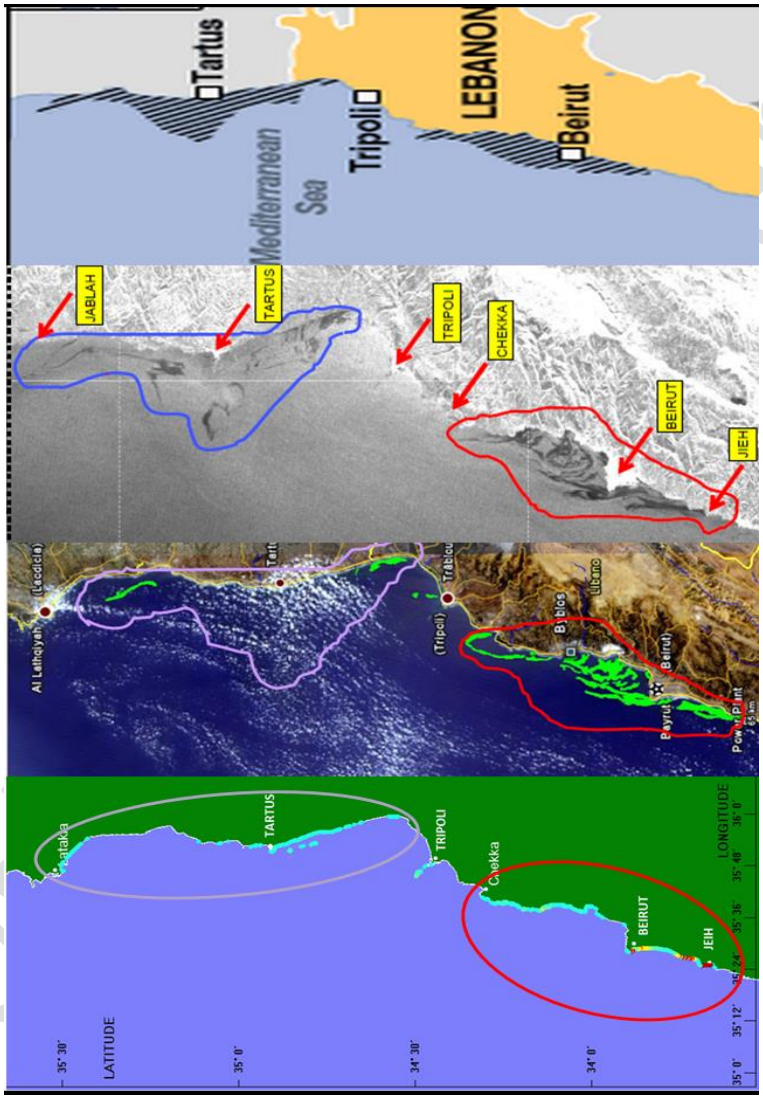

Figure 84: Inter-comparison of oil adhesion to the coast and advection at sea during the Lebanon oil pollution crisis in summer 2006 between: a) oil on coast as modeled by MEDSLIK, b) observed by MODIS, c) observed by SAR and d) after a United Nations monitoring mission (maps after Lardner et al. 2006 and De Dominicis 2013b (Lardner, Zodiatis, Hayes, & Pinardi) (De Dominicis, Pinardi, Zodiatis, & Archetti, MEDSLIK-II, a Lagrangian marine surface oil spill model for short-term forecasting – Part 2: Numerical simulations and validations, 2013)**.**

10. References

References

Abraham Tenne (Head of Desalination Division Chairman of the WDA). (2010, October). Sea Water Desalination in Israel: Planning, coping with difficulties, and economic aspects of long-term risks. *Water Authority, State of Israel, Desalination Division* , 1-13. Retrieved from http://www.water.gov.il/Hebrew/ProfessionalInfoAndData/2012/12-Desalination-in-Israel.pdf

Alves T, M., Kokinou, E., Z. G., Radhakrishnan, H., Panagiotakis, C., & Lardner, R. (2016). Multidisciplinary oil spill modelling to protect coastal communities and the environment of the Eastern Mediterranean Sea. doi:10.1038

Alves, M. T., Kokinou, E., Zodiatis, G., Lardner, R., Panagiotakis, C., & Radhakrishnan, H. (2015, November). Modelling of oil spills in confined maritime basins: The case for early response in the Eastern Mediterranean Sea. *Environmental Pollution, 206*, 390-399. Retrieved from https://www.sciencedirect.com/science/article/pii/S0269749115003759

Alves, T., Kokinou, E., Zodiatis, G., Lardner, R., Panagiotakis, C., & Radhakrishnan, .. (2015). Modelling of oil spills in confined maritime basins: The case for early response in the Eastern Mediterranean Sea. *Environmental Pollution*(206), 390-399. Retrieved from https://core.ac.uk/download/pdf/42523632.pdf

Argonne Venting and Flaring Research Team. (2017). *Analysis of Potential Opportunities to Reduce Venting and Flaring on the OCS.* Argonne Regional Laboratory.

Brenner, S. (2015, November 11). Oil spill modeling in the southeastern Mediterranean Sea in support of accelerated offshore oil and gas exploration. *Ocean Dynamic, 65*(12), 1685–1697. doi:10.1007/s10236-015-0902-2

Broday, D., Dayan, U., Aharonov, E., Laufer, D., & Adel, M. (2019, September 8). Emissions from gas processing platforms to the atmosphere-case studies versus benchmarks. *80*(2020), 1-10. Retrieved from https://www.sciencedirect.com/science/article/pii/S0195925519300800

Brown, C. (2017). Laser fluorosensors. In M. Fingas, *Oil Spill Science and Technology* (pp. 402 - 418). Cambridge, MA: Gulf Publishing Company.

Bulgarelli, B., & Djavidnia, S. (2012). On MODIS retrieval of oil spill spectral properties in the marine environment. *IEEE Geosci. Remote Sens. Lett, 9*, pp. 398–402. doi:10.1109/LGRS.2011.2169647

Coppini, G., De Dominicis, M., Zodiatis, G., Lardner, R., Pinardi, N., Santoleri, R., . . . Kallos, G. (2011). Hindcast of oil spill pollution during the Lebanon Crisis, July–August 2006. *Marine Pollution Bulletin*, 140-154. doi:10.1016/j.marpolbul.2010.08.021

Corden, C., Whiting, R., Luscombe, D., Power, O., Ma, A., Price, J., . . . Shorthose, J. (2016). *Study on the assessment and management of environmental impacts and risks resulting from the exploration and*

production of hydrocarbons. Amec Foster Wheeler Environment & Infrastructure UK Ltd. Retrieved from https://ec.europa.eu/environment/integration/energy/pdf/Study_on_the_management_of_environmental_impacts_and_risks_of_conventional_oil_and_gas%20.pdf

De Dominicis, M., Pinardi, N., Zodiatis, G., & Archetti, R. (2013). MEDSLIK-II, a Lagrangian marine surface oil spill model for short-term forecasting – Part 2: Numerical simulations and validations. 1871-1888. doi:10.5194/gmd-6-1871-2013

De Dominicis, M., Pinardi, N., Zodiatis, G., & Lardner, R. (2013, November). MEDSLIK-II, a Lagrangian marine surface oil spill model for short term forecasting, Part 1: theory. 1851–1869. doi:10.5194/gmd-6-1851-2013

Department of Environmental Health Public Health Services Ministry of Health State of Israel. (2013, June 26). Public Health regulations (Sanitary Quality of Drinking Water and Drinking water Facilities), 2013 . *Collections of Regulations Number 7262*, 1394/ 1-34. Retrieved from https://www.health.gov.il/Subjects/Environmental_Health/drinking_water/Documents/Briut47-Eng.pdf

Diamante, G., Müller, G., Menjivar-Cervantes, N., Xu, E., Volz, D., Bainy, A., & Schlenk, D. (2017, August). Developmental toxicity of hydroxylated chrysene metabolites in zebrafish embryos. *Aquatic Toxicology, 189*, 77-86. Retrieved from https://www.researchgate.net/publication/327797768_Developmental_toxicity_of_hydroxylated_chrysene_metabolites_in_zebrafish_embryos

Dixon A, Butter D, Fewkes A. (1999,, October 13). Guidelines for grey water reuse. *Health Issues (Journal Chartered Institution Water and Environment Management)*(J.IWEM), 322-326.

E. Nolde. (1999, December). Grey water reuse for toilet flushing in multi-storey building over ten years experience in Berlin. *Urban water*, 275-284. Retrieved from https://www.researchgate.net/publication/222561582_Grey_Water_Reuse_Systems_for_Toilet_Flushing_in_Multi-Storey_Buildings_-_over_Ten_Years_Experience_in_Berlin

Emissions from gas processing platforms to the atmosphere-case studies versus benchmarks. (2019, October). *Environmental Impact Assessment Review, 80*, 80. doi:10.1016/j.eiar.2019.106313

EPA. (2014). *EPA Federal Register, Vol. 79 # 125.* Retrieved from govinfo.gov: https://www.govinfo.gov/content/pkg/FR-2014-06-30/pdf/2014-12167.pdf

EPA. (2015). *Federal Register / Vol. 80, No. 230.* Retrieved from govinfo.gov: https://www.govinfo.gov/content/pkg/FR-2015-12-01/pdf/2015-26486.pdf

EPA Handbook: Optical and Remote Sensing for Measurement and Monitoring of Emissions Flux of Gases and Particulate Matter. (2018, August). *EPA 454/B-18-008*, p. section 2.3.

EPA. (n.d.). *QA Handbook Vol II, Section 6.0.* Retrieved from https://www3.epa.gov/ttnamti1/files/ambient/pm25/qa/vol2sec06.doc

Fingas, M., & Brown, C. E. (2017, DEcember 30). A Review of Oil Spill Remote Sensing. *Sensors, 18(1):91*. doi:10.3390/s18010091,

FLIR. (2012). *Technical Note: Oil Spill Detection with Infrared Imaging.* FLIR. Retrieved from https://www.flir.eu/discover/marine/first-respondents/oil-spill-detection-with-infrared-imaging/

Goldman, R., Biton, E., Brokovich, E., Kark, S., & Levin, N. (2015). Oil spill contamination probability in the southeastern Levantine basin. *Marine Pollution Bulletin, 91*, 347–356. Retrieved from http://karkgroup.org/wp-content/uploads/Goldman-et-al-2014.pdf

Government, UK. (2016). *The Offshore CombustionInstallations (Pollution Prevention and Control) Regulations 2013 -Offshore Emissions Monitoring Guidance.* Department for Business, Energy & Industrial Strategy. Crown. Retrieved from https://assets.publishing.service.gov.uk/government/uploads/system/uploads/attachment_data/file/574899/Offshore_Emissions_Monitoring_Guidance_Rev_3__Dec_2016_.pdf

Harahsheh, H. A. (2016). OIL SPILL DETECTION AND MONITORING OF ABU DHABI COASTAL ZONE USING. *The International Archives of the Photogrammetry, Remote Sensing and Spatial Information Sciences, XLI-B8*.

Heather Murphy. (2017, May 10). Persistent of pathogens in sewage and other waters types. *Global Water Pathogen Project*. Retrieved from https://www.waterpathogens.org/book/persistence-in-sewage

IMO. (2011, May). Definition of the dispersant-Guidelines for the use of dispersants for combating oil pollution at sea in the Mediterranean region Part I: Regional approval Regional Information System – Part D, Section 2 (RIS/D/2) . (I. -I. Organization, Ed.) Retrieved from http://www.rempec.org/admin/store/wyswigImg/file/Information%20resources/Guidelines/RIS%20D2%20%28Dispersants%29/EN/DispersantsGuidelinesPartI.pdf

Israel Ministry of Environmental Protection. (2017). *Tamar 2016 Emissions report.* Retrieved from www.sviva.gov.il: http://www.sviva.gov.il/PRTRIsrael/Documents/miflas_2016.pdf

Israel, G. o. (2016). *Israel Clean Air Act.* Retrieved from Sviva.gov.il: http://www.sviva.gov.il/infoservices/reservoirinfo/doclib/air/avir30.pdf

J. Ottosson, T. A. Stenstrom. (2003). Faecal contamination of grey water associated microbial risks. *Water Research , 37*, 645- 655. Retrieved from https://kundoc.com/pdf-faecal-contamination-of-greywater-and-associated-microbial-risks-.html

J. W. Doerffer. (1992). *Oil Spill Response in the Marine Environment ISBN:0080410006.* Pergamon Press.

Klemas, V. (2010, September). Tracking oil slicks and predicting their trajectories using remote sensors and models: Case studies of the sea Princess and deepwater Horizon oil spills. *Journal of Coastal Resources, 26*(5), 789–797. doi:10.2112/10A-00012.1

Lardner, R., & Zodiatis, G. (2017). Modelling oil plumes from subsurface spills. *Marine Pollution Bulletin*. doi:org/10.1016/j.marpolbul.2017.07.018.

Lardner, R., Zodiatis, G., Hayes, D., & Pinardi, N. (n.d.). Application of the MEDSLIK oil spill model to the Lebanese spill of July 2006. *European Group of Experts on satellite monitoring of sea based oil pollution,.* European Communities ISSN 1018-5593.

Last Name, F. M. (Year). Article Title. *Journal Title*, Pages From - To.

Last Name, F. M. (Year). *Book Title.* City Name: Publisher Name.

Leifer I., L. B.-B. (2012). State of the art satellite and airborne oil spill remote sensing: Application to the BP DeepWater Horizon oil spill. *Remote Sens. Environ.*, p. 185–209. doi:10.1016/j.rse.2012.03.024.

List of Oil Spills. (2019). Retrieved from Wkipedia: https://en.wikipedia.org/wiki/List_of_oil_spills#cite_note-97

Liu, Y., MacFadyen, A., Ji, Z., & Weisberg, R. H. (2011). Monitoring and Modeling the Deepwater Horizon Oil Spill: A Record-Breaking Enterprise. *International Journal of Remote Sensing Geophysical Monograph Series, 34*(12), 4508-4509. Retrieved from https://www.tandfonline.com/doi/abs/10.1080/01431161.2013.767576

Liu, Y., Weisberg, R. H., Hu, C., & Zheng, L. (2011, February 8). racking the Deepwater Horizon oil spill: A modeling perspective. *EOS, Transactions American Geophysical Union, 92*(6), 45–46. doi:10.1029/2011EO060001

Liu, Y., Weisberg, R., Hu, C., & Zheng, L. (2011). Trajectory forecast as a rapid response to the Deepwater Horizon oil spill, in Monitoring and Modeling the Deepwater Horizon Oil Spill: l: A Record-Breaking Enterprise. *Geophysical Monograph Series, 195*, 153. doi:10.1029/GM195

Marzialetti, P., & Laneve, G. (2016). . Oil spill monitoring on water surfaces by radar L, C and X band SAR imagery: A comparison of relevant characteristics. *Proceedings of the 2015 IEEE International Geoscience and Remote Sensing Symposium (IGARSS)*, (pp. pp. 7715–7717). Beijing, China.

McMichael, A. (1988). Carcinogenicity of benzene, toluene and xylene: epidemiological and experimental evidence. *ARC Sci Publ. (85)*, 3-18.

Menna, M., Poulain, P. M., Zodiatis, G., & Gertman, I. (2012, March). On the surface circulation of the Levantine sub-basin derived from Lagrangian drifters and satellite altimetry data. *Elsevier Deep-Sea Research I (Oceanographic Research Papers) , 59*(65), 46-58. Retrieved from http://www.oceanography.ucy.ac.cy/wp-content/uploads/2013/03/Menna_et_al_DSR.pdf

Moroni, D., Pieri, G., & Tampucci, M. (2019). Environmental Decision Support Systems for Monitoring Small Scale Oil Spills: Existing Solutions, Best Practices and Current Challenges. *Journal of Marine Science and Engineering, 7*(19). doi:10.3390/jmse7010019

Moroni, D., Pieria, G., Salvetti, O., Tampucci, M., Domenic, C., & Tonacci, A. (2016, December). Sensorized buoy for oil spill early detection. *Methods in Oceanography, 17*, 221-231. Retrieved from https://www.researchgate.net/publication/309716141_Sensorized_buoy_for_oil_spill_early_detection

O.K. Buros. (2000). *The ABCs of Desalting* (2 ed.). (S. W. Corporation, Ed.) Topsfield, Massachusetts, USA: International Desalination Association. Retrieved from https://water.ca.gov/LegacyFiles/pubs/surfacewater/abcs_of_desalting/abcs_of_desalting.pdf

OffshoreEnergyToday. (2017). Retrieved from offshoreenergytoday.com: https://www.offshoreenergytoday.com/delek-secures-leviathan-financing/

(2011). *On Scene Coordinator Report Deep Water Horizon Oil Spill.* National Response Team.

Oteng-Peprah, M., Acheampong, M. A., & deVries, N. (2018, July 16). Greywater Characteristics, Treatment Systems, Reuse Strategies and User Perception—a Review. *Water Air Soil Pollut (2018) 229:255*. Retrieved from https://www.researchgate.net/publication/326432835_Greywater_Characteristics_Treatment_Systems_Reuse_Strategies_and_User_Perception-a_Review

Ovchinnikov, I. M., Plakhin, A., Moskalenko, L. V., Neglyad, K. V., Osadchiy, A. S., Fedoseyev, A. F., . . . Voytova, K. V. (1976). Hydrology of the Mediterranean Sea (Gidrologia Sredizemnogo mora in Russian). *Gidrometeoizdat,*, 375.

Pascual, A., Pujol, M. I., G, L., Le Traon, P. Y., & Rio, M. H. (2005). Mesoscale mapping capabilities of multisatellite altimeter missions: first results with real data un the Mediterranean Sea. *Journal of Marine Systems* , 190-211. Retrieved from http://www.aari.ru/docs/pub/070302/pas07.pdf

ProDes. (n.d.). Guidelines for the regulation of desalination. *Promotion of Renewable Energies for Water Production through Desalination (ProDes)*(Deliverable 6.2), 23. Retrieved from https://www.prodes-project.org/fileadmin/Files/D6_2_Legislation_Guidelines.pdf

Public Health, a. t. (2007). Guidance for the Health and Environmental Aspects Applicable to Desalination. *Desalination for Safe Water Supply*, 12-13. Retrieved from https://www.who.int/water_sanitation_health/gdwqrevision/desalination.pdf

Roser, M. (2016). *Oil Spills*. Retrieved from Our World in Data: https://ourworldindata.org/oil-spills

Smaradottir, H. (2018). *Private Communication.*

State of Israel Ministry of National Infrastructure, E. a. (2016 , May 30). *Environmental Guidelines for Offshore Petroleum and Natural-Gas Exploration and Production.* Retrieved from www.energy-sea.gov.il: http://www.energy-sea.gov.il/English-Site/Pages/Regulation/Environmental%20Guidelines%20for%20Offshore%20Petroleum%20and%20Natural-Gas%20Exploration%20and%20Production.pdf

T. Hodgkiess, W. T. Hanbury , G.B. Law, T.Y. Al-Ghasham. (2001, May 28-31). Effect of hydrocarbon contaminants on the performance of RO membranes. *138*(1-3), 283-289. Retrieved from https://www.sciencedirect.com/science/article/abs/pii/S0011916401002740#!

The POM Group. (1992, February). General circulation of the eastern Mediterranean Sea. (Earth Sci. Rev., 32,), 285-309. Retrieved from https://www.seas.harvard.edu/climate/eli/reprints/The-POEM-group-1992.pdf

The Use of Dispersants in Marine Oil Spill Response. (2019). Washington DC, Ref.National Academies of Sciences, Engineering, and Medicine. 2019. The Use of Dispersants in Marine Oil Spill Response. Washington, DC: The National Academies Press. https://doi.org/10.17226/25161: National Academy of Sciences. doi: 10.17226/25161

Topouzelis, K., Muellenhoff, O., Ferraro, G., & Bulgarelli, B. (2006, . The 2nd International SAR oceanography workshop, SEASAR 2008 workshop: 23-26). Satellite monitoring of oil spills in the Mediterranean Sea for 1999-2004. *Advances in SAR Oceanography from ENVISAT and ERS missions.* Frascati Italy: E.C. – Joint Research Centre Institute for the Protection and Security of the Citizen Maritime Affairs Unit. Retrieved from http://earth.esa.int/seasar2008/participants/126/pres_126_topouzelis.pdf

US Environmental Protection Agency. (2015). EPA Method 325 A. Retrieved from https://www.epa.gov/sites/production/files/2016-07/documents/m-325a.pdf

Vaišis, V., & Pilžis, K. (2016). OIL SPILL DETECTION WITH REMOTE SENSORS. doi:10.3846/aainz.2016.20

W. El-Sayed Elshorbagy, A. Awad Elhakeem. (2012). Forecasting the oil spill impacts on coastal desalination plants in United Arab Emirates. *WIT Transactions on Ecology and The Environment, , 164*(ISSN 1743-3541), 263-274. Retrieved from https://www.witpress.com/Secure/elibrary/papers/WP12/WP12023FU1.pdf

Yaron Egozy. (n.d.). Operational experience at varying production capacities in the Hadera Desalination Plant. Retrieved from http://gwri-ic.technion.ac.il/pdf/IDS/398.pdf

Zodiatis, G., Coppini, G., Perivoliotis, L., Lardner, R., Alves, T., Pinardi, N., . . . Neves, A. A. (2017, August). Numerical Modeling of Oil Pollution in the Eastern Mediterranean Sea. *Oil Pollution in the Mediterranean Sea: Part I*. Retrieved from http://orca-mwe.cf.ac.uk/107719/1/2017Dec_handbook_env_chem.pdf

Zodiatis, G., Coppini, G., Perivoliotis, L., Lardner, R., Alves, T., Pinardi, N., . . . Neves, A. A. (2018). Numerical Modeling of Oil Pollution in the Eastern Mediterranean Sea Part I. *The Handbook of Environmental Chemistry , 83*, 215-231. Retrieved from https://books.google.co.il/books?id=KaSWDwAAQBAJ&pg=PA214&lpg=PA214&dq=Zodiatis+George,+Giovanni+Coppini,+Leonidas+Perivoliotis,+Robin+Lardner,Tiago+Alves,+Nadia+Pinardi,+Svitlana+Liubartseva,+Michela+De+Dominicis,+Evi+Bourma,+and+Antonio+Augusto+Sepp+Nev

Zodiatis, G., Drakopoulos, P., Brenner, S., & Groom, S. (2005). Variability of the Cyprus warm core Eddy during the CYCLOPS project. *Deep Sea Research, II Topical Studies in Oceanography, 52*, 2897–2910.

Zodiatis, G., Gertman, I., Poulain, P. M., & Menna, M. (2015, December). The general circulation in the SE Levantine. *Proceeding of the Scientific Conference: Integrated Marine Research in the Mediterranean and the Black Sea.* Brussels.

Zodiatis, G., Gertman, I., Poulain, P. M., Menna, M., & Sofianos, S. (2016). Two decades of monitoring and forecasting of the circulation in the Levantine (1995-2016). *Rapp. Comm. int. Mer Médit., 41, 2016*. Retrieved from http://ciesm.org/online/archives/abstracts/pdf/41/CIESM_Congress_2016_Kiel_article_0079.pdf

Zodiatis, G., Hayes, D., Gertman, I., & Samuel-Rhodes, Y. (2010). The Cyprus warm eddy and the atlantic water during the CYBO cruises (1995-2009). *Rapp. Comm. Int. Mer Medit , 39*, 202. Retrieved from http://www.ciesm.org/online/archives/abstracts/pdf/39/PG_0202.pdf

Zodiatis, G., Lardner, R., Solovyov, D., Panayidou, X., & De Dominicis, M. (2012). Predictions for oil slicks detected from satellite images using MyOcean forecasting data. *8*, 1105-1115. Retrieved from https://www.ocean-sci.net/8/1105/2012/os-8-1105-2012.pdf